La Rivista del Nuovo Cimento (2025) 48:435–536
https://doi.org/10.1007/s40766-025-00071-6

REVIEW PAPER

Perspectives in power applications of low and mainly high temperature superconductors: energy, transport and industry

L. García-Tabarés[1] · F. Toral[1] · J. Munilla[1] · L. González[1] · T. Puig[2] · X. Obradors[2]

Received: 10 December 2024 / Accepted: 10 April 2025 / Published online: 11 July 2025

Abstract
Recent advances in superconducting materials are giving renewed impetus to different power applications, some of which already existed based on previous superconductors with more modest properties while some others have been the symbiosis of new requirements in science and technology and better properties of the new superconductors. This paper constitutes a review of classical and new superconducting materials for power applications (the technological superconductors as they are frequently called) in terms of their structure and their engineering properties (electrical, mechanical and thermal) but also in terms of their manufacturability and scalability for possible scenarios where massive quantities may be required. The second and longer part of the paper is a state of the art of power applications of superconductivity related to energy (generation, transport and transmission), transport (airborne, waterborne and terrestrial) and industrial processes. Practically, all these applications are based on superconducting magnets, which are addressed in the article, including new technologies regarding their design, fabrication and operation. Particularly, these magnets can be the coils of superconducting electrical machines, also described in the paper, where different applications are presented following a scheme of problems to be solved versus the solution provided by superconductivity, including benefits regarding sustainability improvement associated with their better efficiency and power consumption reduction.

1 Introduction

Despite superconductivity being discovered more than 110 years ago, the implementation of powerful applications and the penetration of this technology in sectors such

✉ L. García-Tabarés
luis.garcia@ciemat.es

1 División de Ingeniería Eléctrica, Departamento de Tecnología, Centro de Investigaciones Energéticas Medioambientales y Tecnológicas, CIEMAT, Av Complutense 40, 28040 Madrid, Spain

2 Institut de Ciència de Materials de Barcelona, ICMAB, CSIC-Campus UAB, 01893 Bellaterra, Spain

as energy, transport, healthcare, science or industrial manufacturing, has been a long and winding road not only because of the difficulty for operating at ultra-low temperatures, but also because of the limitations of the superconductors themselves in terms of their other critical operating magnitudes (current and magnetic field) beyond which, they lose the superconducting (SC) properties. Only high critical values could make it worth using superconductors at such low temperatures, and these high values were not achieved until 50 years after the discovery of superconductivity. At the present moment, a new generation of superconductors (the so-called HTS—high critical temperature superconductors), discovered "only" forty years ago are starting to become mature and ready for being integrated into many applications such as magnets for fusion reactors, transmission lines, wind energy generators or magnetic energy storage systems, all in the field of energy, motors for propelling planes, trains and ships in the sector of transport, MRI magnets and particle accelerators for radio, proton and ion therapy and also for radioisotope production in the healthcare sector, particle accelerators and colliders for high energy and nuclear physics, NMR facilities in science, and some other applications, which are slowly penetrating in the industrial sector, all profiting of an additional advantage: they can operate at higher temperatures than their predecessors, the LTS (low critical temperature superconductors), with the corresponding benefits or, they can be operated at the same temperature as the LTS but with much better transport properties. Another important consideration when talking about power applications of superconductors is that most of them are implemented in the form of SC electromagnets since, normally, a high magnetic field is pursued for those applications. Power applications of superconductivity are then supported by two different but complementary technologies: SC material development (including wires and cables) and SC magnet development. This paper starts with an introduction to the most relevant properties of the superconductors related to their use in power applications and a state-of-the-art regarding the development of modern superconductors (basically HTS). Next, it introduces the main concepts in SC electromagnets to afford a review of the principal power applications of modern superconductivity in fields such as energy, transportation and industry, most of them based on those electromagnets... These applications are probably less discussed and disseminated in the scientific literature when compared to others related to science or healthcare.

2 Technical superconductors

Superconductivity was discovered in 1911 by Kamerlingh Onnes, three years after he succeeded in liquefying Helium to 4.2 K. This discovery won him the Nobel Prize in 1911. Since then hundreds of materials have exhibited this phenomenon which manifests itself by showing zero resistance below a critical temperature, T_c, and being able to expel the magnetic field from inside the material below this T_c, the Meissner effect. It took many years to discover a microscopic theory capable of explaining superconductivity until Bardeen, Cooper, and Schriefer proposed the BCS theory, which won them the Nobel Prize in 1972. The BCS theory of superconductivity is based on the formation of electron pairs, called Cooper pairs, capable of combatting the Coulomb interaction between the two electrons, with a weak attractive interaction between the

electrons and the atomic lattice vibrations (phonons). All Cooper pairs can condense into the ground state, not being restricted to the Pauli principle of electrons. This creates a quantum coherent SC state with an energy gap between the SC state and the normal non-SC state. This is how SC materials avoid electron scattering, showing zero resistance and keeping the Meissner state up to a critical field, B_{c}. We can distinguish two types of SC materials, Type I and Type II. In Type I superconductors, Superconductivity is destroyed above this critical field, B_{c}, but the corresponding electric currents are quite small. This is the case for most elements such as Hg, Al, Pb, Nb, ... In contrast, Type II superconductors show a low critical field, $B_{\mathrm{c}1}$, below which the Meissner state exists, and above which a mixed state persists up to the upper critical field, $B_{\mathrm{c}2}$. Above $B_{\mathrm{c}2}$, Superconductivity (Cooper pair condensation) is destroyed. In the mixed state, quantized magnetic flux, called vortices, enter the material and determine the physical properties of these superconductors. In Type II superconductors $B_{\mathrm{c}2}$ can be very large, allowing it to sustain very large magnetic fields. Vortices can move by the application of an electrical current, which generates dissipation in the material. However, if vortices are strongly pinned (hard type II superconductors), large electrical currents can be carried in the material without dissipation. The associated maximum current beyond which vortices move generating dissipation is called the critical current, I_c, and the corresponding magnetic field beyond which vortices cannot be pinned (i.e. $I_c = 0$), is called the Irreversibility field, Birr. All these characteristic magnetic fields are temperature dependent, $B_{\mathrm{c}1}$ (T), $B_{\mathrm{c}2}$ (T) and B_{irr} (T). Therefore, Type II superconductors are used to generate large magnetic fields or for large current applications. Examples of Type II are the metallic alloys NbTi and Nb_3Sn, but also the ceramic cuprates, iron-based superconductors (IBS) or MgB_2. We can also distinguish between conventional superconductors, which follow the BCS theory mentioned above, and unconventional superconductors. While NbTi and Nb_3Sn, among others, are low-temperature and conventional superconductors, cuprates (which were discovered in 1986 and gave their name to high-temperature superconductors HTS) and IBS are unconventional superconductors. For these materials, a new microscopic theory is to be discovered yet, since the strong electron–electron interaction cannot be surpassed by the electron–phonon weak interaction of the BCS theory. Nevertheless, there is no doubt that Cooper pairs, mediated by another stronger interaction, give rise to superconductivity in these unconventional superconductors. Figure 1 shows most of the SC materials with their T_{c} and the year of their discovery.

Two very relevant magnitudes help to distinguish between Type I and Type II superconductors. These are, the coherence length, ξ (T), defined as the distance between the two electrons forming the Cooper pair, and the penetration length, λ (T), defined as the characteristic distance where Meissner current circulates at the surface of the superconductor to expel the magnetic field from its interior. Given these two magnitudes, one can define Type I superconductors when $\frac{\lambda}{\xi} \leq \frac{1}{\sqrt{2}}$ and Type II superconductors when $\frac{\lambda}{\xi} \geq \frac{1}{\sqrt{2}}$.

However, from all discovered SC type II superconductors only a few of them could successfully be shaped in the form of wires or tapes to be used in devices. These are the LTS NbTi and Nb_3Sn, MgB_2 and the HTS $Bi_2Sr_2CaCu_2O_8$ (Bi-2212), $Bi_2Sr_2Ca_2Cu_3O_9$ (Bi-2223), $REBa_2Cu_3O_7$ (REBCO, RE = Y, Rare Earth) and

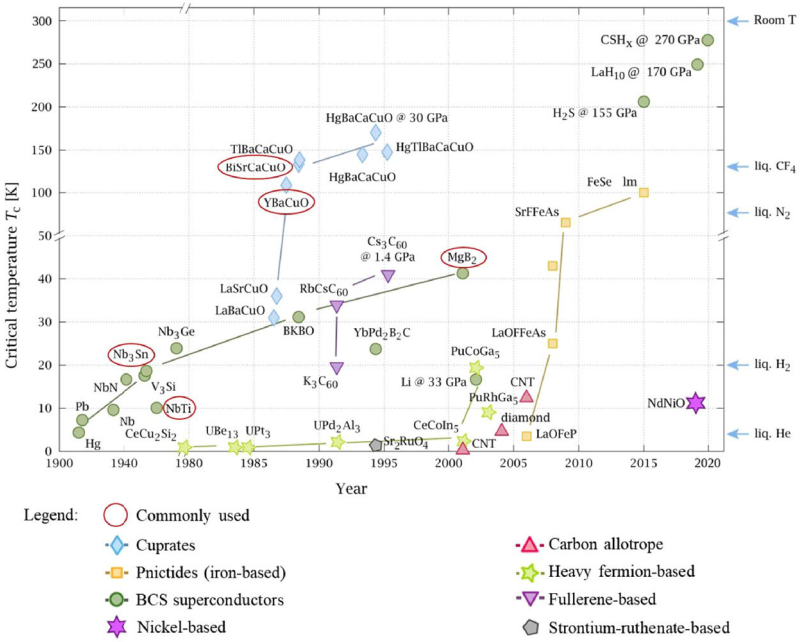

Fig. 1 Evolution of the critical temperature T_c of SC materials with the year of discovery. The colours indicate the different families of materials. Figure from [1]

recently several phases of the IBS families, such as $FeSe_{0.5}Te_{0.5}$-11, (Ba,K)Fe_2As_2-122, $BaFe_2As_{2-x}Px$-122, $BaFe_{2-x}Co_xAs_2$-122 and NdFeAs(O,F)-1111. The reason for this is the very different nature of the materials, the former being relatively simple metallic alloys while the latter being complex ceramics or multicomponent materials. In Table 1 we present a selection of the most representative examples of the different families of SC compounds of interest for large current applications.

All the practical superconductors being used for power applications (either LTS or HTS) are type II [2–4]. In the mixed state, the vortices density continuously increases when the magnetic field increases. To classify type II superconductors we can use, not only the T_c values but also their B_{c2} (T) dependence because this will determine the region of the B–T magnetic phase diagram where they become useful conductors for applications. Nevertheless, an additional parameter needs to be properly considered when one examines the range of B–T region useful for applications. The reason is that to have a useful SC wire under a magnetic field, vortices should remain immobile, by a pinning force, F_p counteracting the Lorentz force $F_L = J \times B$ where J is the SC current density circulating through the material. The critical current density, J_c, defined at $F_p = F_L$, is the maximum current density without losses. In LTS materials, the thermal excitation able to depin vortices is low as compared to the pinning energy, however, in HTS, instead, thermal activation is strong as compared to the pinning energy and so the vortex lattice behaviour increases in complexity. The first significant effect is that the melting of the vortex lattice, i.e. the melting line B_m (T), appears in clean HTS well below B_{c2} (T), generating a free motion of vortices (a

Table 1 Classification of superconductors followed by the materials family, representative composition, and the corresponding coupling mechanism

Classification	Materials family	Representative compositions	Coupling mechanism
LTS ($T_c < 20$ K)	Metallic elements	Nb, Hg, Pb, Al	BCS
	Intermetallic	NbTi, Nb_3Sn	BCS
	Heavy fermion	$CeCu_2Si$, $PuCoGa_3$	Non-BCS (magnetic mediation)
	Organic salts	BEDT-TTF	Non-BCS
	Chevrel	$PbMo_6S_8$, $SnMo_6S_8$	BCS
	Oxides	Niquelates (Nd, Sr)NiO_2	Unknown
Intermediate Tc	Intermetallic	MgB_2	BCS
($T_c < 40$ K)	Carbon based	Carbon nanotubes (CNT), fullerenes (K_3C_{60})	BCS
HTS ($T_c > 40$ K)	Oxides	Cuprates ($REBa_2Cu_3O_7$, $Bi_2Sr_2CaCu_2O_8$, $Bi_2Sr_2Ca_2Cu_3O_9$)	Non-BCS
	Pnictides	Iron based superconductors (IBS), $REFeAsO_{1-x}$, $(Ba,K)Fe_2As_2$, $FeSe_{0.5}Te_{0.5}$, $CaRbFe_4As_4$, $Sr_2ScFeAsO_3$	Non-BCS (magnetic mediation)
	Hydrides	H_2S, LaH_{10} (high pressure necessary)	BCS

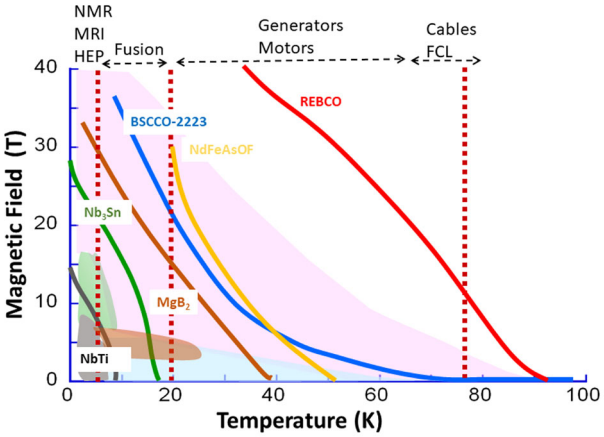

Fig. 2 Superconducting materials irreversibility lines (color solid lines) and regions of operation (color regions) for power applications. There is no coloured region for NdFeAsOF as this material has not been used in applications yet. The magnetic field is applied along the direction having the smallest value of B_{irr} (T) (perpendicular to the CuO_2 planes in the case of cuprates)

vortex liquid phase) where HTS lose the characteristic of having no dissipation [3]. In non-clean superconductors, this melting line becomes the irreversibility line B_{irr} (T), above which the absence of dissipation is lost. For LTS, B_{irr} (T) lies practically at B_{c2} (T). In conclusion, B_{irr} (T) is strongly linked to the defect structure of the material, and it becomes the upper practical limit where the superconductor may preserve its potential as a conductor. Additionally, it is straightforward to note that B_{irr} (T) is deeply correlated with the anisotropic character of the HTS material, because the vortex line energy decreases when the electronic anisotropy of the material is enhanced. If we examine the different typical B_{irr} (T) lines for the practical HTS and LTS materials we can immediately notice that while T_c is a key parameter [5], it is even more relevant that B_{irr} (T) is high enough to expand the B–T range of operation of the superconductor (see Fig. 2) [3, 4, 6].

Theoretical analyses of the vortex lattice determine that B_{irr} (T) (and B_m (T)) is inversely proportional to γ^2, the mass anisotropy of the superconductor, and so the useful range of the superconductors is strongly determined by this parameter which is indicated in Table 2 for the different classes of SC materials, together with other intrinsic or extrinsic useful parameters [3]. As it can be seen in Fig. 2, the combination of a high T_c and a low γ leads to extended regions of the B-T phase diagram where the superconductors may operate. Particularly, REBCO HTS are the materials with the largest cover of the B-T phase diagram (the only one at 77 K), at intermediate temperatures ($\sim$ 20 K) in addition, MgB_2 and IBS superconductors may also properly operate while at lower temperatures (4.2 K) all the superconductors mentioned in Table 1 display attractive performances up to different magnetic fields [5].

The third parameter relevant for applications is the critical current density $J_c(B, T)$, i.e. the maximum current density that a superconductor may support before vortex dissipation starts [4]. This parameter is strongly dependent on B and T and so three axes determine the region where dissipation-less superconductivity is confined (Fig. 3).

Table 2 Typical values of the electronic anisotropy and best values of other intrinsic and extrinsic parameters of most of the SC materials used for practical applications. All the anisotropic parameters are referred to the orientation with the smallest values. REBCO = $REBa_2Cu_3O_7$; Bi2223 = $Bi_2Sr_2Ca_2Cu_3O_9$; Bi2212 = $Bi_2Sr_2CaCu_2O_8$; Sm-1111 = $SmFeAsO_{1-x}H_x$, IBS = iron based superconductors

Material	REBCO	Bi2223	Bi2212	MgB_2	Sm-1111 (IBS)	Nb_3Sn	NbTi
Max T_c (K)	88–95	108	90	40	55	18	9.8
γ	5–7	150	30	2–2.7	1.2–4.5	1	1
$B_{c2}(0)$	> 100	> 100	100	~40	50–100	30	15
$B_{irr}(4.2/77)$ (T)	> 70/ < 13	> 25/ < 1	> 60/0	~25/0	> 50/0	~30/0	~ 15/0
$\xi(0)$ (nm)	1.6	1.5	1	6.5	1.2–2.4	2.7	4
$\lambda(0)$ (nm)	120	240	1	150	1	150	160
J_c (4.2/77 K) (MA/cm^2)	150/10	1	1	1/0	20/0	1/0	1/0

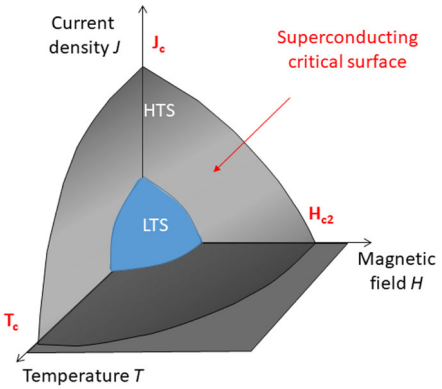

Fig. 3 Typical regions of magnetic field—temperature–current density where type II superconductors occur. The superconducting region of high-temperature superconductors (HTS) is strongly expanded as compared to low-temperature superconductors (LTS)

In practice, when one intends to manufacture SC wires or tapes, there are two types of materials: those which require to be textured (uniaxially or biaxially) and those which can remain polycrystalline. The main reason for this distinction is that grain boundaries in polycrystalline materials may behave as weak links, i.e. defects which limit the current density when the coherence length, $\xi(T)$, is small enough [2, 3]. This is not the case for LTS and MgB_2, while it is very detrimental for HTS materials, although less stringent for the iron-based superconductors (IBS) [7–9]. The exponential dependence of $J_c(\Theta)$ with Θ, i.e. the decrease of the critical current density across two grains with a misorientation angle Θ, determines if a single-axis texture is enough or if a biaxial texture is required [3].

The practical LTS conductors (NbTi and Nb_3Sn) are manufactured following a well-standardized procedure which enables the fabrication of multifilamentary wires. In the case of NbTi superconductors, the alloy is melted, formed into rods, and drawn into fine filaments, which are embedded in a copper matrix for stability. For Nb_3Sn, separate Nb and Sn components are combined via a diffusion process, where the Nb filaments react with Sn at high temperatures to form the Nb_3Sn compound which requires a wind and react process. In the last case, recent studies have demonstrated how the pinning force can be increased by the addition of Hf, Zr or Ta during the diffusion process [10, 11]. To manufacture MgB_2 wires, magnesium and boron powders are packed into metallic tubes (copper, iron or niquel), which are then drawn into fine wires, using a powder-in-tube (PIT) process. The wire is heat-treated to react the magnesium with boron, forming the MgB_2 SC phase and they are considered good candidates to become commercial conductors for MRI [12, 13]. It has also been demonstrated that high-quality SC joints can be prepared valid for MRI [13, 14].

In the case of HTS conductors, there are essentially two processing methodologies based on texturing HTS materials. The first one, used for Bi2212, Bi2223, and the IBS is the powder-in-tube (PIT), where polycrystalline precursors fill a metallic tube (usually Ag) being subjected then to a thermomechanical process inducing a uniaxial orientation of the grains. The supercurrents flow as described by the so-called "brick-wall" and "railswitch" models, i.e. the supercurrents flow along strong links even if only uniaxial texture is induced [2, 7]. For the case of REBCO, the critical angle Θ_c where $J_c(\Theta)$ starts to decrease is very small ($\Theta_c \sim 4°$) and so a biaxial growth is required, leading to the architecture called coated conductors (CC) [15, 16]. The CCs

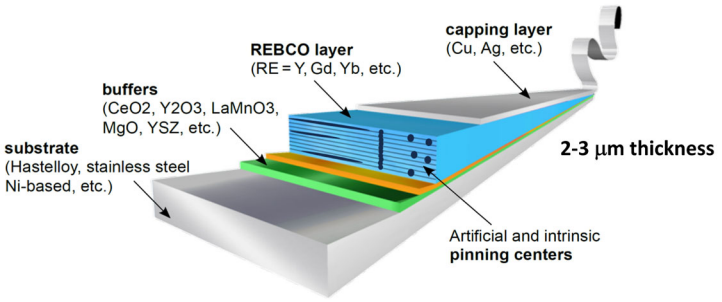

Fig. 4 Typical coated conductor architecture

consist of a metallic substrate with a selected set of buffer layers which protect the substrate from oxidation during the growth of the REBCO layers and, at the same time, protect the REBCO phase from substrate elements contaminations and finally confer the biaxial texture to the REBCO layer during growth (Fig. 4). Several approaches are being used nowadays to generate the biaxial texture. The most accepted one at present is ion beam assisted deposition (IBAD) which allows to achieve biaxially textured oxide buffer layers on top of polycrystalline substrates (Hastelloy, Stainless Steel). The most widely expanded IBAD layer is MgO while YSZ was also used in the past. Another successful approach is inclined substrate deposition (ISD) where MgO layers keep a single inclined orientation on top of a polycrystalline metallic substrate. Finally, the process rolling assisted biaxial texture (RABiT) where the biaxial texture is created on the metallic substrate (Ni, Cu) was also shown to be suitable for creating high-performance CCs, although the mechanical properties of the substrates limit their attractiveness for high magnetic field applications [15, 16].

The first boost in the development of CCs was associated with the demonstration that biaxial REBCO layers could be grown on top of these metallic substrates with very low intergrain misorientation and so $J_c(B, T)$ was not limited by grain boundary effects [2, 15, 16]. There exist several REBCO film growth methodologies which have become competitive to reach long length ($\sim$ 1 km) CCs at a thickness of the order of 1 μm or above. We can classify the processing methodologies based on three different principles: vapour-solid growth, solid-solid growth and liquid–solid growth [16, 17]. In the first group, the most outstanding techniques are pulsed laser deposition (PLD) and metalorganic chemical vapour deposition (MOCVD). In the second group, the main approach is the use of chemical solution deposition (CSD) using trifluoroacetate (TFA) precursors [18, 19]. Finally, in the third group we mainly find reactive coevaporation and direct reaction (RCE-DR) and transient liquid-assisted growth (TLAG) [17, 20, 21]. In these last cases, an intermediate liquid is formed at high temperature after the deposition of amorphous metal precursors for RCE-DR [22], and an inorganic nanometric crystalline phase is deposited by CSD for TLAG [23]. The main challenge in the manufacturing process of CCs at present is to decrease the figure of merit cost/performance (Eq. 1) which implies the use of techniques requiring low capital and running expenses and achieving high throughput manufacturing and high yield while they keep a high SC performance, mainly high $J_c(B, T)$ values. Significant progress has been demonstrated in all the growth approaches but a very significant

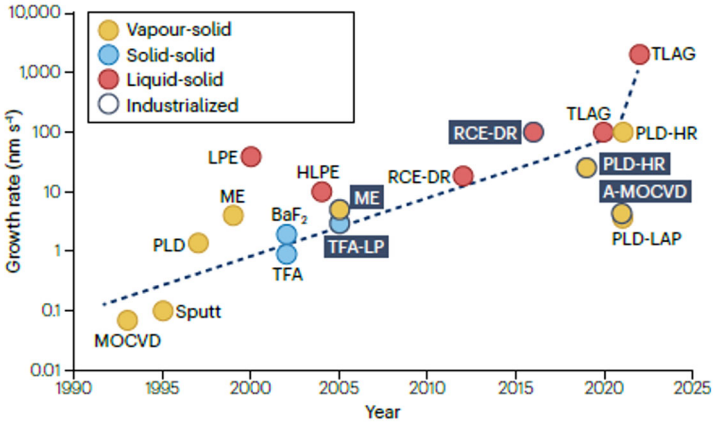

Fig. 5 The industrialized methods are highlighted in dark-blue. The dashed line indicates a steady annual increase of the growth rate up of 3 nm s-1 until year 2020, when an abrupt increase with TLAG was observed up to 2000nms^{-1}. *A-MOCVD* advanced metal organic chemical vapour deposition, *HLPE* hybrid LPE, *LPE* liquid phase epitaxy, *MBE* molecular beam epitaxy, *ME* metal evaporation, *MOCVD* metalorganic chemical vapour deposition, *PLD* pulsed laser deposition, *PLD-HR* high-rate PLD, *PLD-LAP* liquid-assisted processing PLD, *RCE-DR* reactive coevaporation and direct reaction, *Sputt* sputtering, *TFA* trifluoroacetate, *TFA-LP* low-pressure, *TFA* transient liquid assisted growth, TLAG—Figure from [17]

parameter is the enhancement of the REBCO growth rate to be able to maximize the yearly production of CC and so reduce the figure of merit (Fig. 5) [17, 22].

$$\frac{\text{Cost}}{\text{Performance}} = \frac{\text{total cost per year}}{G \cdot L \cdot W \cdot \left(\frac{I_{c-w}}{d}\right)} = \frac{€}{\text{kA} \cdot \text{m}} \tag{1}$$

where G is the growth rate, L is the CC length, W is the CC width, d is the REBCO film thickness and $I_{\text{c-w}}$ is the total critical current density.

The second boost in the performance of CCs was associated with the novel developments in the growth of biaxially textured REBCO nanocomposite cuprates. As it was previously mentioned, a key challenge of HTS materials is to be able to pin vortices in non-SC defects to refrain them from moving under the effect of Lorentz force under high magnetic fields. Pristine REBCO films always contain a certain amount of defects which already help to enhance $J_{\text{c}}(B, T)$, however, artificial pinning centers (APC) are required to further enhance the HTS efficiency at high magnetic fields. The main approach to generate nanocomposite films is to introduce non-SC nanometric phases embedded in the REBCO layer [4, 16, 17]. There are essentially two methods to achieve this goal: the simultaneous growth of two phases, for instance REBCO and $BaMO_3$ (M = Zr, Hf), or to implement a sequential process where both crystalline phases, REBCO and the secondary phase, are formed separately at different times [17]. The final nanostructure differs in both cases and so their performance also needs to be optimized following different approaches. In the first case, we find essentially PLD and MOCVD while in the second group we find CSD, TLAG and RCE-DR. The typical nanostructure generated in the first case is self-assembly of the $BaMO_3$ epitaxial phase to form nanorods along the c-axis allowing the decrease of the interfacial elastic

energy, although randomly distributed nanoparticles of RE_2O_3 can also be a useful approach depending on the region of the magnetic phase diagram where the CC needs to have high performance [4, 16, 20]. In the second case, instead, nanoparticles are used which then are randomly distributed during the REBCO film growth [17, 18, 24, 25]. The nanoparticles can be either preformed and then dispersed in the metalorganic solution to achieve a colloidal ink or can be nucleated in the same growth process at lower temperatures than the REBCO film. In this case the nanoparticles may remain randomly oriented or partially oriented and they also enhance the defect generation in the REBCO matrix (nanostrain, stacking faults) thus enhancing the high field critical currents as well. The influence on the $J_c(\Theta)$ anisotropy differs in both types of APCs again depending on the anisotropic character of the defects.

Nowadays, REBCO CCs are commercially produced in km lengths and the annual production rates are already beyond 5000 km/year with annual growth of manufacturing rates in the range of 50% which overall pushes a continuous decrease of the figure of merit which is expected to reach that of Nb_3Sn in the next 1–2 years [26]. The main advantage of REBCO CCs is their suitability for uses requiring either high magnetic fields or high temperatures. Of course, the conductors having not as high intrinsic performances (Bi2212, MgB_2, LTS) have several advantages, such as low cost and wire geometry instead of the flat geometry of CCs. In particular, LTS also benefits from a consolidated knowledge of fabrication, engineering manipulation and device design and testing that positions them especially in the already settled applications where cryogenic liquids are accepted (medicine, science industry). So, they are expected to continue meeting the practical requirements, especially for those applications [27–29]. However, we anticipate that improvements in application use at even higher magnetic fields, higher sustainability values, and an increase in demand will be progressively uptaken by HTS CC.

Concerning the future expectations related to performance improvement of CCs, we should mention that recent works have demonstrated that modified electronic structures may further enhance SC performances. Most of the CCs manufactured up to now were oxygenated to achieve the optimal T_c, however, the analysis of the critical currents of REBCO films and CCs in the overdoped state, i.e. with an excess of charge carrier concentration, has shown that the pinning energy is higher in this state and so the APCs should also become more effective in the overdoped state [20, 24, 30, 31]. Therefore, this area of research is now getting very active due to the expected increased margin of J_c(T,B) of CCs and further decrease of the figure of merit (Eq. 1) by just modifying the oxygenation post-treatment. The powerfulness of cuprates to reach an overdoped state to increase performance has also been demonstrated by Bi2212, which also poses the advantage of being isotropic when shaped as a multifilamentary wire, though it has the disadvantages of having a react and wind fabrication. When practical power applications of superconductors are considered, the real defining parameter is the so-called engineering current density $I_e(B, T)$ which considers the current circulating in a wire or tape taking into account the whole wire/tape cross section (substrates, stabilizing metal, metal sheath). In the case of LTS and the PIT HTS wires the volume of the stabilizing metal may reach up to 40–70% which in the case of Bi2212 and Bi2223 strongly increases the cost taking into account that the stabilizing metal is Ag [5]. In the case of REBCO CCs, the main parameter determining $I_e(B, T)$ is

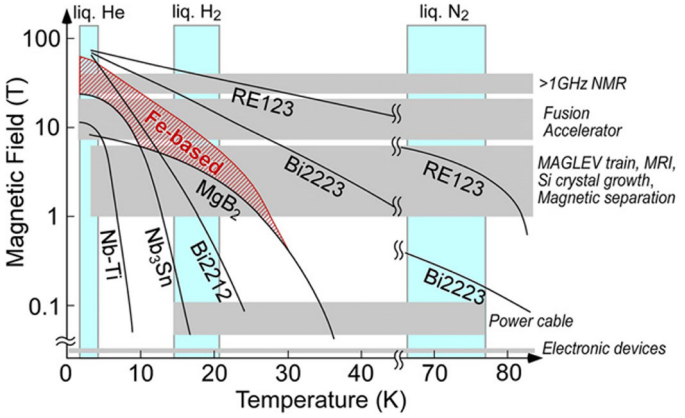

Fig. 6 Maximum conditions of B–T where the different materials can be used for specific applications. The criterion was to have $J_e > 10^4$ A cm^{-2}. Figure from[8]

the metallic substrate thickness and the copper stabilizer, as well as the maximum thickness of the REBCO layer. At present, Hastelloy substrates in the range of 30–50 μm can be used to manufacture CCs, and REBCO thicknesses up to 3–4 μm may be grown with high performances, which overall strongly enhance the $I_e(B, T)$ to be considered in the design of cables, motors or magnets. At present, commercial tapes are usually of ∼2 μm SC film on 50 μm thick substrates.

The values are typically achieved at present at 4.2 K and self-field with the existing SC wires and tapes are the following: ∼ 500 A/mm^2 for Bi2223 tapes, ∼ 1500 A/mm^2 for Bi2212 wires, ∼ 5000 A/mm^2 for YBCO CCs (50 μm substrate), ∼ 300 A/mm^2 for MgB_2 wires and ∼ 200 A/mm^2 for IBS wires. The summary of the potential applications where the different SC materials may be useful based on having a minimum performance of $J_e \sim 100$ A/mm^2 is summarized in Fig. 6. It is clear that while REBCO CCs are the unique material useful at high temperatures, it is still the best at liquid H_2 and high magnetic fields but other conductors are also useful at lower fields (MgB_2, IBS). At 4.2 K, in addition to the well-known LTS and those useful at 20 K, also the Bi2212 wires may become competitive at very high magnetic fields.

There are, however, other performance parameters which need to be considered when the selection of SC material needs to be done. These are the mechanical, thermal and electromagnetic properties under the corresponding working conditions [19, 27, 28, 32]. Also, as it is well-known, superconductors have zero dissipation under direct currents (DC) but they display losses under alternating current (AC) magnetic fields, for that reason the conductors need to be thermally stabilized with high thermal conductivity metals and the superconductor itself must be prepared in small transverse dimensions, typically as filaments surrounded by a Cu or Ag matrix. The preferred geometry for wires is, therefore, a multifilamentary structure. In the case of REBCO CCs, silver and Cu coatings are used to stabilize and protect the SC layer. Unfortunately, however, HTS materials display a relatively low normal zone propagation velocity (NZPV) under the working conditions and so they are prone to being destroyed in case of a quench event. For that reason, several modifications of the CC architecture have been investigated to enhance the NZPV and so transform them into a more

resilient behaviour without stringent modifications to the manufacturing procedures. For instance, the idea of implementing CCs with a current flow diverter (CFD) profile has been successful in enhancing the NZPV by a factor of 5–10 which is already high enough for most magnet or fault current applications (see Sect. 4.1.3) [33, 34]. The main idea is to increase the interfacial resistance of the REBCO layer with the top metallic layer which then diverts the current during the quench event and this results in a fast propagation of the normal zone further protecting the conductor.

Another parameter which needs to be quantified in any practical conductor is the tolerance to stress under the temperature and magnetic field conditions required for any specific application [32]. One of the most relevant parameters is the irreversible strain limit, which indicates the strain at which the SC properties degrade irreversibly, defining therefore the mechanical flexibility for device designs. For the different wires/tapes for each material, this can vary considerably. We can therefore indicate this limit to be in the range of 1% in NbTi wires [35], while this decreases considerably in Nb_3Sn wires, down to 0.2–0.4% [36, 37] due to the brittleness of the Nb3Sn phase. For MgB_2 wires, it is in the range of 0.5–0.7% [38], though this depends on the metallic sheathing. In general, for IBS wires, the irreversible strain limit is in the range 0.2–0.4% [39], varying depending on the specific compound. For Bi2223 and Bi2212 PIT wires, it is in the 0.2–0.4% [40–42]. Finally, for the REBCO CC, it is generally around 0.4–0.5% strain [43]

The other relevant mechanical parameter is the irreversible stress limit, indicating the stress beyond which permanent damage to SC properties occurs. This varies based on the fabrication technique and wire configuration, but indicates the irreversible damage in the material. For NbTi wire, the tensile stress irreversible limit is 600–800 MPa [35], for Nb_3Sn is in 150 to 200 MPa [36, 37] since it is relatively ductile. MgB_2 wire is a bit more brittle, being in the range of 150–200 MPa [38]. IBS wires are around 150 MPa, but this varies with the specific compound and fabrication process. IBS wires are less brittle than Nb_3Sn, but still have limited tolerance. In the case of Bi2223, a laminated reinforcement using a pre-tensioned metal strip contracting the Bi2223 filaments axially shifted the irreversible strain limit from 200 MPa up to 400 MPa [40, 41]. For Bi2212 PIT wire, also increased up to 200 MPa by reinforcement [42]. Finally, REBCO CC Tape has a higher stress tolerance, >500 MPa [43], since it is grown usually on a stainless steel substrate.

In the case of REBCO CCs, several conductor assemblies have been proposed to overcome the thermo-mechanical and AC losses limitations, as well as the anisotropic behaviour of the REBCO tapes. For instance, van der Laan et al. have implemented the so-called conductor on round core (CORC®) cables where REBCO CCs are wrapped around a hollow metallic tube where coolants can flow, either liquid N_2 or H_2 gas at high pressure [44]. The main advantage of these cables is that they display an isotropic behaviour under magnetic fields and the AC losses are minimized. The achieved $I_e(B, T)$ values are also very competitive (16 kA under 20 T at 4.2 K) owing to the fact that multiturns of REBCO may be applied on hollow tubes of small diameter ($\sim$ 2–3 mm). These cables are now fully considered excellent candidates to implement power systems in electrical planes, for instance. For magnet applications requiring higher currents, a cable including several CCs under perpendicular stacking or twisted stackings has been proposed: the vacuum pressure impregnated, insulated,

partially transposed, extruded, and roll-formed (VIPER) and twisted-stacked conductor [6, 27, 28]. This conductor architecture has been demonstrated to display a robust mechanical behaviour even under very demanding conditions of $B > 15$ T and high current (> 25 kA) applications. They also display reasonable stability against quench events while joints can be easily performed. VIPER cables are being used to build up magnets for compact fusion at present (see Sect. 4.1.1). Finally, when a comparison of different materials for a specific application needs to be done, the ultimate factor is cost, a parameter which is continuously evolving, mainly for REBCO CCs [20, 26–28, 45]. Of course, cryogenics cost is also a key parameter at present and if cooling can be performed at 20 K instead of 4.2 K because REBCO CCs can be used with enough performance it is certainly worth comparing the system cost as a whole. This is the case, for instance, of HEP and fusion applications where using magnets cooled at 20 K and generating magnetic fields in the range of 20 T is now a very promising option [6, 26].

3 Superconducting magnets

Magnets are devices able to create a magnetic field in a region of interest. From the point of view of the source of the magnetic field, there are two types: those based on permanent magnets and those using coils, that is, electrical circuits to create the magnetic flux, so-called electromagnets. It is well-known that ferromagnetic materials are able to concentrate the magnetic flux. Soft iron (low carbon content) is the most common one, because of the high saturation field and moderate cost. The iron is saturated when it is not able to enhance anymore the field created by the electrical circuit and the transfer function between field and current becomes non-linear. There are some magnets not using iron (air-core), but most of them benefit from the magnetic properties of iron [46]. The iron is also able to shape the magnetic flux in the region of interest. From the point of view of the applications, there are magnets to create fields with constant amplitude in time (DC) or with variable amplitude (AC). Variable magnetic fields create induced power losses both in the electrical conductors and the magnetic materials. These losses can be reduced by narrowing the path for the flow of the induced currents: in the case of conductors by subdivision into thinner wires, and in the case of iron by using thin laminations. The maximum achievable magnetic field for permanent magnets and electromagnets based on conventional conductors (mainly copper) is about 2 T for continuous operation. This limit is determined by two features:

- The properties of the materials creating the magnetic field: on one hand, the maximum remanent field of the permanent magnets is about 1.4 T. In the case of electromagnets, the limit is given by the maximum achievable current density, which is about 4 A/mm^2 for air-cooled coils and 10 A/mm^2 for water-cooled coils.
- The saturation field of the ferromagnetic materials: above this field, the capacity to concentrate the flux lines diminishes. It is about 2.2 T for pure iron. It could

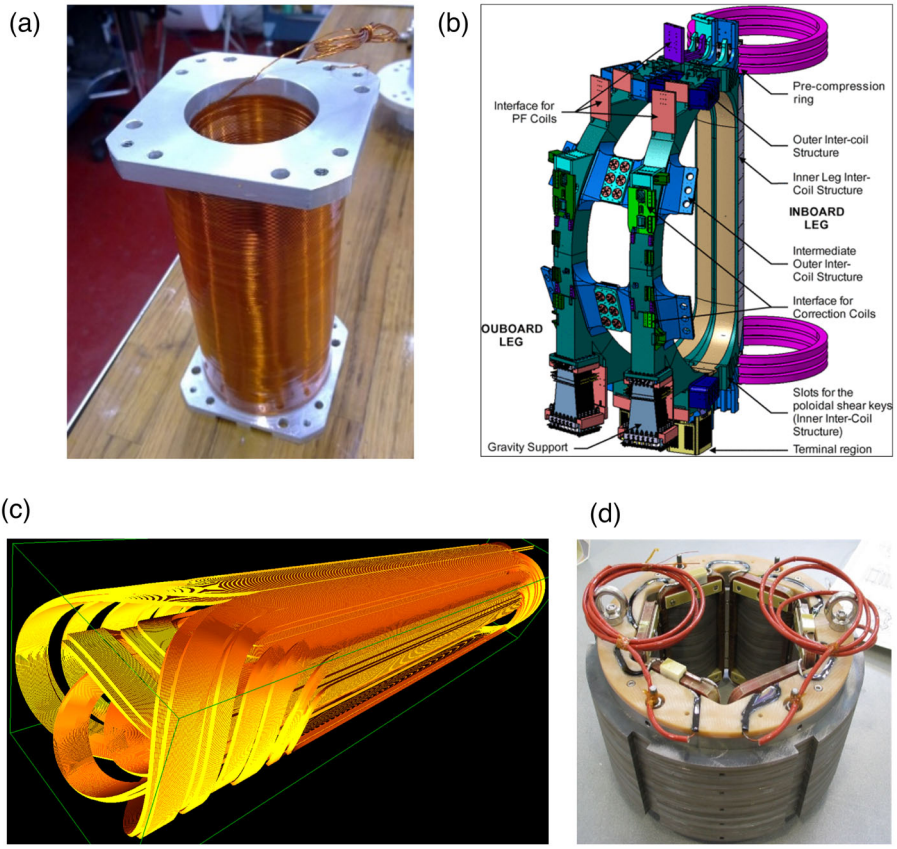

Fig. 7 (**a**) IFMIF solenoid [48]; (**b**) partial view of two coils of the ITER toroid [49]; (**c**) nested cos-theta dipole for HL-LHC [50]; (**d**) superferric sextupole [51]

reach values close to 4 T for some expensive metallic alloys based on rare earths [47].

One could think that the magnitude of the magnetic field created by a magnet could be increased progressively by adding more permanent magnets, coils or iron. This is not possible because of the intrinsic behaviour of the magnetic field. As stated by Biot–Savart's law, the amplitude of the magnetic field at a point decreases with the square of the distance to the field source. In consequence, the efficiency of far coils or permanent magnets decreases noticeably. In practice, conventional magnets can achieve a maximum field about 2 T in the region of interest. For higher fields, the cost of the magnet and the electricity is not affordable. The best alternative is to increase the current density in the coils, which is enabled by the use of superconductors, that can reach about 500 A/mm^2 as a typical value. This current density broadens the maximum field up to 20 T. At these high magnetic fields, the contribution from the iron yoke is modest, limited at around 2 T as aforementioned. Ampere's law provides a hint on how big a resistive magnet coil must be for this field, neglecting the contribution from the iron. Assuming a useful field region of 10 cm, a copper coil of 400,000 mm^2 would

be necessary, while only 3200 mm^2 would be enough for an SC coil. The comparison would be even more unfavourable considering the distance from the current to the region of interest (Biot–Savart's law). Implications in the dimensions and weight of the magnet and, especially in its power consumption, would be very limiting. A SC magnet fed with a constant current does not dissipate any power, but it does when the current varies [52, 53]. The power losses are associated with the hysteretic behaviour of the magnetization of the superconductor or with the coupling currents that appear for practical superconductors, which are multifilamentary embedded in a metallic matrix and, in many cases, later braided as cables.

A SC coil can take any shape, but there are some topologies that are commonly used and receive specific names (see Fig. 7):

- *Solenoid*: a helical coil with straight axis. It creates a uniform field in the aperture, parallel to the axis. For a very long or infinitely long solenoid powered with a current I, that field is $\mu_0 nI$, being n the number of turns per unit length. Practical applications are scientific experiments, particle detectors, accelerators, NMR and MRI, magnetic energy storage, transformers and others.
- *Toroid*: a helical coil with curved axis, typically a circumference. If the difference between the inner and outer radius is small compared with the average radius r, a uniform field is created in the aperture, parallel to the axis, with a negligible fringe field. For a toroid with N turns powered with current I, the field is $\mu_0 NI/2\pi r$, being r the mean radius. These magnets are usually arranged as a number of flat solenoids with their axes aligned along a circumference. Typical applications are Tokamaks, particle detectors and magnetic energy storage systems.
- *Dipole magnet*: two symmetric coils create a region of uniform field, typically a cylindrical or prismatic aperture where the field lines are perpendicular to the axis. In the case of a cylindrical aperture where the cables are placed following a cosine distribution around, the coils are so-called cos-theta. For a non-saturated iron-core dipole with a rectangular aperture of height h, the field is given by $2\mu_0 I/h$. Typical applications are accelerator magnets, magnetic separation and electrical machine windings.
- *Multipole magnet*: similar to the dipole magnet but higher order of periodicity, that is, quadrupole, sextupole, octupole and so on. Their main use is in particle accelerators [54].
- *Superferric magnet*: an iron-core SC magnet where the iron is not saturated. In this case, the field lines are shaped by the iron boundaries. Fields can not be high, but these magnets yield very good field quality, given by a precise iron geometry. They are used in particle accelerators and electrical machines.

The typical input data for the magnetic design of a magnet are the field amplitude and shape, the region of interest and the maximum external dimensions. In some cases, the maximum current is also fixed, given by the available power converters. There is not a type of SC magnet that is a universal solution. One of the main challenges arising from the SC magnet design is to find the optimal topology for a given need. One can notice that the coil topologies previously highlighted are quite symmetric. Therefore, analytical expressions based on basic equations (Ampere's law, Biot–Savart's law) can be used to choose the magnet topology and compute the main dimensions of coils

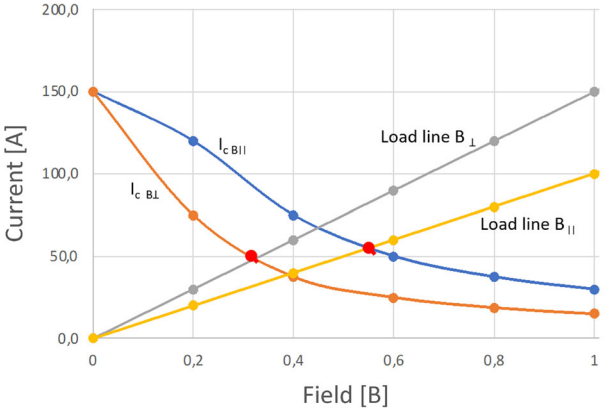

Fig. 8 Load line of an HTS solenoid. Due to the anisotropic properties of the superconducting tapes, the performance depends on the magnetic field direction: it is better when the field is parallel to the broad side of the tape, that is, in the central region of the solenoid. The safety margin of operation is the ratio between the operation current I_{op} and the short sample current I_{ss}

and iron (if present). The value of nominal current is linked to the choice of the cable. The expected peak field and the coil topology will determine the SC material to use:

- The current density that the superconductors can transport, as already stated in Sect. 2, depends on the magnetic field and the temperature, and also on the direction of the field lines in some cases (for instance the REBCO tapes, because of their anisotropy [55]). The load line of a SC magnet is defined by the peak field in the superconductor as a function of the current (see Fig. 8). When the superconductor is powered with a current that creates the critical field, that is, the short sample current, the magnet is powered at 100% on the load line. The difference between the operation point and the critical one provides the operation margin, that is, the capacity of the magnet to withstand instabilities (temperature, flux lines displacement, wire movements) without becoming resistive (phenomenon so-called quench).
- Only those superconductors that can be shaped into long wires with uniform properties can be used in the coils for the magnets. Some superconductors (for instance, NbTi) can be produced as flexible wires which can be braided as cables to be wound in a coil with any topology and transport large currents. Others, such as Nb_3Sn, can be produced flexible just as non-reacted cables to be wound in any shape, but then they should follow a heat treatment to become SC. Other superconductors used after the reaction have large minimum bending radius, such as MgB_2 [56] or REBCO tapes. There are many research lines open to solve this problem and to improve the current density, as explained in Sect. 2. For all of them, it should be evaluated if it is worth developing a given SC wire or cable, because the cost or the development time can be excessive, and the magnet design must use one existing wire or cable.

The detailed electromagnetic design is usually made with the help of numerical methods, mainly finite-element (FEM) or boundary-element (BEM) methods or codes

solving the Biot–Savart's law numerically. When the iron is saturated, which is very common in an SC magnet, the problem becomes non-linear and the use of numerical methods is mandatory. Present efforts are towards the integration of electromagnetic, mechanical and protection studies in the same software environment [57]. The target is to avoid the time-consuming transfer of the magnet model from one software to another, depending on the type of calculation to do. Besides the definition of the cable, the coil and the iron, the magnetic design will also yield the field map, the self-inductance, the stored magnetic energy and the electromagnetic forces, which will be used in the next stages of the design of a SC magnet.

The mechanical design of a SC magnet has two main objectives:

- To design a support structure to hold safely the large electromagnetic forces, both from the point of view of the SC coils and the parts of the support structure.
- To avoid cable movements that could spoil the magnetic field quality or trigger a quench.

The electromagnetic force density is proportional to the current density and field (Laplace equation), so it achieves large values in a SC magnet. In the same way, stresses are proportional to the magnetic field to the square. In fact, the magnetic field exerts a pressure equal to the magnetic field to the square over $2\mu_0$.

One should take into account the differential thermal contraction of the materials used for the support structure, since all the SC magnets are assembled at room temperature but operated at cryogenic temperatures. It is difficult to accurately know the material properties at low temperatures, mainly the non-metallic ones. In the case of SC coils, numerical simulations allow to compute the smeared-out properties of the complex mix of materials. Nevertheless, it is very common to prepare test samples to measure those properties. The most common solution to avoid cable movements is to preload the cable blocks during the assembly at room temperature in such a way that they are still in contact with the support structure after cooling down and energization. Besides, the mechanical design aims to avoid tensile stresses in the SC cables which could open cracks in the resin (if impregnated) and trigger a quench. High compressive stresses could also degrade the superconductor properties, and must be checked. For instance, in the case of Nb_3Sn cables, the maximum allowed pressure is in the order of 150 MPa at cold conditions. In the case of REBCO tapes, it must be checked that the stress distribution does not delaminate the superconductor from its substrate, phenomenon so-called peeling. The superconductor itself does not withstand large axial tensile stresses, but it is reinforced with high-strength materials included in the substrate, for instance Hastelloy [58].

A SC magnet usually stores a large magnetic energy, since it is proportional to the magnetic field to the square. When there is a quench, a given length of the wire becomes resistive. The generated heat spreads and the resistive zone grows. There is always a good electrical conductor (pure copper, silver) in parallel with the superconductor to transport the current when the superconductor becomes resistive because they feature large resistivities in normal state. Due to the large current densities, the power dissipation density is very high, and the current should be reduced as soon as possible to limit the peak temperature, which could damage the coils. The stored magnetic energy must be dissipated by warming up the coils or by the Joule effect in a resistor connected

in series. The dissipated power in the near electrically conductive parts is of second order. There are different methods to protect a magnet during the quench, with the objective of achieving safe maximum values of voltage and temperature. These are the most common:

- Dump resistor: it is connected in series with the magnet when it quenches. A fast switch is necessary, usually quite expensive because of the large transport currents. It must be carefully designed as the larger the dump resistor, the faster the current decays but also creating a higher voltage, which could be dangerous for the coil integrity. Its value is limited by the maximum allowable voltage at the magnet leads.
- Quench heaters: some resistors which are in good thermal contact with the SC coils. They are powered when a quench is detected. Since all the coil becomes immediately resistive, there are no hot spots. The main difficulty is the reliability, both because of the electrical insulation and the risk of failure of the electrical connections of the heaters.

The calculation of the quench propagation is cumbersome since the thermal problem is linked to the electrical circuit and the material properties change sharply with the temperature and magnetic field. Some basic computations can be made based on the heat balance equation assuming a given quench propagation velocity. More detailed calculations are usually made with numerical methods, mainly based on finite elements of finite difference methods. There are important differences in the quench propagation velocity between the different superconductors. HTS feature usually smoother transition to resistive than LTS ones. The detection of a quench is made by measuring the voltage drop across the coils. The standard criterion uses 0.1 μV/cm as the threshold to consider that the superconductor has transited into the resistive state. The relation between the developed electric field and the current density is exponential, being the exponent the so-called n-value. LTS features large n-values between 50–80, while HTS yield lower n-values, ranging 40–50 at liquid helium (LHe) temperature but decreasing to 20–30 at LN2 temperature [59]. It means that the current is shared between the HTS and the stabilizer, leading to moderate power density and, in consequence, slow quench propagation velocity. In some HTS coils, when the voltage drop is large enough to be detected, it is too late to keep the peak temperature at safe values, and the coil is damaged.

The last topic about SC magnet design to be covered here is its thermal design. There are different ways to cool down the SC magnets. There are two main methods:

- Conduction cooling: the magnet is in good thermal contact with a cold source, usually a cryocooler or a cryogenic line. No cryogens are necessary. Available cooling power is usually moderate, so the magnet should be very well thermally insulated. The temperature gradient can be large in case of applications with local heat sources, for instance due to AC losses.
- Cryogens: the magnet is immersed in a cryogenic bath. The cryogen can be operated in a close loop, by means of a liquefier or a re-condenser with a cryocooler; or open loop, when the cryogen boils-off without recirculation. There is a variety of techniques, using different cryogens and pressures, depending on the operating temperature. Several working temperatures can be highlighted:

- 1.9 K using superfluid helium at low pressure, taking advantage of the good thermal conductivity and specific heat of the superfluid helium, but at a high cost.
- 4.2 K using LHe at atmospheric pressure, very simple to operate, but it is still quite expensive.
- 77 K using liquid nitrogen (LN2) at atmospheric pressure, economic, but the critical current density of the superconductors is low at this temperature.
- Helium gas flows at intermediate temperatures (20–50 K), usually at high pressure to enhance the heat exchange, or other gases such as hydrogen or neon [60]. The cooling gas can be in direct contact with the coils or cool a heat exchanger.

The cooling system should have enough power to compensate the steady thermal losses and the AC losses. The former depends on the thermal insulation of the cryostat enclosing the magnet. Radiation losses are very important at cryogenic temperatures, and are usually reduced using several nested thermal shields working at intermediate temperatures. Conduction losses are diminished by using poor thermal conductors, such as stainless steel or glass fibre composites (Fig. 9).

The latter depends on the rate of variation of the magnetic fields. There are three types of AC losses in a SC cable: magnetization, which can be reduced by using thin SC filaments; AC losses in the metallic matrix where the SC filaments are embedded, that can be reduced using a worse conductor, but has an impact on the quench propagation velocity; and AC losses in the electrically conductive parts of the magnet, than can be reduced by using the right materials or laminating them. On the one hand, HTS operating temperature is usually higher than LTS, so it would be easier to extract the power losses due to induced currents. On the other hand, presently LTS superconductors are produced with smaller filaments, so their AC losses are intrinsically smaller. There are ongoing efforts to reduce AC losses in HTS, for instance some REBCO tapes are coated following complicated patterns [63].

The fabrication and assembly techniques for SC magnets depend on the specific topology and the requested geometry accuracy. It is in the order of hundredths of millimetre for a SC magnet for a particle collider, but in the order of some tenths or even a millimetre for energy or transport applications. First step of fabrication is the winding (see Fig. 10). SC coils can be wound with a wire, a tape or a cable, which can be made by braiding wires or stacking tapes. In some cases, there are spacers inserted in between groups of cables to achieve the requested field quality. Some clamping tooling can be necessary to keep the cables in the right position. The SC coils are usually impregnated with resins to provide mechanical stability and hold the large aforementioned stresses. Those resins should be compatible with the operating temperatures. In some cases, the resin is applied by brush during the winding (wet impregnation), in other cases, it is injected in a vacuum-tight mould (vacuum impregnation). A magnet is usually composed of several coils connected in series. It is very difficult to produce an SC splice, so usually, they are resistive, but with very low resistance. The splices are usually reinforced with copper to provide good thermal stabilization and avoid premature quenches because of thermal instability. One common technique to save splices is to wind double pancake coils (see Fig. 11),

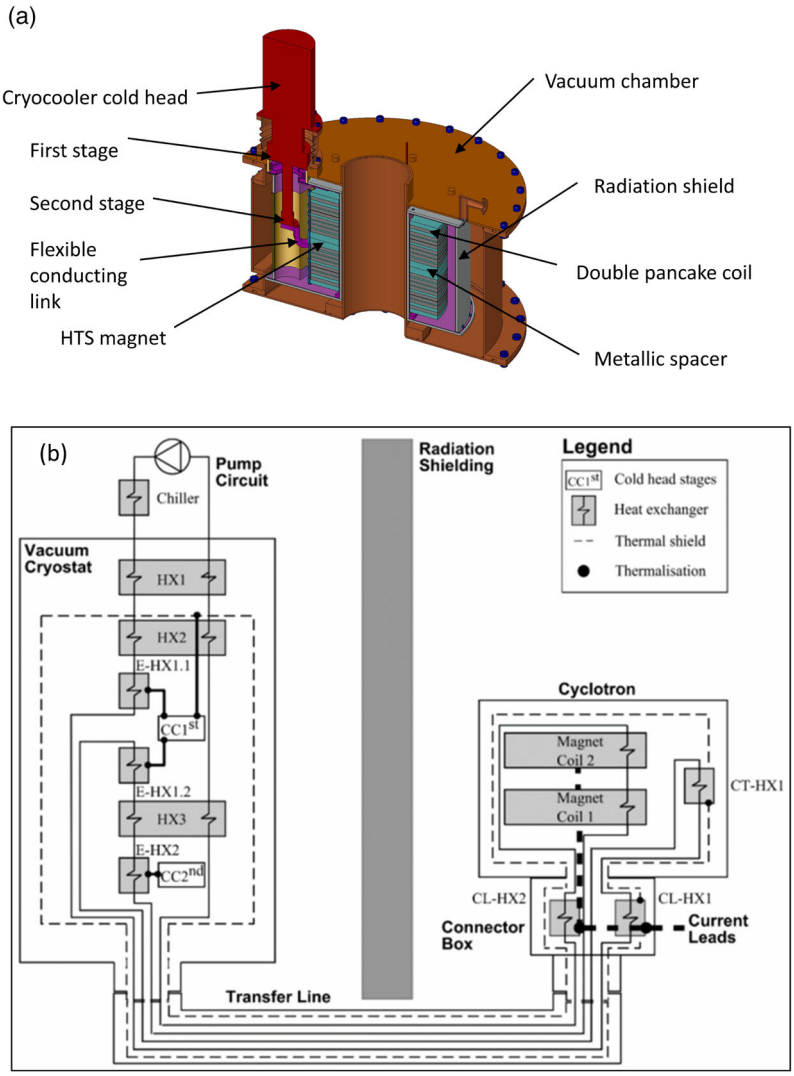

Fig. 9 (**a**) HTS magnet made of double pancake coils cooled by conduction from the second stage of a cryocooler. The thermal shield is cooled down by the first stage [61] and (**b**) cryogen circulation cooling of the AMIT SC cyclotron [62] using LHe which is cooled down using a cryocooler and heat hexchangers

where two layers of cables or tapes are wound with a single unit length by means of a layer jump at the inner diameter. Moreover, in this topology, both leads are located in the outer diameter, which gives an additional advantage for easier assembly while the splices are outside the bore and the high field region. For HTS tapes, two remarks are convenient. Firstly, long lengths are challenging to produce, since a local zone with poor properties would spoil the whole length. HTS coils can be wound with no insulation between the tapes, since the metallic substrate will not take any current as

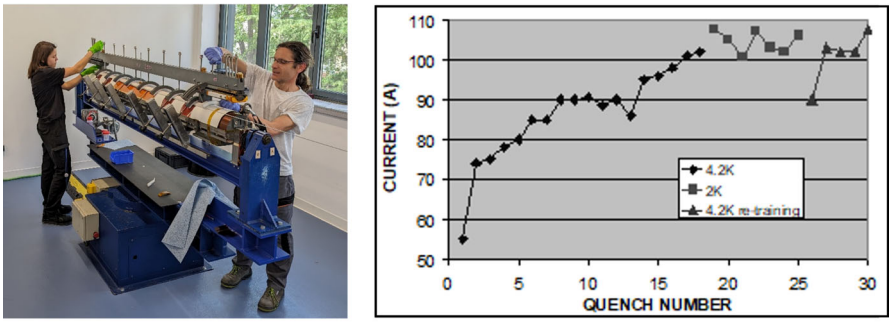

Fig. 10 (**a**) Winding of a cos-theta coil [50], (**b**) training test of TESLA500 combined superconducting magnet: when a quench happens at a lower current than the previous one is called de-training, usually due to a mechanical limitation. The quench current increases when the working temperature decreases: it shows that there is no mechanical limitation at that moment. A training test after a thermal cycle is called re-training [64]

it is running in parallel with the superconductor, or partially insulated. This layout would ease the magnet protection: in case of a quench, the current can be transferred to the neighbour tapes, and the heat transfer is much more efficient in decreasing the hot spot temperature. Quality assurance is based on different types of measurements: dimensions, electrical parameters and magnetic field quality.

The testing of SC magnets is usually done in test stations. The objective is to validate the magnet performance before integration into the final cryostat, which can be difficult to disassemble in case of need. When an SC magnet is powered for the first time, the first quench usually happens below the nominal current. However, the current at which the magnet quenches increases time after time. This process is known as training, because the magnet is following a learning curve. The reason for this behaviour is that these premature quenches are triggered by cracks in the resin or cable movements that do not happen in the next powering ramp, because the support structure and the magnet parts are mechanically more stable. In some cases, the magnet is not able to reach the nominal current. There can be different reasons, being the most common deficient mechanical design or fabrication, where the SC coils are not properly preloaded to avoid tensile stresses or sudden movements. During the training tests, the magnets are usually heavily instrumented: temperature sensors and voltage taps to identify the origin of the quench, where the voltage drop due to the resistive state starts to develop; strain gauges to measure the deformation of the support structure and coil parts; and magnetic test benches to characterize the field quality. In operation, the magnets are equipped with fewer sensors, keeping only the most important temperature sensors and voltage taps.

Table 3 Magnetic field and power applications of superconductivity

Fundamentals	Application form	Examples of interest	Why high fields are important
Laplace force ($F = B \cdot I$)	Electrical machines (magnets)	Energy generation. Ground, aerial and marine transportation	Increasing the force and power density > e.g. renewables, efficient ships, clean & light airplanes…
Magnetic pressure ($P = B^2/2 \cdot \mu_0$)	Electrical machines (magnets), magnetic bearings	energy generation & Ground transportation	Increasing the global force and power force density > e.g. Ultra-high-speed transport
Magnetic rigidity ($p = R = \frac{Bp}{q}$)	Magnets	Accelerators, gantries & fusion	Reducing the sizes of circular accelerators gantries and fusion coils > e.g. Ultra-high energy accelerators. Ultra-compact accelerators. Medical devices
Larmor frequency ($\omega = B \cdot \gamma$)	Magnets	NMR, MRI systems	Increasing the resolution of the system > ultra high field NMR, MRI systems
Magnetic energy density ($\epsilon = B^2/2 \cdot \mu_0$)	Magnets	Energy storage	Increasing the specific and global energy > e.g. *G* Joule range SMES for grid applications. Hybrid energy storage systems
Faraday's law ($V = -N\frac{d(B \cdot S)}{\mathrm{d}t}$)	Transformers (magnets), fault current limiters (FCL)	Energy transmission & distribution	Compact and environmentally friendly transformers. New FCL types > e.g. grid protection
B itself	Magnets	Science & industry magnetic separation, induction heating…	Affects all scientific phenomena involving high fields > semiconductors, biology…
I itself	Cables	Energy transmission & distribution	Increasing the current density > e.g. DC links. Urban networks

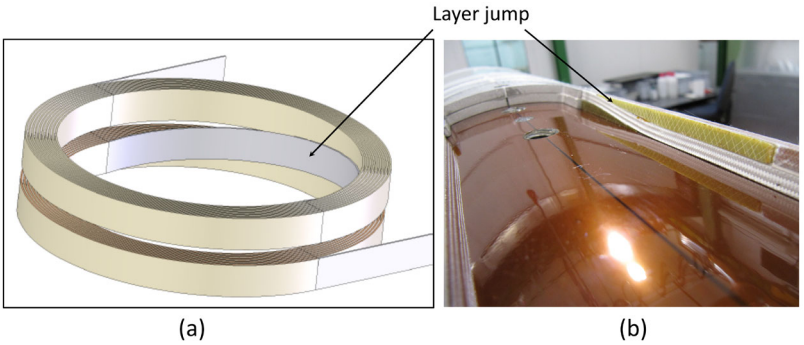

Fig. 11 (**a**) Schematic description of a double pancake coil with HTS tapes [61]. (**b**) Layer jump of double pancake cos-theta dipole of the MCBXF orbit corrector [50]

4 Power applications of superconductivity

Although there are some devices for which the use of superconductivity becomes mandatory and they would simply never work with conventional conductors, most of the applications using superconductors, exist in a normal conducting version; superconductivity simply converts them into superapplications with enhanced performances. Now, where is the advantage of using superconductors in power applications? In practically all the cases, the answer is increasing the magnetic field present in the corresponding fundamental equation on which the application is based [65] Table 3 shows these fundamental equations affected by the magnetic field, associated with the different groups of applications, how this field is achieved (the form of application) and why it is important that it becomes as high as possible.

As it can be seen, all applications except one (energy transmission), are based on the existence of a high magnetic field which is produced by magnets, either as its own magnets or as part of electric machines or transformers. This clearly shows the relevant role of SC magnets as one of the two technological pillars of applied superconductivity. Figure 12 presents a classification of these power applications of superconductivity sorted by generic groups of applications. This paper will address solely those applications related with energy, transport and industry (highlighted in the figure in colour) to remark the importance that these selected uses may be significant to achieve some of the goals universally established for sustainable development [66, 67] (obviously, the non-described uses in the paper, will also contribute to the achievement of those sustainability goals).

4.1 Energy applications of superconductivity

4.1.1 Applications to energy generation—Fusion

Fusion energy, one of the most promising generation alternatives for a sustainable world, is based on the combination of two light nuclei to form a new nucleus. This combination is performed inside a Fusion reactor in the form of plasma, ionized gas

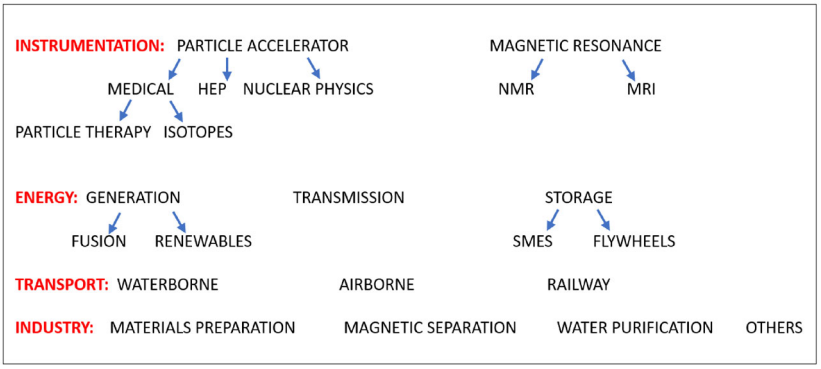

Fig. 12 A classification of power applications of superconductivity

at such high temperatures that ions can overcome repulsion forces and fuse together releasing energy. Fusion reactors require confining the plasma in "burning" conditions: that is, with enough particle density, temperature and confinement time (the triple product) for fusion reactions to occur at a rate that the plasma be mostly self-heated. Probably, the most mature solution for this requirement is magnetic confinement where specially shaped magnets generate a field that guarantees a stable isolation of the plasma. In turn, there are, basically, two consolidated types of solutions to achieve the magnetic plasma confinement: Tokamaks and Stellarators. Tokamak development has been going on for the last 60 years in different laboratories all over the world culminating in the present construction of ITER which is the world's largest Tokamak to be operated as the first fusion test reactor to burn deuterium-tritium plasmas [68]. Although Stellarators were invented before Tokamaks their development has followed closely behind Tokamak somehow limited by their higher complexity. Nevertheless, the successful operation of Wendelstein 7-X in Germany [69], among other projects, also keeps this option as a real alternative for a future Power Plant. In any case, both options present technological and scientific advantages and disadvantages and also both options benefit from the introduction of SC magnets, in general, and HTS SC magnets, in particular. In fact, the two leading realizations for each configuration (ITER for Tokamaks and Wendelstein 7-X for Stellarators) use SC LTS magnets. Tokamaks and Stellarators are based on the toroidal confinement of plasma and they represent two different options for the requisite of twisting the magnetic field lines that an array of magnets distributed in a toroidal configuration would create and which would not result in a stable plasma confinement [70, 71]. In a Tokamak the twisting is produced by a poloidal field generated by a plasma current while in a Stellarator it is produced by the external non-axisymmetric coils. In Tokamaks the plasma current is normally induced by a transformer, which makes the device prone to current-driven instabilities and more difficult to operate in a stable state, while stellarators are plasma current free and easier to operate in a stable state. Figure 13 represents the basic magnet configuration for both, Tokamaks and Stellarators.

Another important difference between both configurations is the geometrical parameters, particularly the aspect ratio referred to the ratio between the external and

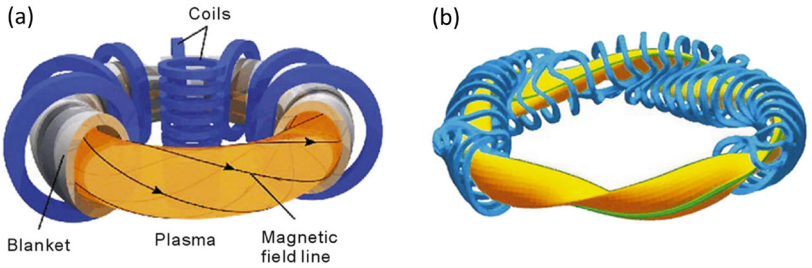

Fig. 13 Coil configuration and magnetic lines for a Tokamak (**a**) and a Stellarator (**b**)

the internal radius, which for Tokamaks is much smaller than for Stellarators, leading to much larger effective plasma volumes [72]. Finally, a last consideration with a high technical impact, is the fact that for Tokamaks the coils are planar (2D coils) while for Stellarators they are truly three-dimensional (3D coils) with an extremely complex geometry much more difficult to fabricate and assemble. Not only the shape and configuration of the magnetic field is important but also its magnitude may have a tremendous impact on the overall characteristics of the reactor. In this regard is worth mentioning that one of the figures of merit associated with the performance of a fusion device is the so-called fusion triple product $\eta T \tau_e$ (ion density, ion temperature and energy confinement time) which, in turn, is proportional to B^4 (Magnetic field density) and V (plasma volume). Typical values for the fusion product are $6.7 \cdot 10^{19}$ KeV sm^{-3} for Wendelstein 7-X, $4.7 \cdot 10^{20}$ KeV sm^{-3} for the JET Tokamak or $7.4 \cdot 10^{21}$ KeV sm^{-3} expected for ITER [73]. The dependence on the fourth power of the magnetic field density times the volume, indicates the relevance of achieving high fields to develop compact machines. Nevertheless, the compactness of the reactor will also be limited by other factors like those related to neutron production issues or plasma stability. The optimization strategy of maximizing the magnetic flux density to achieve net fusion energy in a more compact, lower cost and faster-to-build Tokamaks has been historically—known as the "high field path to fusion energy". Chronologically this path can be divided into different eras according to the involved magnet technology and the materials they were made from. A comprehensive description of this path can be found in [74]. In a summarized way, the first attempts to produce high-field magnets started by using advanced Bitter-type copper coils able to generate pulses up to 8 T in the plasma centre. Some examples included a Tokamak at Frascati (ENEA) and three at MIT which were the origin of many other realizations worldwide. The copper route was finally abandoned due to the difficulty of scaling resistive copper magnets to fusion power plants and also to the advent of reliable LTS magnets in the 80s and 90s. Again [74] supplies a list of different realizations based on LTS magnets which have provided the necessary background for affording the ITER project, a Tokamak based on Nb_3Sn and NbTi coils able to produce a plasma centre field of 5.3 T. To achieve sufficient plasma performance (fusion triple product) with such field values, it is required a big outer Tokamak radius leading to high capital costs, long construction times and, in general, severe limitations complex to manage. The history of Stellarators starts in 1951 when Lyman Spitzer developed its concept,

starting the construction of the first prototype [75], a tabletop machine named Model A in 1952 to show the confinement capability of the stellarator geometry. Then came several Model B machines which, in spite of the presented problems with the magnet supports, were able to demonstrate that the plasma could be heated to relatively high temperatures but extremely short confinement times. Research continued with the last series, Model C, where many improvements were made to increase confinement time and temperature but, still, they were far beyond what was needed for energy generation and the machine was converted into a Symmetric Tokamak. In fact, a renaissance of tokamaks occurred in the following years but instability problems due to the circulating current in the plasma and above all, different advances in magnet technology, remerged the Stellarator approach and three big projects were launched: The Helical Symmetric Experiment (HSX) in the US, Wendelstein 7X in Germany and the Large Helical Device in Japan, using these last two machines, SC magnets. The absence of confinement provided by the circulating currents in the plasma implies using more powerful magnets in the Stellarator-type reactors. On the positive side, Stellarators are inherently steady-state operating machines (constant field in time) and this has very significant implications when using SC magnets. The requirements of intense fields to achieve high values of the fusion triple product have practically discarded any magnet technology other than the SC one. As in many other applications, stationary high magnetic fields in wide volumes can only be achieved using SC magnets in spite of the complexity that their use represents. For the moment, several fusion reactors have been based on the use of Low Critical Temperature SC Magnets (LTS Magnets) either using Nb_3Sn or NbTi, depending on the magnetic field peak value at the conductor. For the case of Tokamaks, these realizations include EAST in China [76], K-STAR in South Korea [77], SST-1 in India [78], T7 and T15 in Russia [79], Tore Supra/WEST in France [80] and TRIAM-1M [81] and JT60SA [82] in Japan and obviously the international collaboration ITER [83]. For the group of Stellarators, two significant realizations have been made using NbTi technology: Wendelstein 7X [84] and the Large Helical Device (a type of Stellerator known as Heliotron) [85]. Although ITER is mainly based on LTS Technology, it is worth mentioning that it also represented the transition from the classical to the new SC technologies since it includes one component which uses HTS, the so-called current leads which are those elements connecting the external power supplies at room temperature with the internal magnets at cryogenic temperatures. Since the heat entrance to the magnets must be minimized, ideal connections made from materials with an infinite electric conductivity and simultaneously a null thermal conductivity should be used. The most similar materials to this ideal behaviour are HTS since they are ceramic and superconductors at the time. For the case of ITER, these current leads able to transport up to 69 kA (for the toroidal field coils) are made from Bi2223 tapes with a specially alloyed Ag matrix [86]. The need for compact reactors to increase the fusion triple product with reasonably affordable machines, along with the improvements in the performance of the HTS superconductors at an industrial scale, quickly triggered the idea of making both types of fusion reactors using HTS-based magnets.

The case of Tokamaks has been the most ambitious and, among all the initiatives, the project SPARC is the most emblematic where significant and promising results have been achieved [74]. This new “high field path to fusion energy approach based

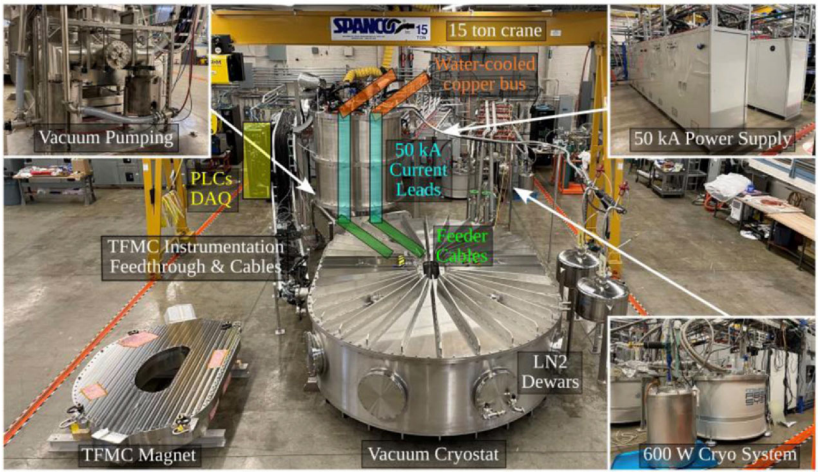

Fig. 14 Test station for the TFMC magnet (also shown) at the MIT PSFC

on HTS magnets" was started at MIT in the mid-2010s and proposes the use of 20T peak Toroidal Field Coils based on REBCO, a material with the notorious advantage of being available in industrial quantities by roughly a dozen of suppliers, with very good mechanical and electromagnetic performances, at affordable prizes. The programme started in 2018 and finished in 2021 and it was executed jointly by the MIT plasma science and fusion centre (PSFC) and Commonwealth Fusion Systems (CFS) as a technology enabler of the SC high-field pathway to fusion energy [87]. The goal of the program was to demonstrate the feasibility of non-insulated coils (NI Coils) to be used as the toroidal field coils in a Tokamak (SPARC) [88]. A toroidal field model coil (TFMC) was fully developed and tested. A peak field in the conductor of 20.1 T @ 20 K was achieved with 40.5 KA of external current in a coil with 256 turns wound in 16 single pancakes and storing 100 MJ of energy. The coil is placed in a liquid-free cryostat based on a helium recirculation system [89]. which is cooled down using cryocoolers which provide 600 W of cooling power @ 20 K [90]. Figure 14 shows the complete test station where the TFMC (which is also present in the figure is also shown) was tested. It includes the vacuum vessel, the power supply, the vacuum and the cryogenic systems.

Probably, the most relevant challenge to address in this project was how to take the leap from the small HTS demonstration magnets in the range of tenths of MA-turns to a coil in the range of tens of MA-turns. Using commercial tapes as supplied by their manufacturers, even if the biggest ones are chosen, is not an option for these big magnets since it will lead to an inadmissible number of turns and consequently an excessive inductance, incompatible with the required magnet time constant for fusion applications [74]. Higher currents and fewer turns are then required and this implies the fabrication of cables able to transport several thousands of amperes inside a high magnetic field values. In this situation, two types of cables were developed in the frame of the project: the so-called VIPER cable and the NINT (non insulated-non-twisted coils), the first based on twisted batches of HTS tapes placed along helical grooves

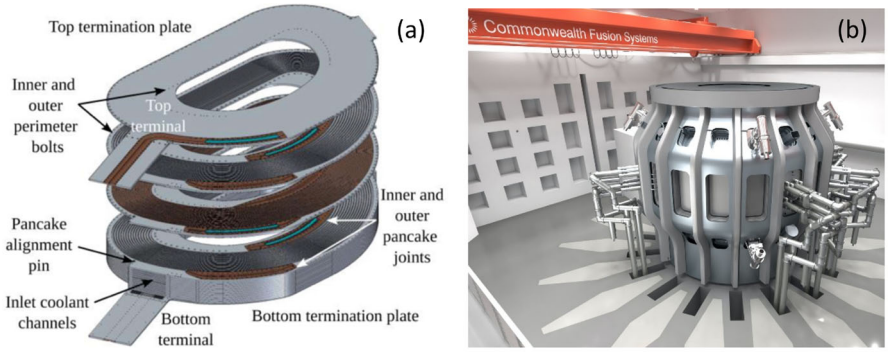

Fig. 15 (**a**) SPARC Coil configuration including an explosion of two and (**b**) artistic view of the SPARC tokamak under commercial operation

along a copper bar externally insulated and constituting the cables with which the magnet is wound from, and the second one formed by non-twisted batches of tapes which are placed in grooves machined in metallic plates with no electrical insulation to the plate. Each groove constitutes a turn of each pancake forming the coil. The first option is aimed at transient magnets where ramping cycles are frequent (this is the case for the central solenoid and the poloidal field coils) while the second option is reserved for magnets mainly stationary (like the toroidal field coils). This is the case for the TFMC and this was the selected option. Figure 15a shows the final configuration of the TFMC, including an explosion of two pancakes, the end plates and the cooling channels. Figure 15b shows an artistic view of what could be the complete SPARC commercial system in operation.

In the last years, several companies proposing HTS-based fusion Tokamaks have been launched, achieving a significant amount of public and, fundamentally, private investment. In 2023, the overall funding for Fusion Companies was slightly above $6.2 bn from which more than $5.9 bn came from private investment [91] . Apart from the significant case of CFS, which has already been mentioned (they have been able to raise more than $2bn to date), some other cases are Tokamak Energy [92] a company founded in 2009 as a spin-off from the UK Atomic Energy Authority (UKAEA). Their proposal is based on using a compact spherical tokamak with HTS magnets and they also have announced collaboration with General Atomics. Alternatively, to Tokamaks, Stellarators have also drawn the attention of companies (most of them new ones) which defend that this family of fusion reactors in the HTS version can derive in a really compact and stable machine with a great potential for on-grid electricity generation but also for other applications such as off-grid production, neutron sources, marine and space propulsion, etc. Although Wendelstein 7X demonstrated the global soundness of the concept of SC stellarators, it also showed the tremendous difficulties of fabricating and assembling SC 3D coils and here is where these new companies are contributing with original proposals. An example is Thea Energy [93], a spin-off of the Princeton Plasma Physics Laboratory which has proposed a new topology of SC Stellerator based on planar coils [94] exclusively as shown in Fig. 16a. Basically, there are two types of coils: The encircling ones which are optimized to generate the

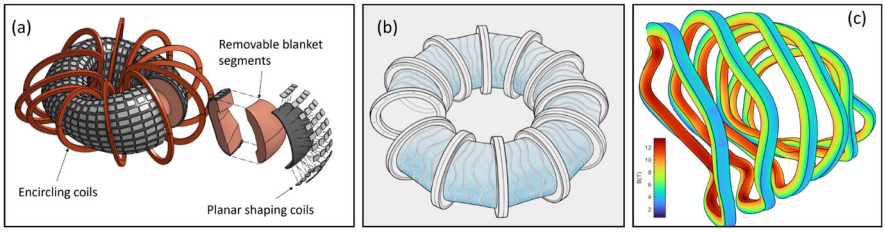

Fig. 16 Proposed configuration from Thea Energy with exclusively planar coils (**a**) and proposed solution by Renaissance Fusion based on depositing and patterning HTS material (**b**). (**c**) Magnetic field calculations of the WISER Stellerator at CIEMAT

majority of the target magnetic field and a number of small dipolar coils to generate the remainder of the target magnetic field. They are called the planar shaping coils. The second approach comes from Reinaissance Fusion [95] a company founded in 2019 and located in Grenoble (France). Their proposal for fabricating the complex form of the required coils, consists of directly depositing and patterning HTS material on a large surfaces like a torus sector to draw equivalent coils to those made from tapes or conductors. This company also claims that the method can be used for making SC magnets for MRI, accelerators, SMES or electrical machines (Fig. 16b).

Other companies developing HTS Stellarators are Proxima Fusion [96], a German Company based on Munich, in the process of developing a SC Quasi-Isodynamic Stellarator profiting of the achievements of Wendelstein 7X and Type One Energy [97], a US company who has announced the Project Infinity One based on a modular HTS magnet-based Stellarator. Figure 16c shows the magnetic field calculation for the superconducting coils of a Stellerator, in the framework of a Private-Public initiative for the construction and exploitation of WISER (WInd tunnel for a StEllarator Reactor) at CIEMAT, with the goal of promoting the development of critical technologies for the construction of a type of reactor with a high commercial potential.

4.1.2 Application to renewable generation

Renewable energies are the cornerstone of a sustainable future, offering clean and increasingly cost-effective alternatives to traditional fossil fuels while addressing the urgent need to reduce greenhouse gas emissions and combat climate change. Among all the renewable energy sources, wind and hydrokinetic energy generation are the two candidates that can potentially benefit from the use of superconductors. Those are the ones that relay their strategy in capturing and transforming kinetic energy from wind or water into electric power by using generators. In the case of water, in turn, the energy source takes different forms such as waterfalls, river flows, ocean waves, ocean currents and tides. Most of those generators are rotative with two sides: The stationary one, which constitutes the stator of the machine and the rotating one, constituting the rotor which turns around the stator. For some particular applications, the generators are linear with also a steady stator and a moving side which is now called translator and travels along the stator. In both cases, the relative movement of the rotor or translator with respect to the stator is converted into electricity. There are

many different configurations of electrical machines and in general terms, the moving part has either electromagnets or permanent magnets to generate the excitation field or, is a solid piece of only iron or iron and other highly conducting material that interacts with the field generated by the stator creating a torque or a force which can either be opposite to the velocity (generator) or in the same sense (motor). The stator side has windings (coils) which are normally circulated by AC currents which are in charge of generating the magnetization field when it is not created by the rotor/translator and also of the conversion of the mechanical energy into electric energy. For the case of wind energy, depending on their operating location, wind turbines can be classified into two main groups, namely, onshore and offshore. Onshore wind farms are generally easier and cheaper to install and maintain compared to offshore wind farms. Access to the sites is simpler, and the infrastructure required (such as roads and electrical connections) is often already in place or easier to develop. Nevertheless, even if onshore wind technology is well-developed, there are certain aspects in which offshore wind farms offer unbeatable advantages. Offshore wind farms benefit from higher and more consistent wind speeds compared to onshore sites, leading to greater energy production and efficiency, allowing for the deployment of much larger turbines, providing greater capacities. Apart from the capacity of single generators, offshore wind farms can be built in expansive ocean areas, offering the potential to install large amounts of turbines and generate renewable energy without competing for the space with other interests such as agriculture, urban development or even population comfort.

The world has seen a rapid growth of wind power [98] over the past two to three decades. The added global capacity of wind energy reached 1017 GW, of which only 7% (73 GW) comes from offshore wind farms [99]. By the decade of the 2030s, wind power generation capacity is expected to increase up to 2000 GW, which is more than 50% of the overall renewable energy generation capacity in 2023. In such a scenario, a larger share of offshore wind power generation is expected reaching 13% of the overall wind power generation [100, 101]. Hydropower on the other hand (hydrokinetic energy from waterfalls in dams, or river-flow and current oceans), is the technology with the largest share (50% in 2019, 40% in 2022) of global renewable electricity generation capacity. It is remarkable how the trend decreases as other renewable generation technologies such as wind or photovoltaics are growing. As of the end of 2022, the projects in the global development pipeline combined total capacity of 557 GW. By 2023, new projects added around 117 GW to the global fleet, representing a 9% increase in global capacity in one single year [102]. Marine power generation is the third hydropower renewable energy source worth mentioning, which by 2023 represented still less than 1% of the total hydropower capacity, leading to a high margin of growth scenario in which, as shown below, important developments are already being carried out. Water turbines are divided into two groups,i.e. reaction turbines and impulse turbines. Reaction turbines are used in very high-head applications (> 300 m). Reaction turbines are used in low-head (< 30 m), and medium-head (30–300 m) applications as well as run-in-river systems in which the turbine uses the natural flow of a river without the need for large reservoirs or significant water storage. In both wind and hydropower applications the energy is transferred through the turbine's main shaft to the generator. The generator transforms then the mechanical energy of the turbine

into electricity. Either for wind or water energy, there is a wide range of generator designs which can be split into two main types, i.e. direct and indirect drives. In the first one, the generator is directly connected to the power source, without intermediate components such as gearboxes, in such a way that the generator shaft rotates at the same speed as the power source. In the second type, the generator is connected to the power source through an intermediate mechanism, typically a gearbox, which adjusts the speed from the power source to an optimal speed for the generator. For example, in a wind turbine, the slow rotation of the blades is increased by the gearbox to a higher speed suitable for the generator. Direct drive (DD) generators are an attractive option for both, wind and hydropower generators. In the two cases, the use of DD generators is particularly well-suited for several reasons like the reduced maintenance requirements derived from the absence of a gearbox, which is one of the most failure-prone components in traditional turbines. This is especially true in the case of offshore wind turbines which are difficult and expensive to access, so reducing the number of components that require regular maintenance is a significant advantage. Moreover, offshore environments are harsh, with high humidity, salt spray, and strong winds [103]. The simpler sealed design of direct drive generators makes them more resistant to corrosion and other environmental factors that can affect traditional gearbox systems. Similarly, small-scale hydropower plants where the low maintenance requirements are crucial, can profit as well from the simplicity of DD generators. Since in a direct drive system the generator is directly connected to the rotor of a turbine, the speed at which the generator operates is directly determined by the speed of this power source. In the absence of a gearbox, which is typically used to increase the rotational speed of the generator, the rotational speed of the source is relatively low. This characteristic aligns well with the necessities of low-head hydropower plants and run-of-river systems where the kinetic energy of water is directly intercepted from a river's natural flow. The major drawback of DD generators shows up when scaling up the generator's power capacity. The electromagnetic power of an electrical machine is defined by the product of the mechanical rotational speed of the machine's rotor times its electromagnetic torque. Since they need to be designed to operate at lower speeds, the elctromagnetic torque must be sufficiently high to achieve the nominal output power. In this sense, two key figures of merit in electric machines are the torque and the power densities, defined as the ratio between the produced torque and the generated power, respectively, divided by the rotor volume (volumetric density). Modern wind and hydropower stations demand high specific power and, especially, high specific torque generators since they must be as light, small and efficient as possible to reduce their LCOE (levelized cost of energy) [104]. For the case of Hydropower applications where new machines are meant to replace old ones increasing their generated power but keeping their footprint, the issue of power and torque densities is especially relevant. The torque density (per unit rotor volume) is the magnetic shear stress which, in turn, is the product of the electric load (stator amperes per unit length distributed in the air-gap), times the magnetic load which is the magnetic flux density in the gap. The power density is the torque density times the rotating speed. To increase the power density of a generator, there are, then, three options: (a) increasing the speed using a gearbox, which is contradictory to what was previously said about system robustness and maintenance, (b) increasing the electric load, which means increasing the current density

in the AC side. (c) Increasing the magnetic load, which basically means providing the machine with powerful excitation-side magnets to work at the highest possible field density [105]. Once discarded option (a), alternative (b) means improving the cooling capacity at the stator side. Different refrigeration techniques are commonly used in traditional generators. Depending on the specific requirements of each system either air, liquid (typically water and oil) or gaseous hydrogen are the most common options. The maximum current densities that can be reached in such cases range between 3 and 50 A/mm^2 [106, 107]. By making use of superconductors such current densities can be dramatically increased up to two orders of magnitude. Finally, regarding option (c) traditional generators use either normal conducting copper electromagnets or permanent magnets with a high content of rare earth elements for generating the excitation field. To increase the field at the airgap, the strategy of upscaling permanent magnet or the normal conducting electromagnets finds a technical limit in the iron magnetic saturation (see Sect. 3), leading to a significant increase in mass and volume. Moreover, the permanent magnet option stresses the already challenging rare-earth supply chain to a greater extent [108]. As an example, the world's largest operating wind turbine is the Vestas V236. It is an offshore permanent magnet-based design. It operates in the direct drive configuration with a capacity of 15 MW [109]. There are other projects under development aiming to achieve up to 18 MW such as the Haliade-X [110], MySE 18.X-28X [111], and CSSC Haizhuang H260-18MW [112]. Such developments are as well based on permanent magnets pushing the performance of such technology to its limit reaching a saturation point in terms of affordable capacity. Under these circumstances, the only possible alternative to increase the generator's shear stress is by making use of superconductivity since this technology can positively affect options (b) and (c), once (a) is discarded.

Following these ideas, there are a number of motor/generators topologies implementing superconductors either in the form of wires/tapes or in the form of bulk conductors (alternatively stacked tapes) [113]. In the first case to build the electromagnets that constitute the stator and rotor windings and in the second one to perform three alternative missions: (a) acting as SC permanent magnets (trapped field magnets) to provide the excitation field, (b) acting as flux shields for reluctance and flux modulation machines or (c) using their flux pinning capability (see Sect. 2) for the case of hysteresis machines [114]. Historically, wind power generators have been one of the main drivers for applications of SC machines, together with aircraft and ship propulsion, each with its own personality. The main developments done so far in these sectors belong to the type of radial field SC topology [113, 115] whose structure is shown in Fig. 17a. It is basically a conventional synchronous machine with an SC excitation which is located in the rotor and, consequently, is turning, involving three associated issues: (a) how to cool down the moving coils (b) how to energize these moving coils (c) how to transmit the produced torque from the cold side to the warm one.

The solution is based on a rotating cryostat and a hollow torque tube through which the current and the coolant are injected into the SC coils, at the time the torque is transmitted to the warm side. Two major shortcomings are associated with this solution: (1) a big air gap is required to allow the presence of the cryostat, (2) a limited electric load is achieved since stator coils are non-SC. A step forward is the development of

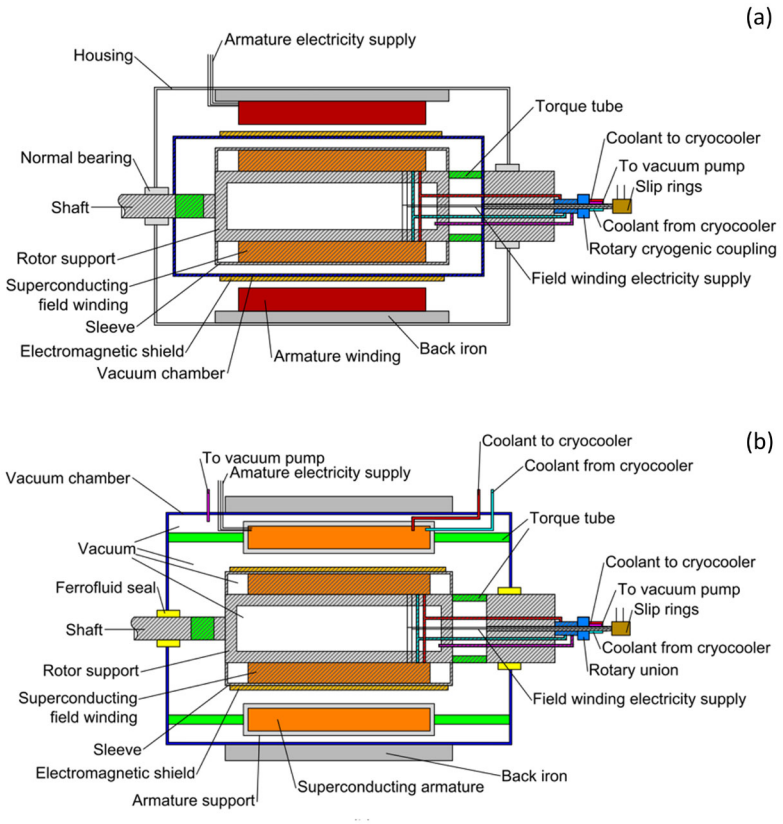

Fig. 17 (**a**) Scheme of a field SC synchronous motor. (**b**) Scheme of a stator and rotor SC synchronous motor

fully SC synchronous machines where both sides (rotor and stator are cold and share the same cryostat) [113, 116] (see Fig. 17b). This allows increasing significantly the electric load and consequently the torque for the same machine sizes but it also generates AC losses in the stator with additional cryogenic loads. Special multifilamentary wires or tapes must be used for this application. Nevertheless, there seems to be a consensus on the fact that only from 20–30 MW, SC machines start to become competitive for wind energy applications. Unlike wind power, in which the goal aims at developing new systems expanding the limits of the achievable capacity, opportunities for superconductivity technology in hydropower are focused on the refurbishment and upgrade of current facilities aiming to maximize the performance and output of existing assets. Among those, special efforts are put into small to medium run-of-river that use reaction turbines, which have the lowest environmental and ecological effects [117].

Superconductivity also offers advantages in terms of grid performance. On the one hand, due to stronger magnetic fields generated by SC windings; a SC generator can be designed with a higher air gap compared to traditional ones without losing mag-

netic flux density. In synchronous machines, there is an inverse relationship between air gap length and the synchronous reactance, which can be defined as the opposition to the flow of the AC at the armature winding due to the combined effects of inductance and magnetic fields. The synchronous reactance of a synchronous machine is inversely related to its dynamic stability during transient grid faults. Higher synchronous reactance typically reduces dynamic stability and the machine's ability to damp oscillations. Hence by allowing a reduction of the synchronous reactance of the machine, the use of superconductors improves the dynamic stability of the machine during transient grid faults. On the other hand, the efficiency (the ratio of the electrical output power to the mechanical input power) of SC machines is almost independent of how effectively electric power is converted into useful work output in an AC electrical system, namely the power factor. The latter is defined as the ratio of the real power (measured in kilowatts, kW) that does useful work to the apparent power (measured in kilovolt-amperes, kVA) that flows through the circuit. For this reason, SC machines maintain high efficiency regardless of the power factor or the amount of excitation current applied. This characteristic allows them to be over-excited to correct the power factor without needing additional equipment such as synchronous reactors or capacitor banks as in the case of traditional generators. As a result, these machines can enhance the reactive power management and overall stability of the power system [118, 119]. This is especially true in the case of small to medium run-of-river turbines which, as mentioned above, are the ones taking the major advantage of superconductor technology. Such hydro stations are subjected to a high degree of variability throughout the year. For these reasons, the focus of the development of SC technology is on applying variable-speed turbine applications at existing stations that contain older, fixed-speed turbines. Such a solution based on the implementation of variable-speed turbines enables the conversion of a greater amount of water energy into electrical energy because they can operate with very high efficiency across a wide range of speeds and power outputs, meaning that when the water flow changes, the SC generator can quickly respond by either increasing or decreasing its power output, matching the turbine's operating conditions almost instantaneously. The latter allows for harnessing the lower power levels drawn from reduced water flows, which eliminates the need for the turbine to operate in part-load (as is the case of traditional fix-speed generators), where their efficiency levels drop dramatically. Despite the above-described advantages that superconductivity can bring to electric generators, there are still several technical challenges that this technology poses. SC generator must be carefully designed to allow for superconductor refrigeration below its critical temperature. For this reason, whereas availability and established processing are major advantages for LTS, the necessity of cooling well below 10 K is a major drawback. This is because usually, such cooling is performed with LHe, which is produced through the radioactive decay of natural gas and is a non-renewable asset. Hence the volatility of LHe price together with the risk of its scarcity are preventing the use of LTS materials and systems in more price-sensitive fields of applications such as the energy sector. One of the enablers of SC generator technology is the possibility of using HTS due to their superior operating temperature which allows to efficiently refrigerate the SC coils at temperatures around 40 K by means of gaseous helium flowing in a closed circuit and cooled down by using cryocoolers, as shown in Fig. 9b, leaving aside the need for huge

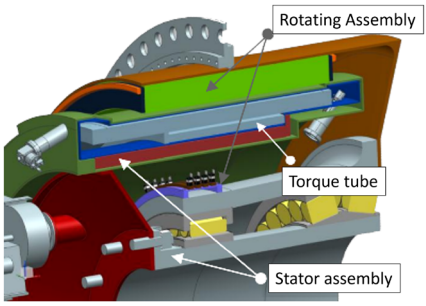

Fig. 18 General electric, GE—ecomagination generator

amounts of LHe. Previous studies [120] have estimated that in a hydropower turbine generator, the power consumed by the cryogenics of a SC rotor is a small fraction of the normal losses in a normal conducting conventional one, being about 25 kW compared to 300 kW for a 25 MW machine.

Moreover, to reduce the heat leakage from the cold section of the machine, the SC parts must be placed in a vacuum vessel at pressures around 10^{-5} mbar [121]. Such a requirement adds extra complexity to the design which implies the use of vacuum leak-tight bearings properly sealed to allow rotary movement as presented previously and shown in Fig. 17. In a similar way, the rotor must be kept at cryogenic temperatures while keeping thermal losses to a minimum when transferring the high torque from the shaft. The choice of the material to be used for such purposes must fulfil not only the low thermal conductivity requirement to behave as an insulation between the cold mass and warm mass of the machine, but also the mechanical resistance to withstand the high torques that in a DD generator act directly on the machine's rotating part. For this purpose, fibreglass and carbon fibre-based materials are commonly used [122].

In parallel, in the search for optimization and adequation to the special requirements of each specific application, many alternative designs have been developed diverging from the above-mentioned mainstream strategy. Especially worth mentioning is the case of the generator developed by General Electric, GE—Ecomagination, aimed to wind power generation one of the novelties of such a generator is that the SC field winding is stationary while the rotating armature is rotating [123] such option eliminates the cryogenic coupler and simplifies the SC coil design, however, the armature requires high current electrical brushes with extremely efficient electrical conductivity. Figure 18 shows a graphical description of its configuration. Moreover, unlike the majority of SC generators, it is designed with the NbTi wires instead of HTS due to the low cost and mature technology, paying the burden of a more complicated cooling strategy. As mentioned above, the following step towards increasing the power capacity of SC generators is to also replace the normal conducting windings of the armature (stator) with SC ones (besides a SC field winding, constituting the fully SC version shown in Fig. 17 b) to boost the machine's electrical load, hence further increase the shear stress. The use of such fully SC generators, drastically increases the power densities achievable, leading to a reduction in generator size, which as mentioned above is one of the motivations for offshore wind farms and hydropower turbines [124]. Illustrative size estimations [125] showed that a 10 m diameter fully normal conducting 10MW

direct drive generator could be downsized to 4.3 m diameter by using superconductive field winding. Moreover, such size reduction can be enhanced down to 3.8 m diameter by using superconductive windings both at the rotor and stator. The major drawback of fully SC generators is the power dissipation due to AC losses generated at the armature winding due to the oscillating magnetic field to which it is exposed. Whereas such an oscillating magnetic field is also present in partially SC machines, power dissipation would not constitute a concern at room temperature, but can become a significant challenge when considering the refrigeration costs. This is especially true when using HTS conductors which are manufactured in the shape of tapes and the winding of SC coils with multifilamentary strands is much more complicated and practical applications are scarce. HTS tape-like geometries with high aspect ratios are especially susceptible of generating AC losses, which are proportional to the area enclosed in the magnetic hysteresis loop that occurs due to the repetitive magnetization of the superconductor as it cycles through AC. Moreover, tape-shaped wires have larger areas exposed to oscillating magnetic fields enhancing AC losses. Such a problem can be tackled from two fronts. The first one is the improvement efficiency of cooling techniques and the second one is to minimize the AC losses following strategies based on a design solution. Regarding the last one, the use of the LTS conductor MgB_2 has been often proposed as a candidate to use in AC windings of fully SC generators [126]. This is due to the fact that it is available in the form of thin multifilamentary conductors to minimize AC losses by limiting the size of current loops (hysteresis) and by increasing interfilament resistance to suppress coupling currents [126]. MgB_2 critical temperature is the highest among all LTS (39 K) allowing it to remain within the current cooling capacities. As of today, fully SC generators are conceived as a long-term solution, allowing SC technologies and cooling techniques to develop into a feasible option. Nevertheless, there are ongoing different proposals to also develop multifilamentary HTS REBCO tapes, aimed at including these types of conductors in AC applications due to their outstanding transport properties [127–129]. Several studies have gauged the average cost of electricity generation over the lifetime of SC-based wind turbine generators through the LCOE metric [101, 126]. These studies have been carried out by upscaling calculations, with current the 5 MW capacity generators as reference. In 2022, it was pointed out that the major bottleneck of this technology is relevant to the price of SC material and cryogenic systems. As a rule of thumb, it was established that only for power capacities above 8 MW the use of SC generators in offshore wind farms would result in favourable values of LCOE [104]. Above such a threshold, due to their high power density, generators are not only lighter but cheaper. Its low weight helps to reduce the turbine mass together with installation costs. In this regard, Fig. 35 presented in Sect. 4.2.2 shows a clear explanation, extracted from [130] on how the power density of SC machines can be dramatically increased with respect to conventional electric ones. Moreover, the figure shows that beyond 10MW an increase in power generation does not constitute a remarkable increase in machine weight. As a result, the estimated LCOE of a fully SC wind generator was found to be significantly lower (about 7% at Pn = 20 MW) compared with its permanent magnet counterpart [104]. Interestingly enough, several projects based on traditional non-SC technology are evolving to reach the 18 MW goal [110–112], very close to 20 MW and well above the 8MW previously mentioned and proving a strong variation of LCOE calculations

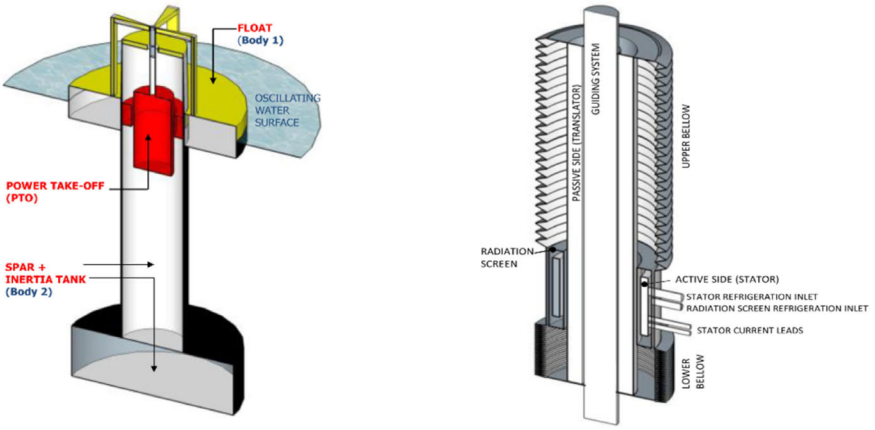

Fig. 19 Left: concept of a Heave Point Absorber 2. Right: concept of a reciprocating SC switched reluctance machine

within a very short period of time. The latter shows that traditional technologies are still rapidly evolving, raising the threshold value that SC technology aims to overpass.

From 2018 onwards, different projects [103, 131, 132] have been focused on the development of SC generators with the goal of optimizing such 20MW goal. In 2019, the EcoSwing consortium [133] successfully designed and comissioned a 3.6 MW partially SC prototype generator based on HTS technology [132]. Such a prototype was a reduced-size demonstrator of a baseline generator design of 30 MW. The prototype was 15% cheaper and 40% smaller than the baseline. Besides, its weight is 68 tons, which is 24% less than a scaled PM generator with the same outer diameter and the same torque. It requires about 35 kW of cooling power to maintain the operating temperature of the HTS field winding at 30 K. The generator's stator is the same as that in conventional electric machines. Noticeably, the air gap shear stress in the HTS generator is 113 kPa, which is about twice that when compared to a conventional DD permanent magnet (PM) generator for wind turbines [134].

Regarding the hydropower sector, SC generators have not yet been widely adopted in commercial hydroelectric power plants. While there has been significant research and development in SC technology for power generation, its application in hydroelectric plants is still in the experimental or pilot stage. As a matter of fact, the last report on advanced manufacturing and materials for hydropower [135] published in 2023, barely mentions the use of superconductors as an immediate goal. In this sector, the installation and operation of the world's first HTS SC generator in a real-world hydroelectric application took place at the Hirschaid plant, in Germany, under the framework of the project Hydrogenie [120]. Hirschaid is a run-of-river plant composed of three reaction turbines. A 1.7 MW SC generator based on HTS rotating coils was installed as a replacement for one of the three originally installed 1.25 MW traditional generators. In 2013 it was commissioned and successfully connected to the German electrical grid marking a significant milestone in the use of SC technology in renewable energy generation. This situation is also very similar to the case of ocean

hydrokinetic energy, particularly currents and waves. For the first case, the specific idea of using a SC magnetohydrodynamic generator is quite old [136]. Some years later and even presently, more advanced proposals have been developed at a prototype scale. The introduction of Helical-Type MHD allows the utilization of solenoidal SC magnets which are easier to manufacture, especially due to their requirements for high field. The hydrogen generation which results in the process has become nowadays an added benefit which makes the application more attractive [137]. Due to the similarities with SC for naval propulsion, additional comments can be found in the corresponding section of this article. To finish this section, a short reference to wave energy generation, another form of water hydrokinetic energy conversion. There are different ways of converting the energy associated with the kinetic energy of the waves into electricity. Their complete description is out of the scope of this paper, but we shall just mention the heaving point absorber formed by a buoy and a moving float with a vertical reciprocating oscillation. In one solution, the float is mechanically connected to the translator of a linear machine, while the stator of the machine is fixed to the stationary (rather pseudo-stationary) buoy constituting a direct drive power take off (DDPTO) [138]. The relative displacement between float and buoy is converted into electricity. The system design is done in a way that resonates with the wave frequency, amplifying the oscillation amplitude and maximizing the extraction of energy. Resonance is achieved by tuning the system and this can be done with the linear generator itself which must provide the required reactive force, usually higher than the active one. Wave energy generators must produce high forces with low losses constituting an ideal application for superconductivity.

Different linear SC generators have been proposed, some of which are in a prototyping phase [139], suggests linear synchronous machines with bulk HTS to create the excitation field while [140] proposes a switched reluctance machine with solely iron in the translator and either MgB_2 or HTS ReBCO coils in the stator. A prototype is now under development and it has the main peculiarity of using a flexible cryostat. Also, a linear generator with stationary SC coils was designed some years ago at the University of Edinburgh [141]. Figure 19 shows, on the left hand figure a schematic view of the heaving point absorber while on the right hand, a 3-D scheme of the SC switched reluctance reciprocating generator.

4.1.3 Application to electric power transmission

A power transmission line is defined by its current and voltage ratings. The first one indicates how much electrical current the cable can safely conduct without overheating or suffering damage. The second one indicates the maximum electrical potential the cable can handle without causing insulation failure or arcing. The combination of current and voltage represents the apparent power rating (in VA or W), which is a key indicator of the power transmission capacity of the line. The ratings of traditional power transmission lines can vary significantly depending on factors such as the type of transmission line, the distance of transmission, and the specific application. The higher the voltage, the more power can be transmitted over long distances with lower losses, which is why extra-high (> 230 kV) and ultra-high (> 800 kV) voltage lines are used for major transmission lengths. Current ratings are lower at higher voltages,

as the same power can be transmitted with less current. This helps reducing losses due to impedance in the conductors that increase with the square of the transmitted current. As a representative example, the Changji-Guquan Ultra-High Voltage Direct Current (UHVDC) transmission line in China [142] is the most powerful and longest distance power transmission line in the world with a voltage rating of 1.100 kV and a transmission capacity of 12 GW to transmit electricity along more than 3000 km.

Moreover, as described in Sect. 4.1.2, renewable energy generation is rapidly evolving to contribute to satisfying such energy demand. In this regard wind, solar and hydropower generation assets are typically sited far away from the populations they serve [143]. Hence as renewable generation increases, so do transmission distances.

Long power lines can use high voltage direct current (HVDC) systems which are more efficient over long distances since they require fewer conductors and are susceptible to less power loss due to impedance than equivalent AC lines. This is because they are not subjected to AC losses. Moreover, power transmitted through an HVDC line can be controlled independently of the phase angle of AC grids at source and load, where AC/DC conversion takes place, even if they are not synchronized. In this regard, HVDC also allows the transfer of power between remote grid systems running at different frequencies, such as 50 and 60 Hz, improving the stability and economy of each grid. However, the strategy based on upscaling voltage ratings according to line length reaches a saturation point. Conventional long-distance transmission systems using aluminium and copper conductors experience power losses of around 10%. This amounts to around 180 TWh annually in Europe, which is enough to power three large cities [144]. Such losses are ascribed not only to inductive effects but also to the need to use power converters and transformers. These converters use electronic components that generate heat. Additionally, converters have voltage limitations that affect the overall efficiency and design of HVDC systems. This leads to the need of finding an efficient solution since higher voltages are needed to reduce transmission losses, but converters cannot always handle such high voltages efficiently. As the world population grows, and consequently its energy demand increases, power line losses must be minimized. Despite the advantages of DC power lines, in the case of urban power grid systems, AC transmission lines are preferred, allowing for shorter distance transmission without the need for using converters within metropolitan areas. In the last 20 years, the electricity consumption of large cities has increased rapidly [145] and power grids have been estimated to need an upgrade to enable an expected 60% increase in electricity demand over the next 20 years [146]. Therefore, municipal power supply systems have been in urgent need of expansion, especially in the central districts. In the case of AC power transmission lines, similarly to their DC counterpart, power losses are a limiting factor, as such lines transmit power in the form of AC current, impedance issues are to be tackled not only due to cable resistance but also to those derived from AC losses. A typical 380 kV 1.1 GW transmission power line shows losses of roughly 1%, or 11 MW, per 100 km [147]. This results in yearly losses of 96 MWh per 100 km.

SC cable systems have a critical role to play in addressing the above-mentioned challenges. Especially those related to power losses. The design of such superconductor cables for power transmission is primarily based on the use of HTS tapes. The development of HTS technology has been an enabler for superconductivity to

be applied to cables for high-capacity power. The major advantages of HTS when compared to the LTS option are the efficiency and operational benefits derived from the use of LN2 as a coolant [148]. The major repercussion of the use of SC power line cables is related to the energy savings associated with near-zero resistance conductors. Even if there is an energy demand associated with SC cooling, the power saving achieved in this way is, in many cases, greater than the energy expended to maintain conductors at a low temperature. The energy demand of an SC transmission line is dominated by superconductor cooling, insulation vacuum pumping and coolant circulation system [149]. These represent passive power losses that apply at any time even when power is not being transmitted. For this reason, the efficiency of a SC transmission line must be carefully evaluated as a function of its load factor, which can be expressed as the average load of the line divided by its peak load. A high load factor means a constant load (or close to the peak load) and an absence of periods in which power is not transmitted [149]. Specially delicate in this regard is the transmission of power generated by renewable energies such as wind and solar, where the energy sources strongly depend on uncontrollable weather-related parameters, leading to low load factors. In the case of wind power generation, as mentioned in Sect. 4.1.2, a solution to this problem is found in the use of offshore wind farms, where wind speeds are considerably steadier than for those onshore. The second important parameter that influences SC transmission lines efficiency is the capacity rating [150]. Higher capacities cause greater thermal losses due to increased diameter, raising heat influx. Thus, power consumption for maintaining cryogen temperature depends on the cooling system's outer diameter, driven by hydraulic diameters meeting mass flow and heat transport needs. Additionally, cooling station distance and cryogen type significantly affect this. In [150] an intensive analysis of the efficiency of SC transmission lines (excluding energy losses originated at converters) with respect to traditional normal conducting ones is carried out. The results show that for load factors between 50 and 100% and capacity ratings of 4 GW and 10 GW, power losses of HTS are between one and two orders of magnitude lower than for traditional normal conducting ones.

Apart from power loss efficiency, the other main advantage is the reduced cross-section area due to the higher current densities that SC power cables can conduct. Thus, the grid capacity can be increased without laying new power reducing the cost of rights-of-way (ROW) [151], i.e. the legal right to use a specific strip of land for the construction of power transmission lines. The latter has a direct positive impact towards the decrease of the amount of land required for transmission lines, which in turn minimizes the disruption to natural habitats, and reduces the costs associated with purchasing land and construction work. An important aspect worth mentioning of SC power lines is the fact that they can be installed underground, buried deeper than conventional ones because heat exhaust is not an issue, meaning that there is no reduction in transmission capacity when other cables are run in proximity and there is no soil drying effect. In [151], the ROW needed for a 5–10 GW capacity SC HVDC is compared to that of a traditional one showing that the use of superconductivity allows to drastically reduce the traditional 125 m to a mere 5.5 m corridor width.

In a SC power cable, depending on the type of electrical insulation of the HTS tapes, the designs can be divided into two main types, i.e. warm dielectric and cold dielectric design. The first one is based on flexible support with twisted HTS tapes

forming the cable conductor. This conductor, cooled by the flow of LN2, is placed in the space between two concentric flexible stainless steel corrugated tubes forming a cryostat. In this way, the dielectric core remains within the space enclosed by the smallest corrugated tube, outside the cryostat, at room temperature [148, 152]. On the other hand, in the cold dielectric cable, the dielectric is impregnated with liquid nitrogen (LN2) providing both an electric insulation and an effective cooling [152]. Figure 20 a shows a schematic description of a cold dielectric SC power cable for DC applications. Cold dielectric designs are by default the option chosen by the large majority of SC power line developments [145].

However, despite the major advantages that cold dielectric strategy offers over its warm counterpart, it implies a more ambitious design involving complicated developments in the field of dielectric materials which shall be impregnated with LN2. In this regard, the cooling requirements are extremely challenging with the need to evacuate power losses along the whole cable's length, ensuring that the nitrogen remains in the liquid state at every point. Any boiling of the LN2 would result in a dielectric breakdown due pressure increase. Typically, LN2 cooling circuits require forced flow provided by a circulation pump. Electrical insulation requirements and height differences forbid 2-phase flow systems. Commonly sub-cooled LN2 at 65–70 K is commonly used. Then, the heat input to the circulation system is removed by re-cooling LN2 in a heat exchanger often cooled by cryocoolers [153, 154]

One important characteristic of the cold dielectric design is that insulation is surrounded by a shielding layer. Depending on the specific application of the cable, such shielding can be formed with normal conducting copper or HTS [148], preventing stray electromagnetic field generation. This allows to minimize effects on nearby infrastructure so there is no interference with surrounding power, telecom and pipe networks. The latter represents a major advantage of SC power cables in comparison to traditional normal conducting ones, in which case stray electromagnetic fields can not be avoided.

In the case of AC power transmission lines, a three-phase system is needed to ensure a constant and balanced power flow for system efficiency. In a three-phase system, there are three separate currents, each with its own sine wave. The sine waves of these three currents are offset by 120 degrees from each other, meaning they reach their peak values at equally spaced times. Since traditional power lines are not shielded, the space between their phases needs to be large enough to eliminate electromagnetic interactions between phases. If the phases are too close together, capacitive or inductive coupling can take place, which could cause unwanted interference, energy losses, or even damage to the power system.

However, HTS tapes allow for compact designs in which three cable phases can be put together into a single cryogenic envelope. Two options are available: (i) three single-phase cables next to one another, i.e. three-in-one configuration (Fig. 20a) and (ii) one single cable arranged in a triaxial configuration (Fig. 20a). The first one profits from the fact that as mentioned above, the stray field of SC cold dielectric power cables can be minimized due to shielding, limiting the coupling between phases. Regarding the second one, in such a triaxial design the three-phase conductors are concentrically arranged on a single support element divided by wrapped dielectric to withstand the phase-to-phase voltage. A specially motivating characteristic of coaxial-

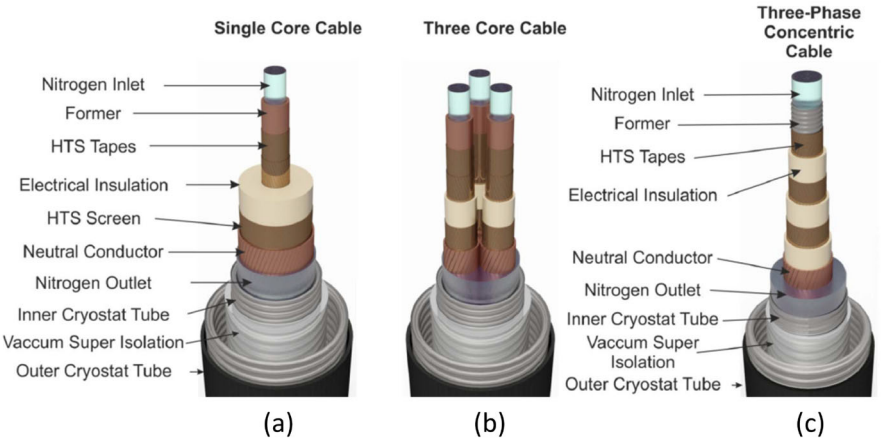

Fig. 20 schematic description of a cold dielectric (**a**) SC power cable for DC applications, (**b**) SC power cable for AC applications. Three-in-one configuration, (**c**) SC power cable for AC applications. Triaxial configuration [155]

Fig. 21 Prototype of the AmpaCity cable and accessories setup for type test in laboratory [153]

type HTS cables is the fact that the amount of SC wires needed can be reduced because self-balancing shielding layers are not necessary in three-phase equilibrium conditions [156] leading to lower superconductor demand together with an even more compact structure. The major drawback of this strategy is related to the critical current diminishment of each phase due to the presence of the magnetic field generated by the other two [157]. Nevertheless, the compactness associated with the triaxial design, brings a major advantage in terms of power line operation and installation due to the subsequent reduction of land take and a reduced need for electrical infrastructure. As mentioned above, rights of way for HTS cables have been estimated to be up to ten times narrower than those for conventional cables and lines. This reduces the need for permitting, minimizes disruption to the public, accelerates deployment and contributes to lower costs [144, 155]. An illustrative example of the latter can be seen in Fig. 21

A very important aspect to take into account when considering SC AC power cables is the potential limitations that AC losses may originate related to the appearance of heat generation when a time-varying current circulates along a superconductor. To address such limitations, SC cables can be designed in such a way that these AC losses are minimized, being able to reduce the impedance to values much lower than conventional cables. Generally, in the uniform current density (UCD) model [149, 158–160], the HTS tapes are twisted around a dielectric core to reduce the effects of flux jumping and eddy currents, which are significant sources of AC losses in superconductors, mitigating the formation of large magnetic flux gradients and reducing localized heating. The twisting is a key process to optimize SC cables in which the main design parameters are the twist pitch and pattern [157, 161], chosen based on the specific application and performance requirements. Special attention must be paid when considering three axial cable designs. In the multi-layer cable, due to different radii between each phase and because of the difference in the magnetic coupling between the inner and outer SC layers, the layer-to-layer current distribution becomes uneven [156, 158, 162] generating complicated electromagnetic field distribution in the superconductors. This results in an increase in the AC losses of the cable which drastically complicates the design of the cables enhancing the complexity of the system.

Another operational thread of both AC and DC transmission power lines is related to fault currents. These are abnormally high electrical currents that occur when there is a short circuit or other electrical fault in the system. Fault currents are potentially dangerous for the integrity of the power line systems and are to be mitigated. Most of the power system works as a voltage source. In a voltage source system, the only way to limit the fault currents is to increase the line transmission impedance, inserting a series impedance into the circuit as fast as possible after the fault current is detected [163, 164]. For these purposes, fault current limiters (FCL) are used. The traditional overcurrent protection in power systems is made with electromechanical circuit breakers, which usually need more than one current cycle to open the circuit. Moreover, often involves mechanical components (such as circuit breakers or relays) that require frequent maintenance. Up to medium voltage levels there are fuses and fuse-like explosive devices that offer such a function. However, they have to be serviced after each trigger and their scalability to high voltage levels is very limited.

Especially interesting are the strategies based on SC FCL devices (SCFCL) which have the advantage of being able to, recover quickly and automatically and can be used even at high voltage levels [165, 166]. There is a vast variety of SCFCL designs, among which the one known as Resistive SC FCL (R-SFCL) has been widely demonstrated on a large scale due to its simple concept and compactness [164]. The R-SFCL operation is based on the SC fast resistivity increasing due to the superconductor quenching caused by the overcurrent during a fault. It is especially attractive due to its self-triggered character. When a short circuit happens, the current passing through the SC becomes much higher than its critical current (I_c), resulting in the fast transition from the SC to the normal state or quench [164]. Figure 22a and b show a 3D CAD model of an actual R-SFCL designed for the ECCOflow project [167] and the R-FCL installation of the AMPACITY project [168] respectively.

Fig. 22 (**a**) 3D CAD model of an actual R-SFCL designed for the ECCOflow project [167]. (**b**) The R-FCL installation of the AMPACITY project [168]

When the superconductor quenches, it suddenly introduces a significant amount of electrical resistance into the circuit. This resistance limits the amount of current that can flow, thereby reducing the peak fault current to a safer level. The main advantage of the Resistive type of SCFCL is that they are fail-safe and can be built to be very compact with negligible impedance during normal operation. On the other hand, the major drawback is related to the need for current leads from room to cryogenic temperature that cause heat losses due to heat conduction even in standby operation without current. Moreover, due to the quench and the heating of the superconductor a recovery time is needed [164]. In this regard, an issue that must be carefully addressed is related to the thermal management of the heat released in the quench and the heat generated in the SC during the fault limitation time. In the case of cold dielectric cables for instance, as mentioned above, no bubbles are allowed at any point during a fault. As a result of this condition, the operating pressure, coolant flow rate, cryostat dimensions and operating temperature must be carefully chosen, adding an extra degree of complexity to the design of SC power cables [169]. A very simple strategy can be applied to further optimize R-SFCL design by introducing an external magnetic field. When a current fault occurs the quench starts at the weakest point of the superconductor and the growing resistance forces the current to flow in the parallel coil. The resulting magnetic field of the coil lowers the critical current in the still SC portions where the quench is therefore accelerated, which in turn mitigates the hot-spot problem. Such a variant is known as magnetic field-assisted R-SCFL.

Besides the resistive type, it is also worth mentioning the SCFCL that focuses its strategy on inductive phenomena. Among those, the most popular is the DC-biased saturated iron core type (SIC-FCL) [127, 170]. It consists of an iron core, which is driven into saturation by a DC SC bias supply wound around the iron. During normal operation, nominal AC power line currents pass through coils wound around the iron in the opposite direction of the DC bias winding, but are not enough to take out the core from the saturation region. Due to the saturation, the cores behave such as air core reactors, presenting a relative magnetic permeability close to 1. Under faults,

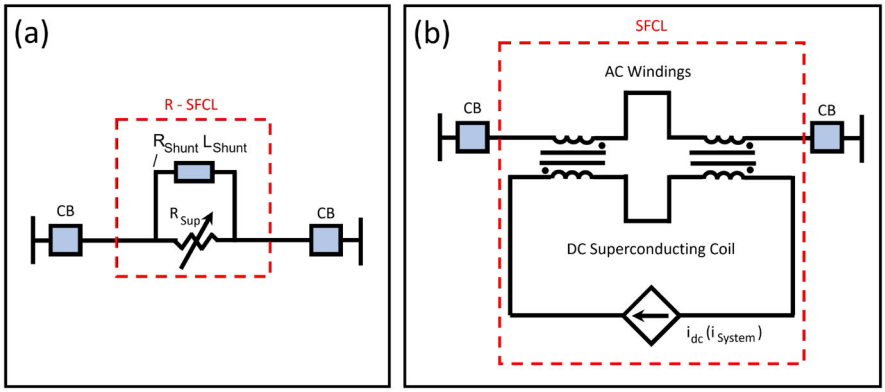

Fig. 23 Electrical circuit of SC fault current limiter [164] in the (a) resistive type configuration and (**b**) DC biased iron configuration

the increasing current in the AC brings the core out of saturation. This causes the inductances of the coils to increase which reduces the rise of the fault current. SIC-SFCLs are not based on superconductor quenching like the resistive type. Hence, since there is no need to cool down the superconductor after the fault current limitation, the device can return to normal operating conditions before the circuit breaker attempts to reclose. The SC coil is in DC mode and not connected to the AC circuit, hence less superconductor material is needed and a small cryogenic system is sufficient to remove the low cryogenic losses [164]. Figure 23 shows schematic descriptions of both resistive and DC-biased FCL electrical circuits. One of the major drawbacks of such design is related to its size and weight since due to the iron core the whole setup is relatively bulky. Moreover, If the fault current increases over the expected value, the reactor will be driven to the saturation region again and will not limit the fault current. Besides, during the limitation of the fault, the iron core is driven from the saturated state to the unsaturated in a strong nonlinear transition, introducing harmonics in the line voltage. It is important to take also into account that in AC power transmission lines a three-phase system is needed, thus requiring three identical single-phase identical limiters adding extra complexity to the overall system [171].

SCFCLs are typically used in all parts of power systems, typically divided into power generation, power transmission, and power distribution. Nowadays there are four technologies, apart from the superconductor-based ones, for FCL that are produced in full commercial application: the high impedance transformer, the neutral earthing resistor, the air coil reactor FCL, and the pyrotechnic FCL, with a TRL index of 9 [164, 172]. The above SCFCL development is currently at the TRL8 level, with a margin for improvement following an actual trend to develop into a more mature technology, evolving into a commercial product.

In 2013, the Zenergy group presented the 15 kV/30 MVA SIC-SFCL, which was installed at the low side of the 115 kV/12 kV Avanti Substation of Southern California Edison [173]. More recently, a 500 kV prototype has been [174] developed. The main coil was built using Bi-2223, and the YBCO tapes were used to optimize the magnetic

field distribution. Also, in the framework of the Innopower research project, a SIC-FCL was developed for medium and high voltage levels (35 kV and 220 kV) [166]. The development of the first fully operating product applications carried out with SCFCL, bringing the technology to TRL8 was carried out within the AMPACITY project, previously described, in which case a resistive SCFLC was implemented to limit 38 kA peak short circuit to about 10 kA as a complement of the 1 km DC SC transmission line. The SCFCL is manufactured using BSCCO operating at 77K. It is remarkable that the line worked successfully during 7 years, without interruption. In that period of time SCFL experienced several faults and operated exactly as designed [175].

The energy efficiency of power transmission lines is dramatically biased by their converters and transformers at each end of the DC and AC power transmission line, respectively. Such effect is especially remarkable when using SC cable for power lines in which the implementation of superconductivity adds considerable design and manufacturing complexity with power efficiency as one specific goal. In this respect, SC solutions are also found to substitute traditional devices. In the case of DC power lines in which power must be converted to AC for distribution SC converter designs have been carried out by making use of SC switches or cryotrons [176]. Such devices consist of a SC pathway surrounded by a coil. While the current is lower than the critical one in the absence of magnetic field, it is passed through the superconductor. When switching is desired, the coil is energized to generate a magnetic field that lowers the critical current of the superconductor below the present value.

In the case of AC transmission lines transformers are used to step up the voltage for transmission (high voltage reduces current and minimizes losses) and step it down at the distribution level. The key components of a transformer are the primary and secondary windings together with a ferromagnetic core. SC alternatives for such transformers have also been developed using SC materials (typically HTS) in their windings (see Sect. 4.3). Different types are available depending mainly on the refrigeration technique (conduction or LN2 bath) and the temperature of the ferromagnetic core [177]. These transformers can operate with minimal resistive losses, significantly improving energy efficiency and increasing energy savings.

The first grid installation dates back to 2001, when NKT operated three HTS cable sections in a grid coupling in a substation in Copenhagen [178]. Since then, during the last decades, SC power transmission cables have taken a big step forward and integrated pilot systems have already been demonstrated. In [151, 164] a very complete summary of AC SC cables projects is presented.

In 2007, a 600 m SC cable was installed under the project LIPA and installed at the Long Island Power Authority grid in New York, representing the world's first installation of a SC cable in a live grid at transmission voltages. It was the cable working at the highest voltage level and power rating (138 kV/574 MVA) at the time of its construction. The cable was developed following a cold dielectric design in the three-in-one arrangement by using BSCCO 2223 as SC material [169]. The project served as a replacement for an existing right-of-way delivering power to 300,000 homes.

In the framework of the project AMPACITY [168] a 10 kV, 40 MVA and 1 km REBCO cable has been developed, manufactured and installed in the city of Essen,

Germany. The cable design is a cold dielectric based on a triaxial arrangement. In this case, there is a common screen concentrical to the former made of stranded normal conducting copper wires. This project represented an important milestone being the first time for a one-kilometer HTS cable system to be installed in a real grid application within a city center area. Moreover, its outcome is representative of the huge improvements that superconductivity can bring to power transmission in metropolitan areas. Four out of ten 110/10 kV transformer substations were removed in the downtown area by using 10 kV cable systems. SC technology allowed to transmit power at 10% of the voltage needed for conventional cables. In comparison to 110 kV conventional cables, 10 kV SC systems allowed a much simpler grid structure, less space for cable routing and smaller areas for equipment installations. Another important outcome of this project is a reduction in the overall costs in comparison to the grid with conventional 110 kV systems.

In October 2024, a prototype of the world's longest SC power cable system was successfully commissioned at the Menzing substation in Munich under the framework of the Super-Link project [179] in collaboration between NKT, Stadtwerke München (SWM), THEVA, Linde, as well as the University of Applied Sciences South Westphalia and the Karlsruhe Institute of Technology (KIT). The cable, designed in a three-in-one configuration, will span approximately 15 kms with a power transmission capacity of 500 MW at a voltage level of 110 kV and is intended to connect key substations in Munich, facilitating efficient power distribution within the city's dense urban environment. Ideally, it will fit into partially existing empty conduits with a diameter of 150 mm. The slim design and especially the long length over 12 km carry considerable technical challenges. The solution was found on a modular HTS cable solution with standardised intermediate cooling stations that are adaptable to various application scenarios and line lengths by cascading.

Besides transmission power lines, especially remarkable are the applications of superconductivity to those transmission systems that, contrary to the above-mentioned long-distance HVDC lines, are related to short-distance DC busbars for application within small-sized premises. As well as in the case of long and medium transmission lines, the benefit of superconductors, therefore, is not only the absence of ohmic losses, but also a substantial gain with respect to smaller size, less material weight, reduced costs and more flexibility at the installation site.

The development of this technology has been considerable within the last years. A representative example is the German government-funded project 3S (German acronym for SupraStromSchiene) within which framework a prototype of a busbar on a medium scale was developed by using REBCO tapes. It was designed for a DC current of 20 kA and a total length of 25 m and installed and tested as a current connection between a rectifier and an electrolysis device at the BASF site in Ludwigshafen, Germany [180]. The main HTS busbar assembly strategy is based on HTS tape stacking. The stack configuration of HTS tapes in DC busbars involves layering multiple SC tapes to enhance current capacity and optimize current flow, making it ideal for DC applications. Figure 24 shows representative examples of HTS tape stacking for busbar applications as developed under the framework of the 3S project. The main challenges of such configuration are related to ensuring uniform current distribution and effective cooling to prevent hot spots.

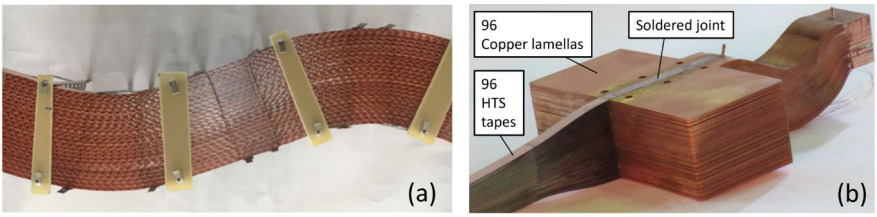

Fig. 24 (**a**) Stack of 23 SC tapes in waveform (overdrawn) with undulated copper tapes as distance holders [180]. (**b**) Flexible Copper to HTS contact with low resistance and a high number of stacks [181]

Interesting feasibility studies on the application of SC power cables to DC oriented to next generation electric railway system feeders (see Sect. 4.2.3) have also been carried out [182–184]. Traditional train feeders are made of normal conducting materials. Such studies considered the option of using SC cable as a feeder of the overhead contact line system, in which case the voltage decay could be significantly reduced and thus also the number of substations along the railway route. This application can potentially have a positive impact on regenerative brakes, which recycle the energy produced when a train slows down by pumping it into a train that is being powered up. The advantages of the regenerative brake are energy saving and reduced wheel wear among others. The regenerative brake systems based on traditional normal conductors carry strict operating conditions which require both trains to be close enough to one another. One of the goals of using SC feeders is to make such conditions less stringent and easier to meet [185].

In the realm of railway applications, the SuperRail project consists in the development, manufacturing, installation and long-term operation of an HTS DC cable system with the objective of reinforcing the power supply of the Montparnasse railway station in Paris [186]. The underground in the center of Paris is saturated and ROW is scarce, hence only the HTS cable technology allows to carry the required power to railway tracks using the few available 100 mm conduits left. The configuration of SuperRail will be two 60-m long 1.5 kV–3.5 kA HTS dc cables installed in parallel able to sustain a 67 kA–200 ms short-circuit current. The cryogenic system is specifically designed for this project based on a Reverse Turbo-Brayton cycle.

Also in the realm of transport, naval ship-to-shore SC power transmission lines are a possibility [187]. The harbour demand for electricity supply is expected to increase drastically due to the regulations that forbid the use of fossil fuel close to the shore. Establishing shore power for naval ships involves using multiple heavy, cumbersome copper cables from pier power substations to ship receptacles. Handling these cables requires coordination between crews on the pier and the ship, often needing a crane. Feasibility studies explored the use of HTS cables instead. In such scenario, connection time would decrease, reducing the ship's reliance on its generators. The lighter weight of HTS cables would also improve safety for personnel handling them.

Moreover, with the rapidly increasing energy demand for internet-based technologies such as cloud computing architectures, Artificial Intelligence and machine learning, global industries and organizations find the need to rely on the uninterrupted operation of data centres [188]. The growth of internet traffic together with a notably

deployment of IT equipments leads to the increase in electric power consumption of data centres [189, 190]. Nowadays, there are some conceptual HTS cable designs for data centers carried out by governments, universities and companies across the world [191, 192] aiming to profit from the use SC DC busbar networks with the advantages of virtually zero energy loss, ultra-high current-carrying capacity, and compact size. In [188] a comprehensive design of a 10MW data centre energy supply system using REBCO-based SC DC busbar networks is presented, evaluating not only the SC their technical feasibility for data centres, but also the technical design and economic evaluation.

Finally, a remarkable contribution of superconductivity to power transmission is found in the framework of the HL-LHC project of CERN and its SC link (SC Link) [193]. The proposed electrical layout of the HL-LHC upgrade requires the location of the power converters of SC magnets at surface buildings in radiation-free areas to avoid problems associated with the radiation damage of these devices and allow safe access of personnel for maintenance. For this reason, the transfer of the current from the surface to the LHC tunnel, where the magnets are located, is performed via SC links transferring more than 150 kA with cable lengths ranging from 300 to 500 m. The R&D process of this project started in 2010 considering both HTS and MgB_2. The superconductor material MgB_2 was chosen due to its higher current temperature in comparison to other LTS, easing the required cooling techniques at temperatures of 25 K, with cryogenic cooling performed with helium gas. The HTS option was discarded since by the time the decision was made, the industrialization of HTS was not yet sufficiently evolved and the associated high costs were not viable. Especially relevant were the limitations on the maximum lengths that, by that time, were possible to manufacture. Given the length of the SC link, the design implied too many non-SC connections, resulting in a difficult and poorly efficient solution.

4.1.4 Applications to magnetic energy storage (SMES)

Soon after the first practical SC magnets were available, the concept of a SMES was proposed and developed. The idea is simple: storing energy in the magnetic field of an SC magnet. Since it has no losses, the current will flow indefinitely in the magnet without requiring any voltage between its terminals and consequently the energy will remain stored permanently. The application of a negative voltage will discharge the magnet and release the magnetic energy which can be recovered (i.e. pumped back to the electric grid). Sequential applications of positive and negative voltage at the magnet terminals will, alternatively, store or release energy with an extremely high efficiency since the magnet has no losses and only those corresponding to the power supply and the cooling system should be accounted for the global energy balance. The first SMES system concept was proposed by Ferrier [194] in 1970 while the first prototype was developed at the University of Wisconsin in 1971 [195]. In 1982, the first SMES to be operated in the power grid was installed at the Bonneville Power Administration [196] in Tacoma. From that moment, many SMES have been developed and operated, first using LTS-based magnets which have been gradually substituted with HTS-based magnets. Most of the applications developed over the years consist of systems to protect sensible loads such as scientific facilities [197, 198], paper

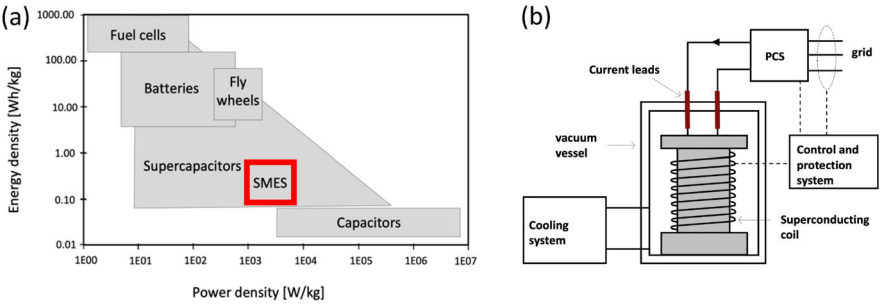

Fig. 25 (**a**) Ragone Diagram for different energy storage systems. (**b**) The main subsystems of a SMES

production machines [199] or a liquid crystal screen factory in Japan [200]. SMES, together with the Supercapacitor-based Energy Storage Systems belong to the group of Electrical Energy Storage Systems which, in turn, are one of the five existing Energy Storage Technologies (electrochemical, chemical, electrical, mechanical and thermal) [201]. In general, any Energy Storage Technology can be characterized by two relatively independent magnitudes: energy and power (sometimes energy density and power density are alternatively used). Those two magnitudes can be taken as the (x, y) coordinates representing a point in an Energy-Power space (Ragone Diagram [202]). Although it is difficult to find in the literature a good coincidence in the results presented for these diagrams for different systems and different authors, some general trends are recognizable. Figure 25a shows a Ragone Diagram in terms of energy and power densities [203] for different storage technologies and where the location of SMES is compared to the location of other systems. As can be seen, the situation of the SMES is quite modest: low energy density and medium to high power density.

Then, why SMES are a real alternative for storing energy? Basically, according to a different classification for energy storage systems, they can also be considered as FESS (fast energy storage systems) together with Supercapacitors and Flywheels. FESS are systems able to start releasing or storing energy in a very short time after they are requested to do it (typically few milliseconds) so that they are able to cope with applications where the actuation has to be very fast (voltage sags in the grid, for example). Since these applications can require many cycles of operation, the life cycle needs to be very high and here is where SMES generically finds applications such as: power quality improvement, power fluctuations compensation, power oscillations compensation, grid stability, voltage stability, sub-synchronous resonance compensation, frequency control, low voltage ride-through, black start, load levelling, spinning reserve, P & Q control, uninterruptible power supplies for critical loads and some others [204], either as individual systems or as part of hybrid storage systems where SMES complement other energy storage devices which are not so fast but are able to provide higher amounts of energy. SMES are in reality complete systems which are composed of four subsystems: The cooling system, the power conditioning system (PCS) the control system and obviously the SC Magnet [205]. Figure 25b shows a scheme of these subsystems and how they are interconnected. The cooling system strongly depends on the type of magnet (LTS vs HTS, basically). Like for other similar

applications, conduction or He circulation are the most common proposal for cooling down the magnet [206]. Nevertheless, for both cases the heart of the cooling system will be one or several cryocoolers, either to cool the magnet down, extracting the heat by using high thermal conductivity materials mechanically connecting the magnet to the cryocooler (conduction) or liquid or gas helium circulating through the magnet which is lately cooled down with the cryocooler (circulation). Proposals for using other types of coolants (directly or indirectly) have also been made [207]. Figure 26a shows a rendering of a conduction-cooled SMES developed at the Lublin Laboratory of SC Technology [208], based on an HTS magnet, where all the main elements can be identified. The power conditioning system constitutes the link between the magnet and the grid and determines how the power flows between both. There are several topologies for the PCS depending on the type of power converter [209]. In the first SMES realizations, thyristor-based PCSs were used since they allowed a direct connection between a single or a three-phase grid and the magnet terminals with no need for an intermediate DC bus. Nevertheless, this type of converter introduces a big current ripple in the magnet with the subsequent increase of the AC losses, but they are still proposed for ultra-high current SMES since thyristors are unbeatable in those ranges of current. Other solutions include current and voltage source inverters normally based on IGBTs. Closely related to the PCS is the Control System which basically commands the power converters to inject or extract power in the grid, according to the instantaneous needs of the application but it also controls the magnet protection system in the event of a quench or the cooling system depending on the internal losses, for instance. The SC Magnet is designed under two global conditions: (a) maximizing the stored energy for a given amount of superconductor, (b) minimizing the stray field. In a non-SC magnet, the first condition is simple to achieve: The magnet with the maximum inductance for a given length of wire is the so-called Brooks Solenoid [210] (same height as inner diameter and twice outer diameter) but for a SC magnet, the result is not so obvious due to the dependence between the magnetic field (modulus and direction), and the critical current in the superconductor. The optimal solution is difficult to accomplish and there is no easy recipe for designing the magnet. Practically, all SMES realizations done so far are based on either two magnet configurations: solenoids or toroids [211, 212]. Figure 26b depicts this configuration for magnets based on pancake coils, the preferable option for HTS SMES. Solenoids have a higher energy density but also a much more intense stray field, while toroids confine most of the field inside the magnet (low stray field) but achieve a lower energy density and present an added problem when the toroid is made from circular solenoids whose axes are arranged along a circumference; the net force for every coil is non zero, trying to pull the coil towards the centre of the toroid. To avoid complex supporting structures, the coils, instead of being circular, have a D-shape, somehow similar to the toroidal coils of a Tokamak (see Sect. 4.1.1). When additional elements are added in the solenoidal version to reduce the stray field (iron yoke, compensating coils, etc.) the higher energy density advantage is reduced, especially for magnets using HTS tapes since the perpendicular component of the magnetic field can be much higher for a solenoid than for a toroid.

Like in other types of energy storage systems (flywheels are the most similar case) it becomes essential to find a figure of merit associated with the maximum amount of energy that an SMES can store per unit volume of superconductor and this is closely

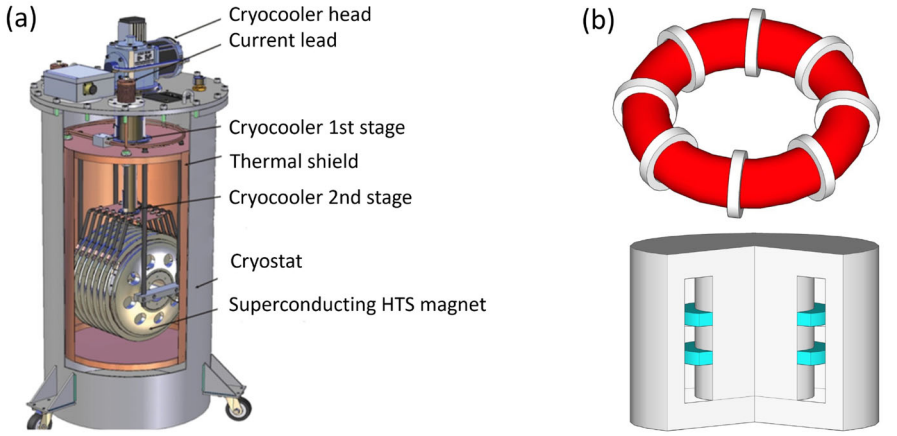

Fig. 26 (**a**) SMES prototype based on a conduction-cooled solenoidal HTS magnet. (**b**) Toroidal SMES configuration vs Solenoidal SMES configuration both based on pancake coils

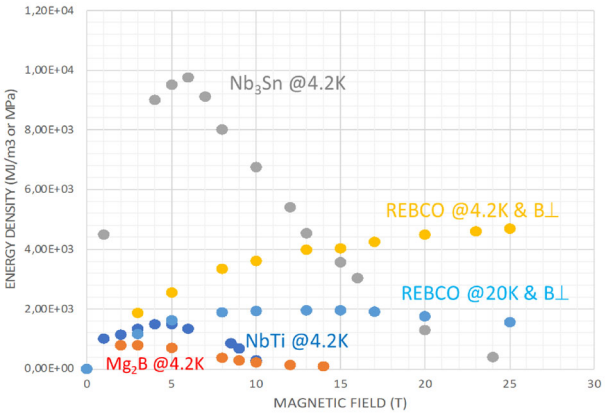

Fig. 27 $B \cdot J$ curve (volumetric energy density) for different SC wires at different temperatures (for the case of REBCO the worst field orientation has been considered)

related to the type of superconductor from which the magnet is made from. For the simple (but non-efficient geometries for SMES applications) of a slender solenoid (much higher than wider) or a slender toroid (average toroid radius much bigger than cross-section radius), easy calculations can be made to find that number which will represent a limit to the SMES performance. In fact, there are not one but two limits for the superconductor: One is electromagnetic as could be expected and it is given by $K_e \cdot (B \cdot J)$ where K_e is one-fourth of the cross-section radius and $(B \cdot J)$ is the product of the field times the current density according to the B vs J curve for a given superconductor at a given temperature. This is an interesting result because if we plot the B·J curve for different materials and different temperatures as shown in Fig. 27, we can decide which is the most "energetic" superconductor and under what conditions.

As it can be seen, Nb_3Sn @ 4.2 K working at a field of 6T should be the best option, followed by REBCO at the same temperature working at around 25 T and REBCO at 20@K working at 15 T. Values as high as 10,000 MJ/m^3 ($\sim$ 0.35 KWh/kg) can be achieved for a 1 m radius solenoid or toroid. Unfortunately, there is another limit which is mechanical and comes from the stresses induced in the SC material due to the electromagnetic forces. Again, for those simple geometries referred in the previous paragraph, the maximum stored energy density can be expressed as $K_m\sigma$ where K_m for this simple case is 0.5 and σ is the stress value developed along the superconductor. Obviously, the maximum energy density value at which a superconductor can work is limited by its maximum allowable stress beyond which its transport properties degrade. While for Nb_3Sn this maximum allowable stress is in the range of 100 MPa, for REBCO tapes it can increase up to 600 MPa, which yields mechanical limits half those values, well below the electromagnetic limit. The relationship between stored magnetic energy and stresses in the superconductors can be expressed in a more general and elegant formulation in terms of the Virial Theorem [213], which establishes that the magnetic stored energy in a magnet is the volumetric integral of the sum of the principal stresses for every elementary volume. Since the energy must be positive, the sum of stresses should also be positive. Avoiding local peak stresses and equalizing them for each direction allows maximizing the stored energy level. In this sense different strategies in the last years have been proposed to improve the performance of the SMES. To overcome the mechanical limit, solutions such as Force-Balance Helical Coils [214] or reinforced wires [215] have been considered, while for reducing the electrical limit (for the case of HTS-based SMES) more complex solenoidal shapes with variable separation between pancakes or different inner radius, have been suggested [215] to minimize the perpendicular component of the magnetic field in the superconductor (The $B \cdot J$ product for a REBCO tape can easily be one order of magnitude higher if the field is parallel to the tape and this could lead to a much higher $B \cdot J$ value for the same B value). And just as a final consideration, SMES is probably the application of SC magnets for which the AC losses become the most relevant. Since the charging or discharging time of an SMES magnet is the ratio between energy and power and since the power for SMES is high, the time can be very small and consequently the term (dB/dt), which determines AC losses, becomes high [216]. To reduce these losses, actions regarding the wire or cable fabrication must be taken, such as the subdivision of the superconductor into filaments, or the transposition of the wires. The requirement of very high currents, on the one hand, along with the importance of reducing a.c. losses on the other, has led to the utilization of special conductors (also used in other applications of SC magnets) such as the CORC conductor (see Sect. 2) [217] or the Roebel cable (After his inventor Ludwig Roebel) [218].

4.1.5 Applications to kinetic energy storage systems (KESS)

Unlike SMES (see Sect. 4.1.4), where the use of SC technology is indispensable to make the system work, in KESS, superconductivity allows improving the performance in terms of stored energy density and efficiency, basically. KESS, more commonly referred as Flywheels, are rotating masses driven by an electrical machine which acts as a motor to accelerate the mass and consequently to store energy in terms of

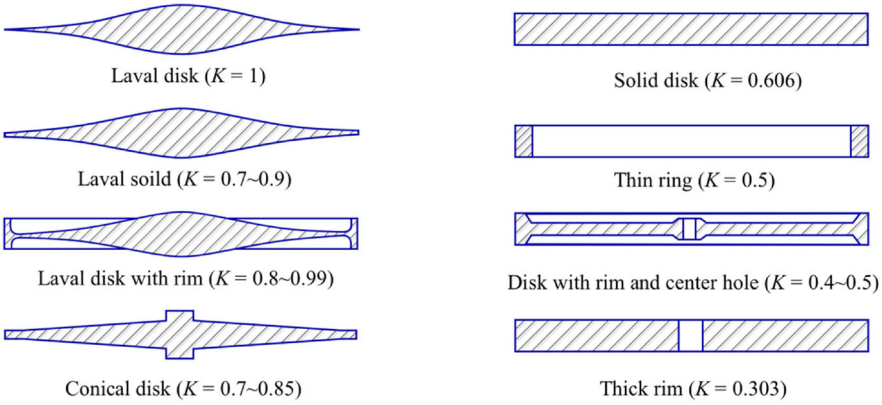

Fig. 28 Form factors for different flywheel geometries

kinetic energy, or as a generator to brake the mass recovering the stored energy and pumping it back to the grid. Although it is out of the scope of this paper, it is quite easy to demonstrate [219] that for an axisymmetric homogeneous rotating mass, the volumetric energy density [J m^{-3}] is proportional to the operational stress in the mass, while the mass-energy density [J kg^{-1}] is proportional to the ratio of the operational stress divided by the material density. The proportionality factor only depends on the geometry of the rotating mass and how stresses induced by centrifugal loads are distributed inside [220]. The best possible shape is the so-called Laval Disk (named after his proponent Gustav Laval). A prismatic cylinder will reduce the energy density to 60.6 % of the best value for the Laval Disk and, amazingly, drilling a central small hole in the cylinder, will reduce by half the energy density that it can store, since it will be unable to develop radial stresses at the centre to compensate centrifugal forces. Figure 28 shows form factors for different geometries. A high energy density is always desired, either in terms of volume to make KESS small and easy to install or in terms of mass to make it light, especially for movable applications. In both cases the "recipe" is working at the highest possible stress, which implies using materials with the highest possible yield strength. In summary, we have to make the material working at the highest possible level of stresses at the time we guarantee that it is able to withstand those stresses. This duality defines the two principal lines of research in modern flywheels. On the one hand developing strong and affordable materials [221, 222] and on the other one, taking those materials to their mechanical limits which, for the case of high mass-energy density flywheels, will be achieved by rotating light masses at ultra-high speeds while for the case of high volumetric energy density flywheels, it will be achieved by rotating heavy masses at moderate to high speeds.

High rotational speeds, in turn, represent a challenge for two of the subsystems of the storage system: the electrical machine and the guidance system besides, obviously, the rotating mass.

Conventional electrical machines have limitations in achieving high rotational speeds from both mechanical and electrical perspectives. Mechanical limitations affect the generation of the excitation field which is normally associated with the rotating

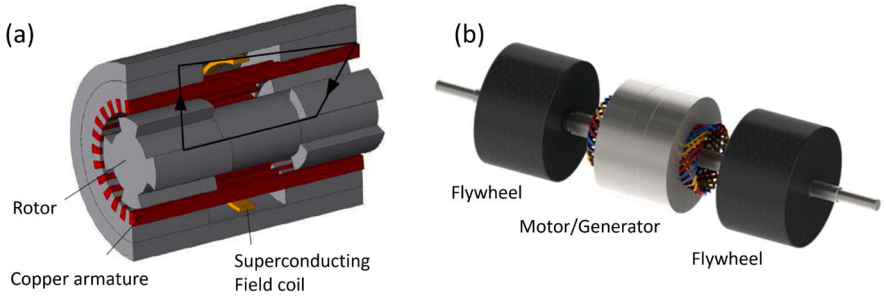

Fig. 29 (**a**) Section of a homopolar SC motor showing the flux main path. (**b**) Rendering of a double flywheel arrangement driven by a single homopolar SC machine

side of the machine. Either this excitation field is generated by electromagnets (coils) or by permanent magnets, centrifugal stresses limit the speed or the diameter of the machine. Regarding the electrical limitations, they basically appear from the high frequency at which the machine operates, which increases the magnetic losses in the iron and also in the conductor due to the skin effect. How superconductivity can contribute to extend the limits? First, conventional topologies involving rotating coils or magnets must be replaced by others with only iron, like those corresponding to switched reluctance or homopolar machines. In this respect, some realizations have been proposed [113, 223] where one step forward has been given: the introduction of HTS coils to create a stronger excitation field [224]. This coil is located on the Stator side creating a homopolar field (since the flux is closed axially instead of azimuthally, all field lines have an outward or inward radial direction for all the poles in the same section, unlike in a conventional AC machine where lines exit one pole radially in the inward direction and enter the opposite one in the outer direction). Figure 29a shows a section of an AC homopolar machine where the field is created by a stationary HTS Coil while Fig. 29b shows a rendering of a double flywheel system driven by a SC homopolar machine [224].

It is interesting to mention that the homopolar AC motor in the non-SC version has already been developed and commercialized in the past for KESS applications using a metallic rotating mass [225]. Also Switched Reluctance Machines with no rotating coils or magnets have been developed in the past for KESS applications [226]. The second challenge to solve for high energy density KESS is how to tackle the problems associated with the suspension and guidance of the rotating mass, since the loads in the bearings can be beyond the limits they can withstand. These loads result from a combination of the high rotational speed and the suspended weight. Even modern bearings with ceramic balls or fully ceramic parts are unable to withstand axial and radial loads beyond a certain speed without dramatically shortening their lifetime. The weight can be eliminated (or reduced) with the presence of permanent magnets or electromagnets. This is a common practice in many conventional flywheels [220, 226]. Nevertheless, this operation does not eliminate the radial forces since there are limits to the achievable dynamic balancing of the flywheel and, consequently to the residual loads. Additionally, ball bearings have a small but non-negligible friction which limits their

application to flywheels where energy must be stored for long periods. The solution to these limitations comes from the electromagnetism in different forms. Globally, there are available three groups of magnetic levitation systems: electro-dynamic suspension (EDS), electro-magnetic suspension (EML) and bulk-HTS suspension [227–229]. In EDS, a magnet is moved along a conducting plate inducing eddy currents in the surface which interact with the magnetic field creating a repulsion force. Eventually, the conducting plate can be replaced with short-circuited copper or aluminium coils. The magnetic field can be created by permanent magnets or electromagnets which, in turn, could be SC ones. In fact, some magnets have been developed, based on non-insulated coils made from REBCO tapes [230]. EDS is robust, economical and can be part of the propulsion system (for instance when using single-sided induction motors), nevertheless they have the drawback of generating losses and drag forces which are inadmissible for flywheels while acceptable for other levitation applications such as high-speed trains [231].

EMS is based on the attraction force between a magnet and a ferromagnetic surface and like in EDS, the magnet can be a permanent magnet, an electromagnet or an SC magnet. In this type of suspension, Earnshaw's theorem [232, 233] (which states that a number of permanent magnets and fixed current coils cannot be in stable equilibrium) is applicable implying that the levitation system requires feedback with regulation of the magnet currents to become stable. A very extended approach uses hybrid magnets (a combination of permanent magnets and electromagnets) where the majority of the force is provided by the permanent magnets while the adjustable current electromagnet contributes to stabilize the system. In this way, the consumption of the magnets is reduced to, solely, the control current and not the full levitating current. This configuration is very frequent for high or ultrahigh-speed transportation [234] and it has also been used for suspended rotating masses as the so-called active magnetic bearings where a set of coils wound in a similar way as in the stator poles of an electrical machine are energized according to the information provided by position sensors to keep the mass always centred and suspended [235]. A way to indicate the performance of the system is in terms of the levitation pressure, the magnetic pressure in this case. For a permanent magnet facing an iron surface, this pressure is given by $B^2/2\mu_0$. With present strong permanent magnets, surface fields in the range of 1.0 T can be achieved yielding a levitation pressure in the range of 400,000 N m^{-2}.

Bulk-HTS suspension is based on placing a bulk-HTS superconductor facing a permanent magnet. In this case, the superconductor will behave as a magnetic mirror for the permanent magnet creating its image with inverted polarity which produces a repulsion force (levitation) Nevertheless, there is a notable exception with respect to the case of having two conventional permanent magnets facing each other, which represents an unstable system as stated by the Earnshaw's Theorem. In the case of the superconductor, the image magnet will always be parallel to the permanent magnet, even if the superconductor tilts, avoiding any destabilizing torque. Flux penetrating in the bulk superconductor in the form of flux lines pinned to the material also acts as a stabilizing mechanism.

In a Bulk-HTS permanent magnet suspension system, the volumetric force density in a certain point of the superconductor will be the gradient of the scalar product of the magnetization vector inside the superconductor, times the vector field generated

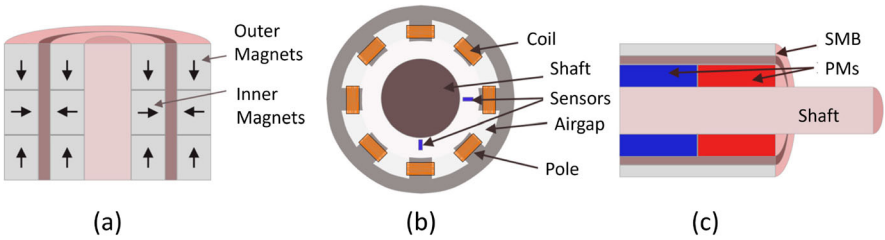

Fig. 30 Axial configuration bearing with PMs, (**b**) radial configuration active bearing based on electromagnets, (**c**) axial configuration bearing based on Bulk-HTS

by the magnet in that point ($f_v = \nabla(M \cdot B)$). To achieve a high levitation force [236], there are three aspects to optimize: (1) A high value of B, which is achieved using strong permanent magnets with surface fields in the range of 1T. Higher fields can be obtained with SC electromagnets. (2) A high magnetization of the HTS material. It is limited by the critical current density at the working temperature and in an ideal situation (where the superconductor is a perfect diamagnetic material, M will coincide with $-B/\mu_0$). (3) High gradients of the permanent magnet field distribution, which is basically achieved with an adequate geometry.

For the simple case of two close identical magnets, magnetized in opposite directions and one in front of the other (representing the model of a permanent magnet facing a perfect superconductor) the levitation pressure is again given by $B^2/2\mu_0$, the same value as when it was facing iron so, theoretically, the pressures provided by EMS and Bulk-HTS are the same. While the EDS and the EMS can be very appropriate for transportation applications where levitation must act along very long distances and the device placed on the stationary side must be cheap, this does not apply to bulk-HTS levitation for which placing superconductors or even permanent magnets all along the track is economically unfeasible. Nevertheless, this system is especially adequate for flywheels where loads are not huge and the required volumes of superconductors are small, making them economically competitive, especially compared to active bearings. Figure 30 shows schematically three types of magnetic bearings: (a) One based on a Halback array of permanent magnets. Since the system is unstable it needs the presence of conventional bearings to achieve radial stability. (b) An active bearing with electromagnets. Stability is achieved by the feedback of the position sensors. (c) A bulk-HTS levitation system.

Once the bulk HTS superconductors achieved the necessary properties in terms of critical current and flux pinning force in the range of LN2 temperature, many institutions started into incorporate them to their flywheel designs with the final goal of increasing the specific stored energy and eliminate the complexity of active bearing control. Selected research institutes and companies which have developed flywheels based on bulk HTS superconductors include: The Boeing Company in the USA [237], ATZ GmbH and Magnet Motor GmbH in Germany [238], RISO in Denmark [233], ISTEC, the Kyushu Institute of Technology [239] and the Railway Technical Research Institute [240] in Japan and others.

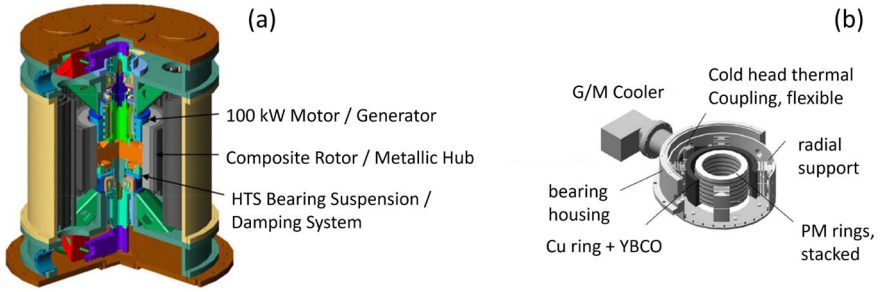

Fig. 31 (**a**) Complete SC KESS by the Boeing Company. (**b**) Bulk-HTS-based bearing installed in a KESS by ATZ

Figure 31a shows a cutaway view of one Flywheel developed by Boeing using a Bulk-HTS suspension bearing [241]. The KESS was able to store a maximum of 5kWh at a power of 100 kW at a maximum speed of 14,500 rpm. The flywheel rotor is passively suspended by a permanent magnet lift bearing which is placed at the top and a stabilizing HTS bearing at the bottom whose stator (in a later version) is conduction-cooled by a cryocooler. Same Figure part (b) shows, specifically, the suspension system of a SC levitated flywheel by ATZ and Magnet Motor. It is an axial type bearing using a multi-seed melt textured YBCO rings with PM rings inside. The SC rings are glued to an external copper ring, thermally connected to a cryocooler. It is capable of suspending loads up to 4700 N (@72 K). The rated energy is 5 kWh and the rated power is 250 kW and it works at a maximum speed of 10,000 rpm [238]. A step forward to increase the performance of the bearing in terms of levitation force consists of substituting the permanent magnets with a SC coil. The Railway Technical Research Institute in Japan developed a Flywheel based on this concept to manage the railway power consumption profile, recovering the trains braking energy and supporting the consumption during the acceleration phase [242]. The coil was on the stationary side while the bulk superconductors at the rotating one. The coil was conduction cooled and the bulk superconductors were refrigerated through the helium gas atmosphere at reduced pressure in which they were immersed. Most of the core research in HTS-bulk levitated bearings was done in the past decade and it is now when business cases start to be identified and, either already established companies or new ones, start to foresee commercial applications for flywheels using bulk-HTS bearings. One opportunity is the area of renewables, where low maintenance, a small stored-energy dissipation and a very high operation cycle capability, are required. Batteries are the perfect candidates except for the last condition. The USA company Revterra [243], for instance, is developing a flywheel based on the three progresses developed along this section: stronger materials for the rotor, motors with lower losses at high speeds and ultralow friction bearings. In this regard, they are making a 100 kWh flywheel with stand-by losses of only 50 W (it will take 2000 h to fully discharge the stored energy by its own friction).

4.2 Applications to transport

4.2.1 Waterborne application

The contribution of international shipping to the greenhouse gas emissions in 2022 was 2% of the world's global emissions [244]. Within the transportation sector, shipping represents the third position in terms of CO_2 emissions after passenger vehicles and heavy trucks and it is foreseen that unless efficient measures are taken, maritime emissions can rise by 50–150% in 2050. Which are those efficient measurements to be taken to counteract the environmental impact of waterborne transport? Different global actions have been proposed so far, including a number of specific technical solutions which can be summarized as follows [245]: (a) Harness renewable energy sources to contribute to powering ocean-going vessels (wind, solar or even waves), (b) switching from traditional marine fuels to cleaner alternatives (liquid gas, hydrogen, biofuels, fuel-cells, batteries for short distances…), (c) more efficient vessels (optimization of hull shapes, increasing the efficiency of the engines…), (d) reducing cruising speed (to decrease power consumption), (e) Leverage technological innovations to enhance efficiency (route optimization, improving on-board energy management…), (f) Providing shore power at the harbour to turn-off ship engines and to ban the use of combustion engines while staying and manoeuvering in the harbour or its proximities. How superconductivity can help to implement these actions [246]? Primarily by installing SC electric motors to propel the ship. SC motors have a much higher force and power densities. As defined in Sect. 4.1.2, a classical figure of merit for rotating electric machines is the shear stress in the airgap [247] (torque volumetric density). For a conventional machine in the range of a marine propulsion motor ($\sim$ 10–50 MW) the shear stress is in the order of 50 kPa while for the corresponding SC version, the shear stress can increase up to 350 kPa. Efficiency for a SC motor in that same range of power can also increase by almost 2% over conventional machines [248] and this affects directly to action (c) not only because the motor is more efficient but also because it is much smaller for the same thrust or power and this allows reducing the sizes of the engine room, improving the hydrodynamics of the stern or, even more, placing the motors in external pods, increasing the manoeuverability of the vessel and also its overall efficiency. Additionally, the size reduction of the engine room allows for an increase in the ship payload for the same overall size and the emission per unit load is automatically reduced. Actions (a), (b) and (f) practically involve switching to electric propulsion where SC motors can be a better option to conventional ones and, finally, improving the energy management of the ship for action (e) is also easier for electric ships which normally require electric power for other significant loads on board. This is the relevant case of cruise ships, which, besides demanding large amounts of electric power for their onboard systems, also require powerful propulsion to achieve high speeds. Other ships such as tug-boats or icebreakers requiring a lot of propulsion power are also in the group of candidates to be equipped with SC motors. A further argument in favour of electric propulsion and hence of SC propulsion is the change of shipping patterns as a consequence of demographic changes, economic developments and more advanced shipping levels and this leads to operate in more extreme

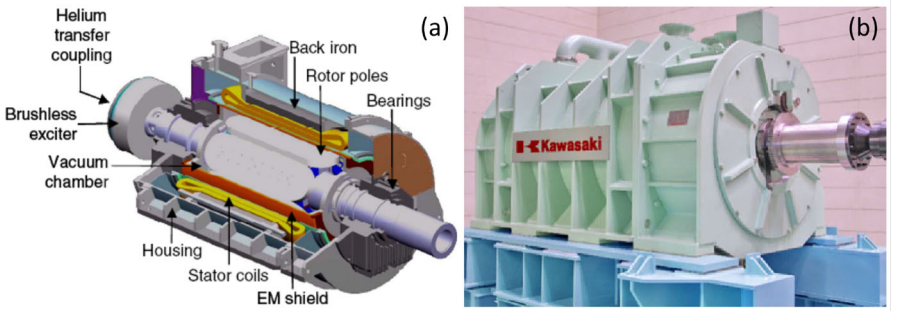

Fig. 32 (**a**) Configuration of the AMSC 5 MW prototype. (**b**) The 1 MW prototype for podded propulsion developed by Kawasaki

environments requiring vessels that can provide more power, in a more efficient way [249].

In this regard, the marine transport sector shares with the renewable sector the same interest in augmenting the volumetric torque density of the electric machines, since in both cases we are dealing with low or very low rpm applications and the only way to increase power density is increasing torque density. Most of the relevant developments done in the naval sector are based on the field SC synchronous generator topology as those described in Sect. 4.1.2. Siemens developed a series of three machines [250] consisting of a demonstrator, a ship generator and a ship motor, respectively. They all had excitation winding based on Bi-2223 and an iron-cored on the rotor side, while at the stator, they had copper armatures and nonmagnetic cores without iron teeth. There was only an outer iron yoke for shielding. The elimination of stator iron led to a big reduction of radial forces and a simplification of the supporting structure. Among all the list of naval propulsion developments done in the past, probably those realizations from American Superconductors (AMSC) are the most notorious. In 2016, AMSC and Northrop Grumman Corporation successfully tested a 36.5 MW HTS ship propulsion motor, based on a 5 MW prototype developed in 2008 [251, 252] whose internal configuration is shown in Fig. 32. This second prototype is less than half the size of a conventional motor and weights only one third of it. It operates at 120 rpm producing 2.9 MNm of torque.

Kawasaki also developed a 1 MW-class HTS motor [253] operating at 190 rpm for podded ship propulsion, which led to a reduction of the size of the stern hull and improved the hydrodynamic efficiency. More recently, they built and tested successfully a 3 MW-class motor operating at rotating speeds between 20 and 160 rpm and loads up to 180 kNm with efficiencies up to 98% [254].

Besides all these approaches based on HTS synchronous field SC machines, there has also been a recent proposal based on LTS and the same topology. General electric (GE) presented in 2019 a notional design of a LTS version in the range of the AMSC motor, also producing 36 MW at 120 rpm [255]. Apart from the conventional approaches for marine HTS motors based on either only field or fully SC synchronous motors, other configurations have been proposed. The main goal of those configurations is to avoid rotating SC coils (and consequently rotating cryostats) and also to

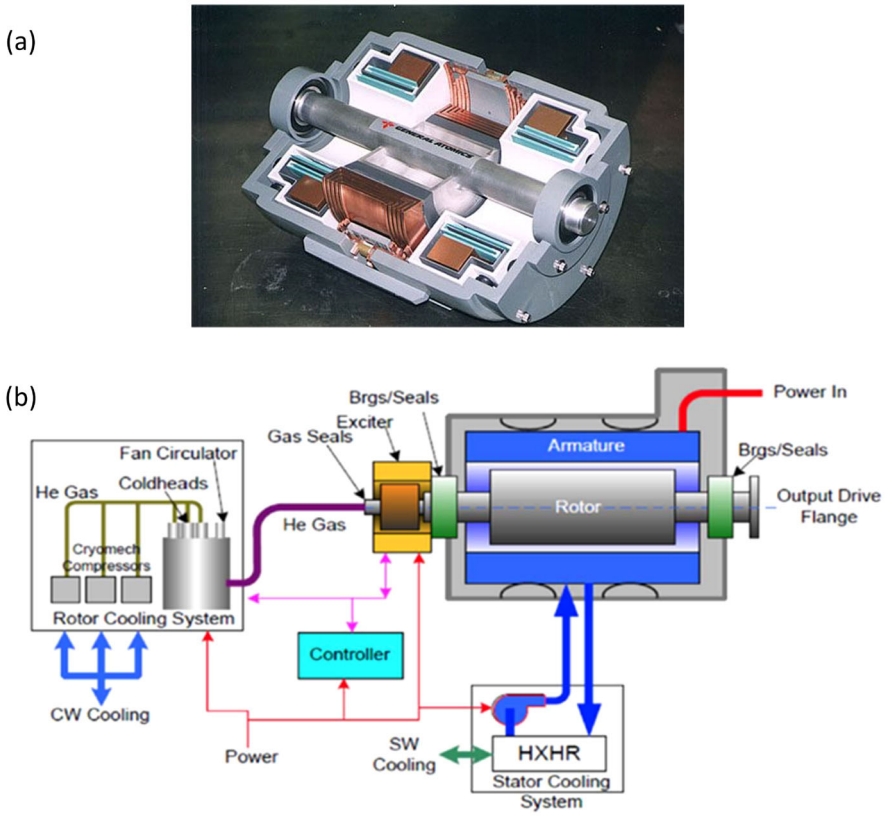

Fig. 33 (**a**) Homopolar SC Motor by General Atomics. (**b**) Cooling scheme for a SC field machine based on He gas

limit the use of superconductivity to the coils on the DC side, eliminating the problems associated with AC losses. In this regard, a compact version of the Faraday's Disk (The homopolar DC motor) was developed by General Atomics [256, 257] making several prototypes of such machine: a 300 kW prototype, a 3.7 MW and finally a 36.5 MW working at 120 rpm. They are truly DC machines and their main issue is the need for brushes (moving contacts) for those enormous currents. Figure 33a shows a section of their SC homopolar motor while Fig. 33b depicts the cryogenic scheme for a rotating field SC motor which is cooled down using gas helium, a preferred option in the marine sector due to its reduced asphyxiation hazard as well as the wider operating temperature margin.

A relatively recent line of activity proposes the use of a Modified Permanent Magnet Vernier type machines for marine SC motors [258, 259]. Due to the significant low speed-high torque advantages, Vernier machines have become potential enablers for direct-drive applications like this one or others such as wind power generators where some realizations have also been proposed. The modification over classical permanent magnet vernier machines consists of the substitution of the permanent magnets with SC

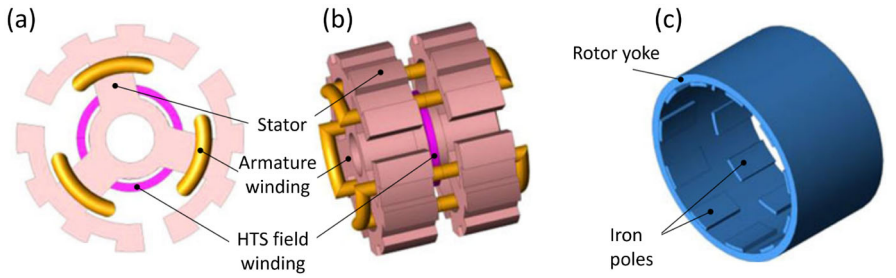

Fig. 34 The two sides of a SC Vernier Type Motor as extracted from [258]. (**a**) and (**b**) Stator with the armature winding and the field winding. (**c**) Passive rotor

coils in their own cryostat. Which is then the advantage of SC Vernier machines over field SC synchronous machines? Since Vernier machines have no coils in the stator but simply a slotted iron cylinder, the stator can become a rotor without introducing any special difficulty and this allows the rotor to become a stator keeping the coils stationary and avoiding rotating cryostats (Fig. 34)

Other approaches have been proposed for SC marine motors like a synchronous one based on a double-helix magnet to create a dipolar field very similar to the so-called canted magnet used in particle accelerators dipoles. This magnet constitutes the rotor of the machine with an SC stator which uses a flux pump [260].

To finalize this section, a short mention to magnetohydrodynamic propulsion which is based on the circulation of seawater inside a volume where an electric field, which generates a current in the water, and a perpendicular magnetic field are both applied perpendicularly to the direction of the motion of the water, generating a force on it. Like for other electromagnetic machines, the force will be proportional to the product of the magnetic field times the current, while the losses will be proportional to the water resistivity times the square of the current. Consequently, to increase the overall efficiency, moderate currents and high magnetic fields are mandatory. The most important realization done so far was the Yamato-1 prototype in Japan [261] in 1985. It used a NbTi-based magnet achieving 4T and an efficiency of 30%. Recent successes in high-field HTS magnets for fusion (see Sect. 4.1.1 have given renewed interest to this type of propulsion. With a 20 T magnet, for instance, efficiencies up to 90% can be expected. Now the challenge is focused on solving another problem: eliminating the corrosion issues in the electrodes [262]. Electric SC motors and generators are the core contribution of superconductivity to more sustainable and efficient shipping but not the only one. Moreover, implementing superconductivity on board must be a global effort affecting the complete vessel, especially for all-electric ships, as it is also for planes as mentioned in Sect. 4.2.2. The full integration of SC components (motors, generators or cooling systems) with non-SC systems (distribution, power electronics or protections) constitutes a necessary exercise in order to optimize the advantages of using HTS on board [263]. In addition to electric machines, there are other SC devices which can find beneficial applications in the maritime sector. One example is the HTS power cables with their high power density for the main distribution bus [264]. Their ability to transport a high ampacity, allows replacing multiple conventional cables operating

in parallel with a single line, reducing the overall weight and volume of the electrical distribution system. Another example is the use of energy storage systems, particularly SC magnetic energy storage systems (SMES) as described in 4.1.4 which can be used to help stabilizing and supporting the on-board ship grid when overloads are required, very especially in case of vessels with electric propulsion (manoeuvering, ship starting or stopping, ship loading and unloading, etc.) [265]. This particular application can be included in action f) described in the section introduction to reduce shipping gas emissions.

4.2.2 Applications to airborne transport

The role of airborne transportation in society has been continuously increasing, and so the number of planes, trips, and accessibility for more population. In fact, air transport shows the fastest growth rate compared to other transport modes and the International Civil Aviation forecasted that by 2050 its emissions could triple compared to 2015 [266]. In 2022 aviation generated 14% of transport emissions, the second biggest source in transportation source after road transport. The fuel efficiency of conventional planes has been greatly improved in the last decades, but not enough to balance the increase in usage [267]. Emissions from aviation are a significant contributor to climate change, not only from the fact of burning fossil fuel to operate but also because of the nitrogen oxides emissions and other vapours which are emitted at high altitude: vapour trails and cloud significantly increase the net effects of conventional airborne transportation to global warming [268]. There are several measures that could be taken to mitigate the effects, ranging from logistic issues to geopolitical limitations and of course, technical improvements. The most common approach up to now has been to increase the fuel efficiency of the plane, by means of engine developments, materials, and optimal sizing according to the route and payloads [269]. Some developments related to superconductivity have been also done in the past when HTS were not discovered yet [270]. At that time the main force for trying superconductivity as empowering technology for airborne transportation was the high-power capabilities for niche applications. At these first attempts, the fossil fuels and turbines for propulsion could not be replaced, being the superconductivity used just for the electrical generator for high power and high voltage internal loads. Nevertheless, in the past decades, there was a common path to gradually substitute a variety of complex systems including hydraulic, pneumatic, electric control systems, etc... into a “More Electric Aircraft” approach where electronics and electrical power supply will integrate as many systems as possible [271]. Historically, the main limitation for full electrification of aircrafts is the power density. Airborne transport demands a very high power density (also known as power-to-weight ratio PTW) to be feasible as propulsion technology. As a rough comparison, commonly needed values are around 10 kW/kg, while conventional electric motors are about one order of magnitude below (Fig. 35). Intense R&D efforts are being developed to improve this value and even surpass this rough threshold for both kW and MW power levels. They are using advanced designs and materials, including rare-earth permanent magnets with promising results also for airborne applications in the future [272]. Up to now, electric aircrafts have been limited to very specific niches of applications such as small and very short-ranged unmanned aerial vehicles (UAV)

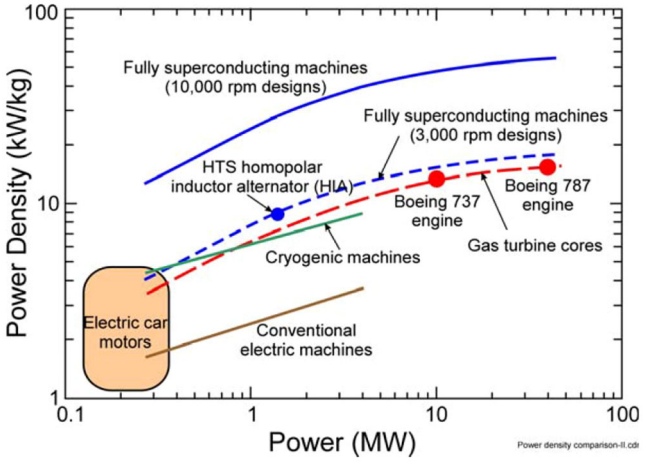

Fig. 35 Power density chart of electric machines [130]

for surveillance, weather monitoring, or air taxi helicopters for city mobility which are not so power and range demanding.

The SC technology could provide significant improvements in two different approaches: hybrid and full electric (Fig. 36)

The hybrid-electric aircrafts include fuel turbines plus SC machines for reducing emissions, fuel-burn, and noise, which are the main required parameters by EU and US for future aircrafts [273]. This approach is also interesting for military aircrafts to increase the electrical power available, making it possible to install MW-class electric systems on board to be used, for example, for electromagnetic launchers and other uses [274]. Two main architectures are being explored: hybrid propulsion and turbo-electric propulsion [275]. It is not so straightforward that a hybrid approach, which requires a certain level of complexity and even duplication of components could result in a positive net result in this field where mass and volume are so critical. The point is that this could provide a breaking change in the design and efficiency of traditional engines for large aircrafts.

The majority of large civil transport are propelled by turbofan engines: a large fan is coupled to a turbine providing most of the thrust to the plane. Part of the air impelled by the fan (defined by the "bypass ratio") is guided to the engine's core, where the fuel is burnt. Exhaust gases are used by turbines to provide torque to the fan shaft, and finally some propulsion thrust is also received by the plane. This scheme is the result of the optimization from previous generations such as turbojets, but conceptual limitations could be foreseen: turbines naturally develop higher efficiency and power density at high speed, while the fan performance is sensitive to its size. Values in the order of ten thousand RPM and high bypass ratios are the most common solutions in modern aircrafts. Being the turbine and the fan connected by a common shaft was therefore a great advance from previous generations which is getting to a technical limit: a hard limitation arises when the tips of the blades are getting supersonic conditions and the efficiency severely drops. Hybrid electric aircraft technology would incorporate an

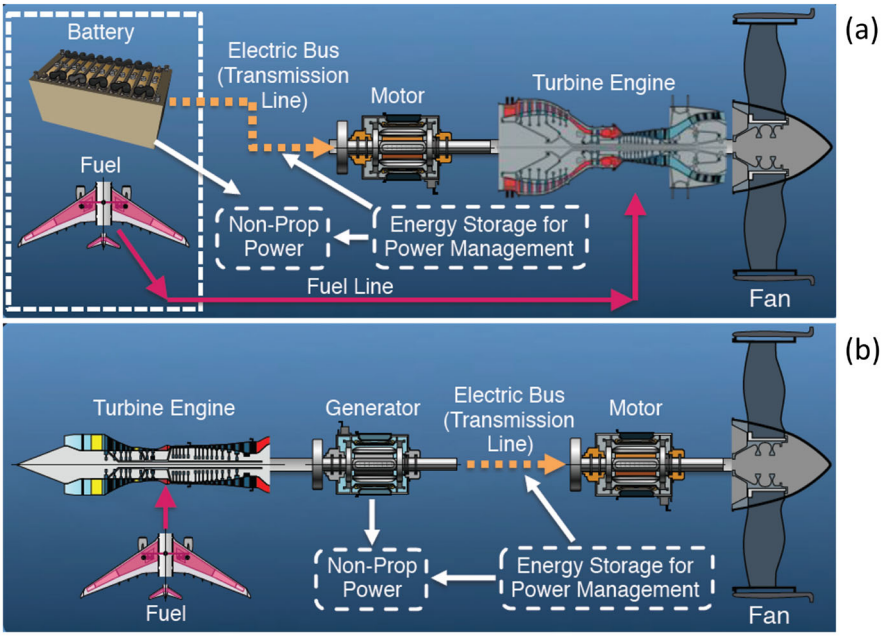

Fig. 36 (**a**) Hybrid electric, (**b**) Hybrid turbo electric, Ref. [275]

electric motor/generator connected to the fan and turbine shaft (direct drive). It could provide torque from electrical energy storage reducing fuel consumption. It could also provide additional peak power when needed (take-off, for example), making it possible to use smaller turbines, or more efficient ones, for cruise speeds. During the take-off, all the power is needed, while just about 60% at cruising speed. The Hybrid Turbo-electric approach is one step further, where the turbine and the fan are completely detached. The turbine could be optimized without the constraints of the fan blades and connected to a generator to produce electric power. This electricity could be stored, converted, or directly used to drive a motor coupled to the fan which, again, could be optimized as an independent component. Electrical motors and fans could provide even better efficiency at low-medium power levels compared to turbines because speed and torque can be independently controlled. Besides the first critical parameter already mentioned (high power density), the second one is the high-speed operation: the generator machine must be coupled to a turbine which is best suited for high speed. On the other hand, torque specification is not so critical, opposite to the usual situation in green power generation applications. For full electric large aircrafts, HTS technology is the only option for propulsion in most of the applications due to the PTW value compared to conventional electric machines. In this concept, as there is no turbine powering a generator, the specification on the shaft speed is not so high, but relatively high values are needed (in the order of one thousand RPM). Both the superconductor generator and motor designs for airborne applications are based on the same physical laws and technological issues already explained as any other SC motor or generator, with a highlight on the importance of the PTW and high speed.

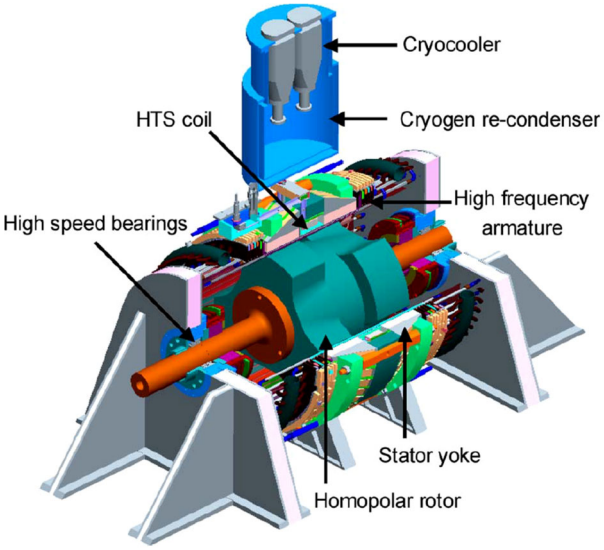

Fig. 37 Homopolar inductor alternator (HIA) design

Finally, airborne machines should be highly reliable: the margin to active corrections or even secondary systems is limited in this field, while the impact of a failure is very high. Because of these reasons, research on the application of SC machines for aircraft propulsion has started relatively late compared to ship propulsion or power generation. Previous experiences in these fields cannot be directly used for aircraft applications, especially the requirement of high speeds when a turbine is to be connected. Gearboxes could be considered but as already explained in previous sections, are prone to defects and additional weight to consider. On the other hand, the direct drive configuration of a SC machine having windings rotating at high speed imposes new challenges. Different possibilities have been explored, for example keeping the HTS materials in the stator (partially superconductor design), simple geometries (cylindrical coils), and HTS bulk materials. One of the possibilities, also explained in Sect. 4.1.5, is the homopolar inductor alternator (HIA) (Fig. 37), such as the one from general electric, designed for 5 MVA generator and 9 kW/kg [276]. HIA is a good candidate when high speeds are needed. The HTS coil is wound in the stator to provide a stationary field, therefore coil geometry and supports are very simple, and centrifugal forces are not present on it. The stator includes also one iron core at each side of the HTS coil and the rotor poles are equal but aligned at different angles. The cryogenics can be quite simple as no cryogen flow is mandatory. Cryocoolers installed in the cryostat are enough. On the other hand, the field is reduced and constrained by the iron saturation of the rotor. Therefore, the magnetic field is quite similar to conventional machines and very high speeds are required to reach MW values.

The other main candidate is a fully superconductor synchronous generator [277], similar to the ones exposed in the renewable energy section. This is the most common architecture being explored at this time because the PTW for these machines is related

to the product between the magnetic field in the air gap and the current on the coils (shear stress as defined in previous Sect. 4.1.2). Thus, iron-less fully SC machines are, in theory, the best solution as they can maximize both parameters. Given the expected high variable dynamic loads, the SC motors for demonstrators are more commonly focused on a slow-speed synchronous motor. The relatively low speed of the rotor reduces the risks on the cryogenic joints and limits the AC losses, which are important constraints as will be explained later. Cryogenics joints and seals are considered a critical technology to be improved in the future for enabling HTS motors in this application, while AC losses are more related to the materials development and/or the cryogenic power availability. Some studies have focused on any possible variation of SC synchronous motors for aircrafts, like [278], from the topologies to the materials combinations both resistive and superconductive for stator and/or rotor. Concepts based on resistive stator and HTS rotor get advantages related to DC current in the SC coil plus the simplified conventional stator. Radial flux machines are typical but also axial flux machines have been proposed [279]. Fully superconductive machines are usually iron-free to reduce weight while reaching magnetic fields higher than the saturation limit of iron (iron shields for limiting fringe fields are anyway needed, the case can cover this function). In any case, the designs are oriented to use as simple coils as possible (solenoids and planar racetrack or double pancake are the main ones). Some other alternatives include advanced wire/cable concepts [280], permanent magnets [281], or superconductive bulk materials [282]. SC linear motors have been also proposed for specific applications such as landing gear actuators [283]. Regarding the materials, MgB_2 [284] and REBCO [285] are the preferred ones to increase, as much as possible, the operating temperature. Besides generators and motors, other components of the power system could be improved by means of superconductivity, such as power trains, bus bars, and fault current limiters (some examples at [286–288]). These can apply to the completely zero emissions aviation scheme and the hybrid schemes. It is important to note that once the cryogenic system is included, it can be more cost-effective if more superconductive devices are included to take advantage of it. The aerospace field is also incorporating other components made of superconductors for electronics and sensors [289]. For cryogenics in airborne applications, there is of course a need for a highly reliable and effective cryogenic system onboard. There are two main possibilities at first sight: liquid cryogen tanks and electrical cryocoolers. From the point of view of efficiency, the first one is the best, but the volume and mass of this tank could be larger than the cryocooler option. Of course, the temperature and thermal loads are critical to determine which approach could be the best one. The first common choices would be LHe or LN2. Helium because of the lower temperature and nitrogen because of its low cost. There is an interesting alternative: liquid hydrogen. Liquid Hydrogen gives a compromise between being cold enough for nice SC properties but warm enough for cryogenic efficiency, while the raw material cost and availability are more convenient than Helium.

Based on these conditions, a liquid hydrogen tank should be provided and refilled for each trip. Refilling should be quite similar to the actual fossil fuels in terms of time, and much better than batteries recharge and/or replace. Additionally, a very interesting synergy can be exploited by combining liquid hydrogen and HTS operating at the boiling temperature of this cryogen (20 K): The liquid hydrogen could serve both as

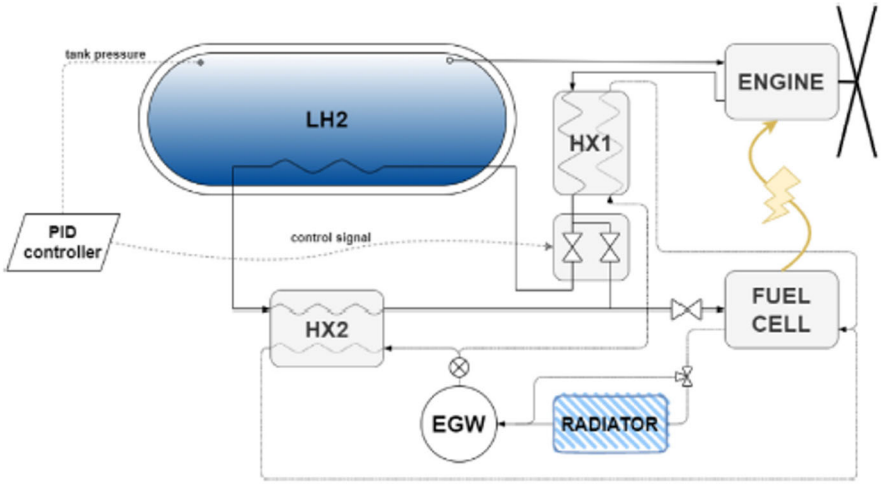

Fig. 38 Fully electric scheme with liquid hydrogen and fuel cell

cryogen and fuel. It can be improved even further if hydrogen is used and the turbine is replaced by a fuel cell: it becomes a clean electricity generator, with no emissions at all from the plane. Using green hydrogen would assure zero net emissions for the whole cycle. This would be a complete full electrical aircraft: the liquid hydrogen evaporation would be used for cooling the SC coils of the motors which will produce the thrusting force from electricity produced in the fuel cell [290] (Fig. 38).

There is, of course, a long path to go before this scheme is proved. Two important problems are to be solved: The main one is cost: this scheme is promising, but the "hydrogen colour" should be green for the environmental advantages (grey hydrogen is by far the most common one and it is refined from fossil natural gas) and its cost is yet too high. A large number of projects and investments are put in both public and private companies to reduce the costs and find actual and imminent applications to elevate the demand [291]. Secondly, the overall efficiency of the liquid hydrogen as an energy vector and its conversion in an embarked system where reliability and safety are critical [292]. Hydrogen is an explosive substance and the density ratio from cryogenic liquid to ambient gas is large. Important dynamic loads and pressure changes are probable in this application which increase the risks and the difficulty of a successful design. Nevertheless, hydrogen has been part of aviation history from balloons and zeppelins to space rockets and more recent developments first as combustion fuel (both alone or mixed) [293]. The historical reasons focused on the density of hydrogen. It is so low, even in liquid state, that its specific energy could be as much as 2–3 times better than fossil fuel (about 33 kWh/kg vs 12 kWh/kg). The counter side is that the volumetric energy density is much lower even liquefied (2.4 MWh/m^3 vs 10 MWh/m^3). Intermediate approaches are also being explored, where warm hydrogen is used in a fuel cell for electric generation while the cryogenic system is Helium based for superconductor refrigeration. In such cases, two independent systems can provide a safer approach with the advantages of the better-established Helium technology [294].

One promising project ongoing about these concepts is the Airbus' Cryoprop project [295]. It represents an initiative to develop a 2 MW superconducting electric propulsion system for hydrogen-powered aircraft, leveraging cryogenic cooling via liquid hydrogen and a helium recirculation loop. This system integrates superconducting cables, motors, and cryogenic power electronics to address the critical challenge of high PTW for aviation electrification. By utilizing liquid hydrogen as both fuel and coolant, Cryoprop takes advantage of superconductivity to improve the current densities up to 100 times higher than conventional copper systems. The helium loop ensures thermal stability, minimizing energy losses while cooling the superconducting elements. Cryoprop aims to validate weight reductions of up to 40% in propulsion systems compared to traditional designs, with projected fuel savings critical for long-range hydrogen aircraft.

4.2.3 Applications to terrestrial transport

When focused on terrestrial transportation, there are quite different agents in this heterogeneous group which account for the majority (around three-quarters) of the transport emissions [296]. The circumstances are very different for the cases of small or large vehicles, for short or large distances and for light or heavy loads to be carried. It is also convenient to distinguish between city or intercity mobility, private or public, programmed or not, and exclusive or shared paths in streets, roads, or railways. There are possibilities for HTS materials to virtually become part of any of them in the future, because of the known advantages that they can provide: specific power, efficiency and emissions reduction. Of course, some other technologies are competing and the situation of HTS performance in terms of current and temperature is very restrictive for most of the applications at this time. Still, the future performance of SC materials could change if their technology keeps evolving in terms of capabilities and costs. This chapter will briefly review the actual working examples and some general views on future developments. For the terrestrial transportation field, trains are one of the flagships of the superconductivity applications because of three reasons: First, the train sector has a well-established technology based on electrical motors, which is not the case for other transport methods. Second, they are operated in railways so the path to follow is perfectly defined and it can be controlled as desired (it can also be a dedicated railway). Third, they are driven by professional operators and used for medium to high loads, from public transport of people to private transport of goods, in a controlled grid. Given all of these circumstances, the trains are well suited for innovations: relatively fast implementation, controlled environment and favourable scale size for testing the improvements, at least at the advanced railway technology development poles: good examples are the huge activities devoted in Japan and Germany in high-speed transportation or worldwide in the hyperloop initiative. HTS technologies could be part of the next generation of trains in three main areas: levitation, propulsion, and power transmission. Considering the levitation, which already existed based on LTS magnets, HTS can provide higher efficiency from the lower cryogenics needs. Regarding propulsion, HTS motors could be an interesting alternative as they are in other kinds of transport. Finally, power transmission is a possibility because of the rail-guided nature of trains, which fits nicely with static supply lines.

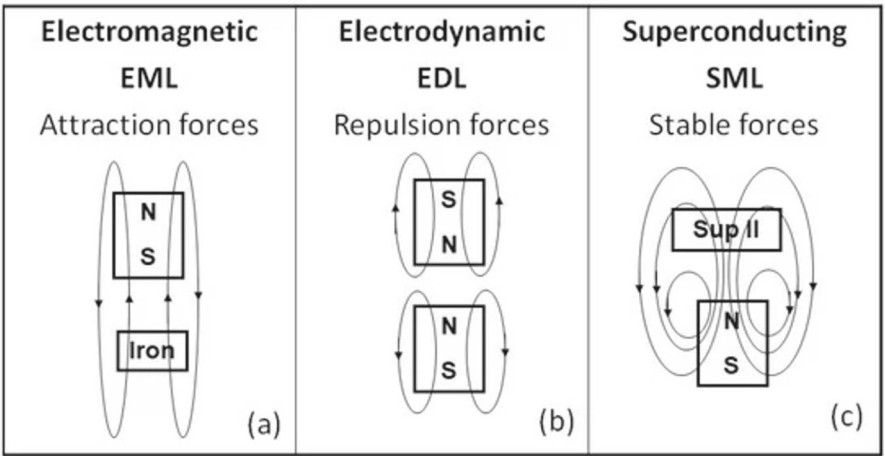

Fig. 39 Magnetic levitation (MagLev) modes [298]

There are three main modes of levitation in trains (MagLev) [236]: electromagnetic (EML), electrodynamic (EDL) and SC magnetic (SML) (Fig. 39). Only EDL and SML types can use superconductivity. The physics behind them is the same as magnetic bearings already explained in Sect. 4.1.5: the main parameter involved is the magnetic pressure (related to the magnetic field). The stability of the suspension force is also critical for these applications. EML is based on the attraction between coils in the rails and the electromagnets installed in the train. It is providing levitation but an additional linear motor is needed to move forward. EDL is based on the induction of current in conductors (rail) by moving magnetic sources (train). The moving magnetic source could be permanent magnets or SC magnets. The combination of magnetic forces could produce not only levitation (guiding) forces but also a linear impulse for acceleration. As relative speed is needed, this scheme cannot levitate and/or start the movement by itself, so wheels and additional coils for starting the movement are still needed. SML is based on the interaction between permanent magnets (rail) and SC magnets (train). This provides stable levitation even at low speeds/static [297].

SML levitation of trains started its development around the 1960s based on LTS. In 2000, the first man-loading HTS Maglev demonstrator was tested in China [299]. It was using YBCO bulk material and LN2. Since then, other testing facilities around the world have been created or oriented to further develop this technology and/or demonstrators as will be explained later. HTS propulsion of a train could be done just at the train side. This would make it possible to take advantage of the superconductivity in the actual railways, while conventional and superconductor trains can share the system looking for the overall optimization and a cheaper transition. The concept, in this case, is quite similar to other applications already explained: a SC motor replacing a conventional one to reduce the weight and slightly better efficiency. The drawbacks are also the common ones: cryogenics system and reliability for an embarked system. In this case, the synchronous motor is again the most common preferred solution for ongoing projects. Nevertheless, while some applications must consider important

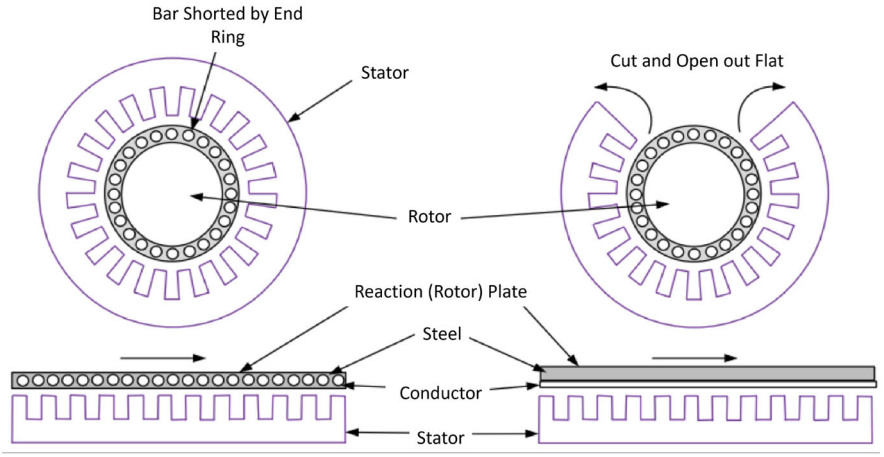

Fig. 40 Structural conversion of linear induction motor (LIM) [301]

constraints such as high speed (airborne) or high torque (wind energy), there are no critical parameters for trains, so the possibilities to look for the best combination in terms of compactness, lightweight and efficiency are open. The specifications are completely different for a levitating train. As there is no contact between wheels and rails (or at least not along the whole trip), the system must provide non-contact forces and so different propulsion schemes are needed. There are two basic configurations for the propulsion system of a Maglev system: Linear Inductor Motor (LIM) and Linear Synchronous Motor (LSM). They can be explained as the result of "unrolling" the circular versions, as shown in Fig. 40 for a LIM. LIM motors have been preferred for low to medium-speed maglevs, while LSM is chosen for high-speed and the SC versions because of higher efficiency [300].

Two significant advances can be obtained compared to conventional wheels: lower friction which results in higher efficiency, and better control of the interface between train and rails, which results in the possibility of higher speeds and reduced vibrations. They produce no emissions and low noise from the train. They can also operate on higher ascending grades than traditional railroads (typical values are 10% compared to 4%). The main disadvantage is related to safety in a situation of malfunction of the system (or a quench if magnets are SC). Additional braking and guidance systems should be defined. The drawback is a more expensive and complicated rail design and operation: copper coils or rare-earth permanent magnets installed along all the rails. Any development on the levitation side must involve the railways, which will be not compatible anymore with conventional trains. The initial costs are therefore a common limitation for this technology, even more for long distances where added difficulties can arise for crossing mountains, rivers, and altitude differences. Operational cost studies and demonstrators are therefore extremely important to verify the technology and its benefits [302]. The effect of getting HTS magnets is a huge change because this could reduce the total weight of the train components to be embarked and levitated [303], reducing the power needs but also the amount of rare-earth permanent magnets.

Fig. 41 (**a**) Aerial view of Maglev-Cobra demonstrator in Brazil

However, using SC materials in the rail is prohibitive for any practical distance at this time. The number of research groups, universities, and projects working in SC trains for test lines or experimental devices is large, some of them are the Yamanashi Maglev Test Line in Japan [304] based on a SC LSM motor, Maglev-Cobra demonstrator in Brazil [297], and the maglev ring test in China [305].

Apart from the motors, some other onboard electrical components of a train could be improved by SC technology. One of the most critical parts (and up to a few tons of weight) is the traction transformer. It is devoted to transforming AC voltage from the grid to the appropriate value for the motors. For example, a 6.6 MVA HTS traction transformer refrigerated by subcooled LN2 is being developed in China [306] (Fig. 41), with an overall weight reduction of 33% compared to the conventional equivalent one (Fig. 42).

Some other possibilities are being also explored looking for compromise solutions. For example, SC linear actuators in the stations for the first acceleration of the train, when maximum power is needed, but conventional railways and smaller electric motors are installed in the train for cruising speed along the route. If the rail is to be replaced by an evacuated tube, the hyperloop concept [307], all of the previous possibilities should be redefined as the specifications could drastically change: the installation cost of the cryogenic rail could be lowered (in relative terms) if the evacuated tube is to be manufactured. Maintenance costs could be reduced because it would be in a much more controlled environment and vacuum insulated. The dramatic change in aerodynamic friction could reduce the power specifications of the motors. Linear HTS acceleration system at the station could provide a significant amount of the power needed for the whole trip, especially if HTS levitation electromagnets are embarked instead of the conventional heavy permanent magnets or copper electromagnets. The HTS Maglev-ETT is an example of a SC hyperloop design [308] (Fig. 43).

HTS Power transmission in trains is the last possibility to be covered here. It can provide significant advances to the overall efficiency, even for non-SC trains. The main point is that the instant power that a train needs is not constant along the trip. Its maximum power needs are typically located in the station areas, where the whole train must speed up a huge inertia. One clever approach is to recover the braking energy from the trains getting into the station and releasing it to the starting trains leaving the

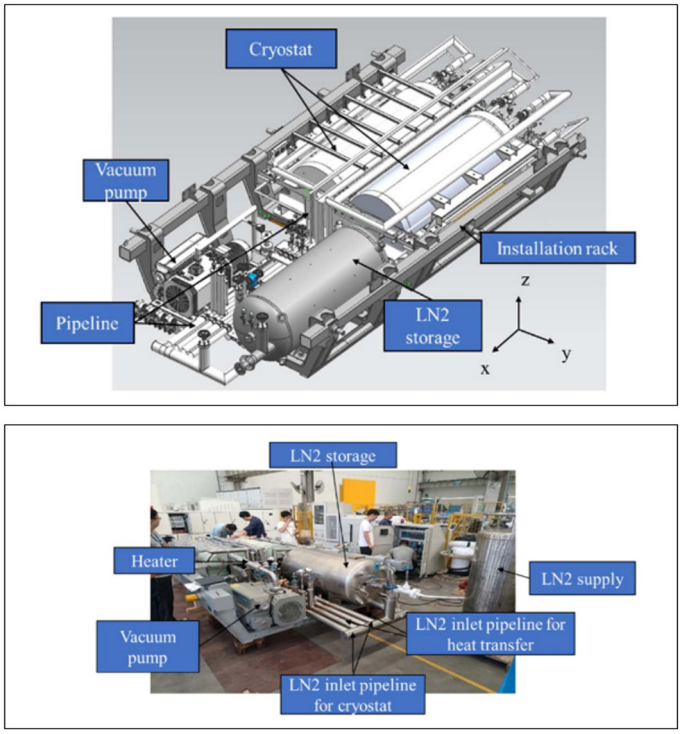

Fig. 42 Concept design and test setup of the 6.6MVA HTS traction transformer [306]

station. This can limit the overall net power needed in the station, but it is not always easy to synchronize the instant energy requirements, and it could not be even possible at small stations or certain time slots. In any case, it does not reduce the installed power capabilities of the station itself. Therefore, SC power transmission inside the stations and/or the connection between the station hub to the power station is an interesting option to increase the efficiency of the system (Fig. 44). This can be applied to any kind of electric train, including conventional resistive ones, and projects have been launched in this direction for subways and local train hubs [309].

SC applications for road transportation are being also considered. Theoretical examples or scale demonstrators on transferring the HTS levitation technologies to roads can be found for being used by any kind of vehicle such as automobiles or trucks [311]. SC motors are also used in cars for conventional roads [312]. The specification in power is not so high in this case: in the order of tens of kW for common-size vehicles. From the cryogenic point of view, they are usually based on LN2 for compactness and reduced cost. One of the most common configurations being developed is the partially superconductor (resistive stator coils, HTS rotor) synchronous motors as a compromise between simplicity and efficiency for lightweight at this power level. When they are improved with bulk superconductors (the conventional equivalent approach is to use permanent magnets), the magnetic field increases by one order of magnitude and the energy density up to two orders [312]. MgB_2 is also interesting for this application

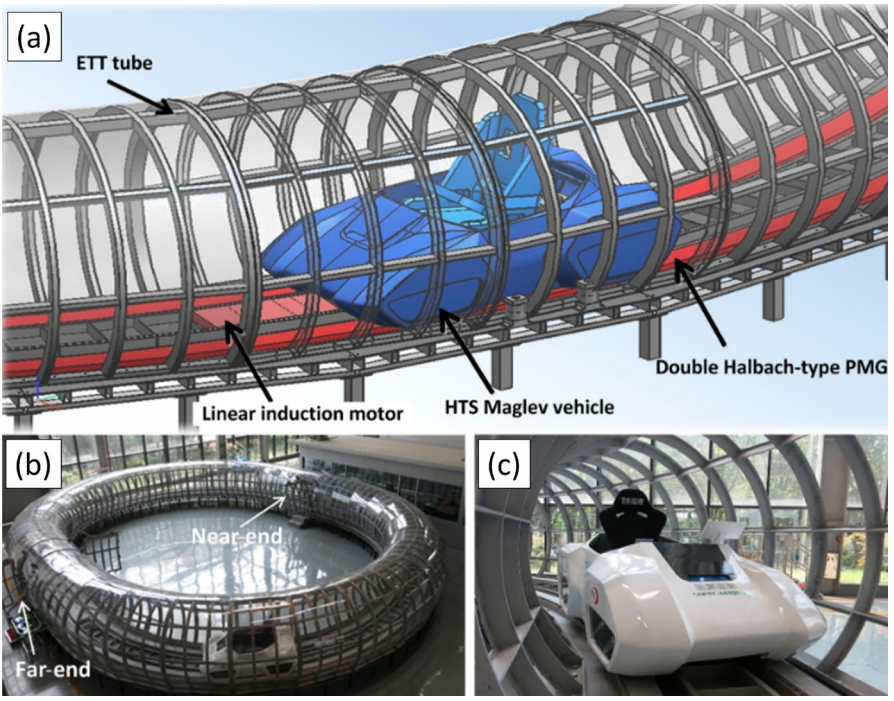

Fig. 43 HTS Maglev-ETT test system. (**a**) Concept design, (**b**) panoramic view, and (**c**) HTS Maglev vehicle

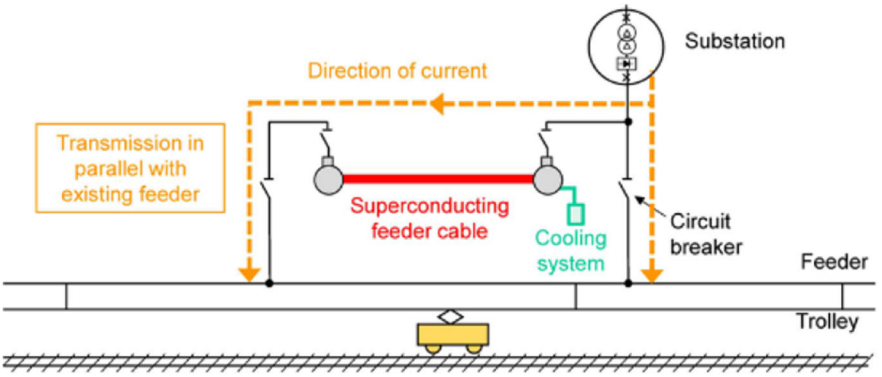

Fig. 44 100 m feeder line in operation [310]

due to the possibility of being produced in wires and its common raw materials [313]. Another possibility is a SC squirrel-cage induction motor instead of a wounded rotor [314]. In any of these cases, the electric energy should be stored or generated on board. While the improvements of the HTS on electrical motors are clear even for these power levels, it is not so clear for other systems. In the case of the energy storage system, moving from a liquid fossil tank to an advanced alternative, SC magnetic storage systems are not so well suited compared for example to batteries. SC transformers,

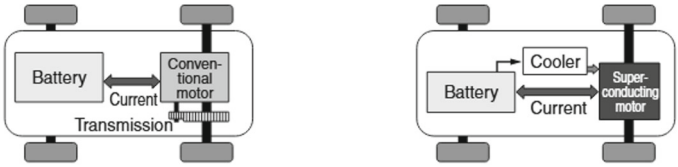

Fig. 45 Electric vehicle comparison: conventional and SC versions [315]

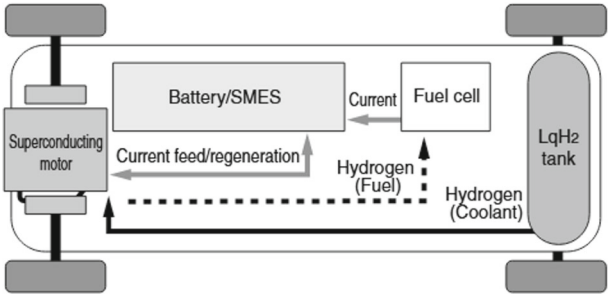

Fig. 46 Concept design of an SC car with fuel cell and liquid Hydrogen cooling system [315]

generators, and other components could be of interest in road vehicles under some circumstances if for example, renewable energy is to be produced on board.

In the future, much better performance can be theoretically achieved when combining HTS motors, regenerative braking, generation, and electromagnetic storage systems [316] if a source of cryogen is available and cheap. Liquid green hydrogen with fuel cells seems more promising in the future Fig. 45 and 46 [315], especially if this technology matures thanks to airborne transport advances. At this moment such a system seems to be too complex for small vehicles, but large trucks for long-range trips or niche applications could benefit from such full electric, autonomous, and green approach in a shorter time scale.

Finally, as an additional note; HTS technology will be probably part of electric transportation mobility even if no SC motors or devices are widely installed in future vehicles. In the scenario where a significant amount of fully electric automobiles are connected to the grid, its capabilities must evolve to take care of this new paradigm, as explained in Sect. 4.1.3.

4.3 Applications for industry

Superconductivity is also present in industry, where new commercial or niche applications can be developed or the conventional ones improved, due to the benefits that the SC technology can provide.

4.3.1 Magnetic separation and water purification

Conventional magnetic separation is a well-established technology. Their applications were first devoted to the purification of feed with magnetic components or for the

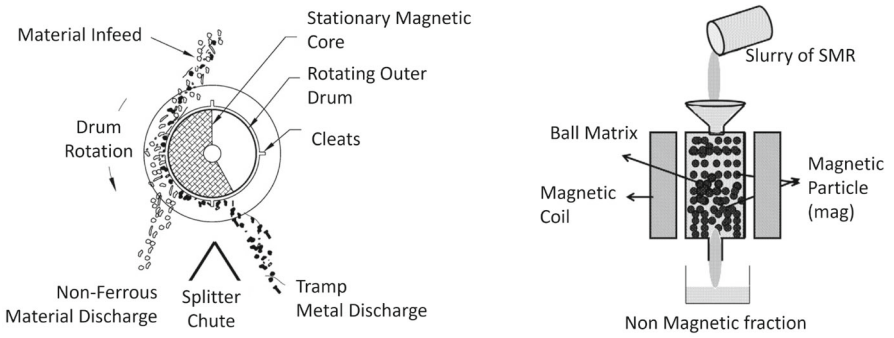

Fig. 47 Dry drum separator [319] and filtered one for wet separation [320]

beneficiation of ferrous ores and it can be as simple as a permanent magnet. The idea is to apply a magnetic force to a bunch of particles depending on the magnetic properties of each particle, based on the dipolar magnetic force. In the case of a magnetizable particle in a non-homogeneous magnetic field, the net force is proportional to the magnetic susceptibility, the magnetic induction field (the value and the gradient) and its size [317]. This magnetic force can be compared to any other competing force to obtain the desired separation. These competing forces could be the weight, adhesive forces between particles or even drag forces if the particles are immersed in a fluid. It is interesting to briefly compare different scenarios. For example, the weight and the magnetic force of homogeneous particles depend on their volume, while the drag forces depend on the length (Stokes' drag, for laminar flow) or the surface (for turbulent flow). Therefore, in dry magnetic separation where drag force is negligible, the efficiency of the separation does not depend on the size of the particles, and only purely magnetic properties are relevant. On the other hand, magnetic wet separation is more challenging when the particles are smaller (Fig. 47). The two most important values of these systems are the capability of separation (minimum size of particle and/or minimum ratio of permeabilities which are correctly separated) and the capacity (volume that can be treated for certain time) [318].

The first magnetic separators were based on ferrite permanent magnets achieving typical values lower than 1 T field and 1 T/m gradient. If replaced by rare-earth permanent magnets, fields up to 2 T and 100 T/m can be produced for certain geometries, but just for small effective volumes as the field decays quickly from the magnet surfaces. Electromagnets can provide a much more versatile solution, with or without iron yoke. For resistive separators, the volume can be greatly increased at the cost of large equipment and operating costs from the electricity. A great step further in improving the magnetic separator capability (not the capacity) is to include magnetic ancillary components (filters) in the effective volume. The magnetic field will not increase but the gradient can be enlarged two or three orders of magnitude. High field and high gradient make it possible to focus not only on the separation of ferromagnetic materials but also to separate diamagnetic particles from paramagnetic ones. It can be used to separate very small particles immersed in liquids, for water treatment or biology and health research: for these tasks a high gradient magnetic separator (HGMS) is needed,

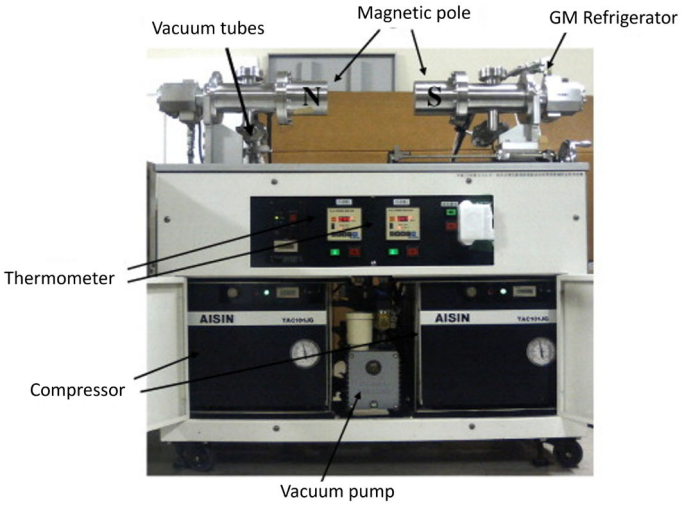

Fig. 48 Waste water purification system based on HTS bulk magnets and pulsed field magnetization [326]

reaching values in the order of 10^4 T/m, enough to separate weakly magnetized particles in the range of 10^{-1} mm [320]. When LTS superconductors were used in these systems, starting around the 1980s, the main specifications that could be improved were the effective volume for a given size, which allow for reciprocating devices (two ferromagnetic filters are alternatively used for almost continuous operation) and operational cost as the magnet can be operated in persistent current mode. Nowadays, a renewed interest in SC HGMS has been pushed by the possibilities of HTS, which provides the advantages of SC at higher temperatures, for example [321].

Water treatment is therefore one interesting application of SC magnetic separation. Both LTS NbTi [322] and HTS bulk magnets [323] can be used for water purification after industrial processes or common wastewater (Fig. 48). Being the water quality so critical from the environmental point of view, magnetic-assisted methods for purification can complement other treatments [324] for efficient and affordable management of its standard specifications for safety according to the sustainable development goals [325].

4.3.2 Superconducting transformers

Transformers for power transmission lines are designed to transfer electrical energy between two circuits through electromagnetic induction, with its primary role being to either increase (step up) or decrease (step down) voltage in an AC system. The operation of these transformers relies on AC because the changing current produces the alternating magnetic field needed to induce voltage in the secondary coil. HTS transformers, defined by high-current density HTS conductors and LN2 dielectric, have many potential advantages over conventional oil-immersed transformers. Substitution of the common copper conductor windings of a transformer by SC ones has been proven to be an effective method possible to reduce the transformers average

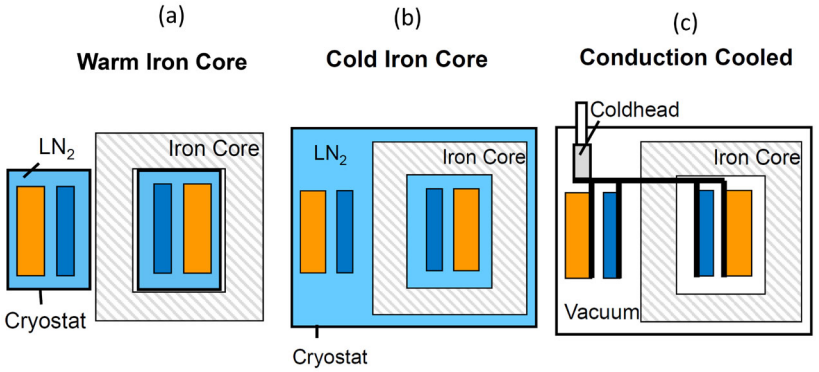

Fig. 49 Schematic description of SC Transformers in the (**a**) warm iron, (**b**) cold iron and (**c**) conduction cooled configurations as extracted from [177]

energy losses by 60% [327]. Moreover, in comparison with conventional ones of the same power rating, HTS transformers can be reduced as much as 40–60% in weight and size. Due to the zero resistance character of superconductors, SC transformers bring the advantage of a very low short-circuit impedance which limits the voltage drop during short circuits and allows for more effective handling of fault conditions without damage to the transformer. SC transformers are highly efficient because they experience minimal energy loss as heat, The reduced energy dissipation enhances the stability of the electrical grid, allowing for better control over the power distribution system and reducing the likelihood of failures [177]. SC transformers, while highly efficient, face several challenges. The use of HTS tapes leads to AC losses and can suffer from thermal runaway when overloaded, causing rapid failure of the windings. Additionally, their low thermal mass makes them vulnerable to rapid heating during fault currents. The mechanical properties of the conductor are another concern, as HTS tapes have limited formability for winding and can experience high stress from fault current forces. The use of LN2 for cooling introduces further complexity [328]. Cryogenic operation increases costs and adds difficulty to the system. Moreover, during short circuits, gas evolution from LN2 presents an additional risk, further complicating operations. These drawbacks highlight the technical challenges in implementing SC transformers on a large scale. HTS power transformer development has mostly followed conventional designs quite closely [328], employing similar iron yokes and winding solenoidal LV and HV coils around them. In the case of SC transformers, the whole structure is not enclosed in an oil-filled tank, but the windings for each phase are contained in cryostats. Regarding the design of such cryostat and the position of the iron with respect to it different designs are available [177]. Associated with the cryogenic system of a SC transformer there is a cooling energy penalty that reduces efficiency. To optimize performance, warm iron [329] (Fig. 49a) is often required, necessitating nonmetallic cryostats with core penetrations. In such a case, the cooling power required for the transformer operation is low. The drawback of such concept is associated with the complexity of the cryostat design and its consequent high cost. Moreover, in a three-phase system, three such complex cryostats are needed.

Cold iron design [330] (Fig. 49b) is also possible in which the core is kept at cryogenic temperatures within the same cryostat as the SC windings. The latter carries the advantage of a simple design of a single cryostats. Nevertheless, such a fact carries the burden of high cooling power requirements. The iron core losses at low temperatures increase the cooling power demand, making the system less efficient since the cryogenic system must cope with the hysteresis and eddy current losses that take place at the transformers iron core. A solution that solves the drawbacks derived from both cold and ward iron configurations is based on the use of cryocoolers to cool down the transformer windings by conduction (Fig. 49c). The latter option allows for simple cryostat designs with a warm iron core. However, the recovery time of the SC coils after a quench is rather long due to the low cooling capacity of a cryocooler. Moreover, such a solution does not represent a competent option for high-voltage applications.

In 1998 Worldwide first field test of a SC transformer was carried out in the framework of a 630 KVA HTS transformer project developed by ABB [329]. The design was a warm iron core transformer with Bi2223 windings cooled at 77 K that served to prove the feasibility of operating HTS transformers in the network. As SC transformer technology evolved, fault current limitation was implemented as a valuable feature of SC transformers since it is possible to facilitate effective current limitation in case of a short-circuit event in the power grid [331]. Such a transformer is called a SC fault current limiting transformer (SFCLT). It utilizes the intrinsic properties of the superconductor material in the windings of the transformer to effectively limit currents above an adjustable current threshold level. The fault current limiting feature of the HTS transformer, which is one of the most important advantages of replacing conventional windings with the SC type (see Sect. 4.1.3), provides protection and significant mitigation of circuit breaker failures and other station equipment and reduces the maintenance cost of system components [332].

4.3.3 Induction heating

There is a well-established technology around induction heating (IH) which has boosted applications in industrial, domestic and medical environments since the first patent as soon as 1887. The concept is based on Joule and Faraday laws and it can be as simple as one varying magnetic field on a conductor producing eddy currents in it, these currents will produce heat. The conventional approach is shown in Fig. 50, the AC generator can operate at a frequency between Hz to MHz, according to the specific design, for the desired application. The most important parameters are the skin depth (related to electric conductivity, magnetic permeability and the operating frequency) and thermal diffusivity: The higher the frequency and permeability and the lower the resistivity and thermal diffusivity, the more localized the heat and temperature increment in the surface are. Among other electromagnetic heating processes (resistance, infrared radiation, plasma, electric arc, laser…), IH is a high efficiency, non-contact and versatile technique ranging from the typically high power/low to high frequencies for industrial applications (low frequencies for mass heating, high for surface heating), low power/high frequency and accurate control for medical and medium frequency/low cost for domestic ones. Throughout the history of IH, the preferred solution has been typically focused on using AC current in static coils, and so the development has fol-

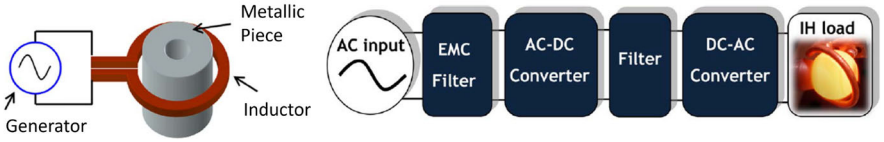

Fig. 50 Typical configuration of IH and its power conversion flow [334]

lowed the power systems evolution. Nowadays, impressive capabilities can be found and used in very intensive energy industries such as heat treatment of steels, joining metals and melting, for processing or recycling, where systems up to the MW levels are commercially available [333].

Electrical heating, and particularly IH, has been gradually replacing other heating systems for energy costs and emissions reductions. Moreover, in the last decades, SC technology has been considered for further efficiency improvements. Although, there is a major situation in this case. As already seen in previous chapters, SC are best suited for DC applications, as the AC component reduce efficiency. Fortunately, the AC component is not a must for IH even if it is used in almost every conventional IH system. According to Faraday's law the source of heating is the varying field, and it can be produced by motion instead of by alternating currents. This is a new (and old at the same time, induction motors are based on this) concept for IH which takes advantage of the great capabilities of SC coils for producing static fields while the material to be heated is moved (typically rotated) to generate eddy currents inside. The best part is the null resistance of the field-generating coils, which drastically reduces electricity consumption. Additionally, the coils can be smaller and/or the operating volume larger for a given total system size. The drawbacks are the cryogenics for keeping the SC state of the coils, and the need for one additional motor for the mechanical movement of the heated part. This last point imposes one additional limitation: the maximum magnetic field variation rate based on mechanical movement is orders of magnitude lower (tens of Hz) than the achievable electric variation of the currents (MHz). Nevertheless, this is not an issue for some of the most energy-consuming industries as they are already focused on low frequencies for higher skin depths (mass heating applications), so IH improved by SC seems to be a great opportunity for a new generation of highly efficient IH furnaces. HTS prototypes for IH have been developed since the first one in 2008, reaching power values up to 400 kW in 2023. The typical configuration includes one or two HTS flat coils and one iron yoke to guide the magnetic field and support the coils. The material to be heated (billet form) is placed in between. Once the HTS coils are energized and the magnetic field applied, the billet is rotated. Each part of the billet will feel an alternating magnetic field according to the rotation speed and, therefore, heat power and torque are generated on it. The external electric motor counteracts the torque to keep the system rotating and the heat power is completely absorbed by the billet (Fig. 51). System parameters including the rotation speed and magnetic field value should be matched to the thermal and electromagnetic properties of the billet and its size for optimized cycles.

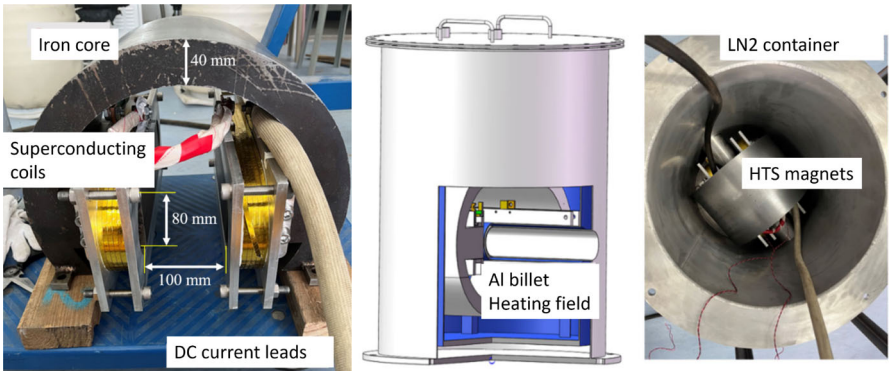

Fig. 51 HTS induction heater [335]

5 Global new trends in power applications of superconductors and concluding remarks

Previous sections have described in detail the status of the applications of superconductors in different sectors including transportation and energy generation, transmission and management and how superconductivity can contribute to develop solutions in those sectors which can impact significantly in their progress. As a summary and from a general perspective, a number of conclusions can be derived from the previous survey:

- For all the commented applications except for one (energy transmission), the way that superconductors contribute to those applications is in the form of magnets, which, with respect to conventional ones, create a magnetic field that can be far more intense. The magnets themselves can be much smaller and also more efficient, and this is why they represent a step forward in their respective applications.
- In most cases, the real advantage of using superconductors is that they allow current densities that can be two or three orders higher than those for conventional magnets. This, in turn, allows reducing considerably the dimensions and weight of the corresponding magnet and this is what really makes the difference, rather than increasing by a few percentages the overall efficiency; smaller motors for ships and especially for planes, smaller generators in offshore wind turbines or much more compact magnets for fusion reactors can make a tremendous leap in those applications. These two considerations are also fully applicable to other applications which have not been considered in the paper such as scientific instrumentation such as particle accelerators or MRI for medical applications and others.
- Most of the presented solutions are relatively old and they were previously considered in the past using LTS superconductors but some were discarded due to the complexity of dealing with temperatures in the range of a few kelvins. The advent of mature HTS tapes and wires allows a reincarnation of those applications where the advantages of operating at significantly higher temperatures or the same temperatures but with much better performances, make them very attractive.

Nevertheless, they also present for the moment, limitations which impact their application, especially those regarding time-varying field applications.

- Parallel advances in cryogenics are also helping to foster the applications of HTS magnets. The relatively recent development of cryocoolers with a high heat rejection is making possible compact and autonomous use in all sectors. The combination of the trendy liquid hydrogen with HTS magnets, especially in energy and transport can become very convenient, simplifying the overall operation.

Specifically, and according to what has been said along the paper a number of comments for each concrete sector can be presented to provide an overall perspective of potentially massive applications of superconductivity in a number of key sectors. The first comment has already been exposed and concerns the idea that those applications are mainly supported by the advancements in two areas of activity: materials development and magnet technology progress including cryogenics.

Regarding the first one, both academic and industrial efforts are steadily advancing. The academy is focused on understanding the physics behind superconductivity and the overall manufacturing scheme for each one, which are the fundamental pillars for finding the optimal paths to enhance the properties of the known SC materials and, possibly, to find new ones that could push the limits for further applications and wider usage. Critical current density is the most relevant parameter for each SC family (according to their specific temperature margins), and the most popular and promising approaches are based on the custom texturing of the materials to improve crystallinity, flux pinning, and thermoelectrical stability. From the point of view of the industry, the most important parameter to optimize is the ratio between manufacturing cost and performance for a given applied material. Non-physical variables are therefore important and are under study nowadays, such as raw materials availability, expectations on actual and future demands, and matureness of the technology. Each of the companies involved in this industry is getting their own know-how and specialization yielding sometimes in significantly different specifications between suppliers. The slow but constant evolution from NbTi (by far the most mature) to other technologies for higher temperatures or fields is resulting very promising but, at the same time, it requires a large demand for resources and investment in it: new products are made for custom designs and/or they will become obsolete quickly after a not-so-high amount of production. The general thinking in this field nowadays can be summarized as follows: there is a need for a clear and large application of a specific advanced SC material to establish standard specifications while reducing uncertainty on future demands. This ideal position could provide a game-changing leap for easier accessibility and reduced costs, a domino effect that the rest of the applications, even the niche ones, would take advantage of.

Concerning the second, the progress direction is basically addressed towards the development of magnets producing higher magnetic fields, working at higher temperatures and globally being more sustainable. On the one hand, new magnet configurations are being explored, like curved magnets to save space, simple geometries like common coil magnets for high fields in circular colliders, new coil geometries suitable for superconductors with a large minimum bending radius or stress-managed coils to deal with the large Lorentz forces in high field magnets. New fabrication and assem-

bly techniques are under development: aluminium shells assembled with a bladder and keys are more convenient for brittle superconductors; new resins, in some cases doped to increase the heat capacity; or new insulating materials able to withstand the high temperatures of the reaction cycles to sinter the superconductors. The high fields imply a large amount of stored magnetic energy, so intense efforts are being made to develop new protection methods in case of quench, with special attention to the specific features of HTS magnets.

On the other hand, most of the superconductors with high critical magnetic fields raise challenges to produce cables with large current capacity which would enable its use in fusion reactors or particle colliders. Presently, these superconductors feature large AC losses, but several research lines are being pursued to decrease their impact: finer filaments, new geometries of HTS tapes or cables made with transposed or twisted tapes and strands.

The combination of those two lines allows to manufacture magnets (and this includes electrical machines and transformers) producing higher magnetic field densities and higher force and power densities leading to more compact applications. In the energy sector, superconducting devices are starting to be highly promising when not indispensable. This is the case for magnetic confinement-based fusion reactors for which conventional magnets were practically discarded a long time ago and the first generation of magnets based on LTS have been recently replaced with HTS ones, allowing to achieve much higher fields in smaller volumes working at higher temperatures and making the full system more reliable and efficient. This application and its enormous demand for HTS tape are having a huge traction effect over the HTS production sector which is increasingly improving their performances, augmenting their available lengths and reducing their prices, also impacting other uses.

For other applications of energy generation, particularly renewable generation, the situation is different and superconductivity becomes one of the competing solutions rather than the only alternative. Applications related to hydrokinetic energy are still in the first steps (low TRLs). In some cases, such as the extraction of ocean energy, their success will be mainly conditioned by their reliability in such harsh environments. In others like low and medium-head hydropower plants and run-of-river systems, the added value relies on the size reduction and ease of maintenance of power plants located in remote regions of difficult access close to the areas they serve. For the case of wind turbines where several prototypes have been successfully developed (medium to high TRLs) the main question now seems to be the determination of the threshold power from which the superconducting solution defeats other alternatives, especially permanent magnet-based generators. Technically speaking, there is a variety of proposals closely related to those for other applications, especially ship propulsion. Nevertheless, the predominant solution is the synchronous alternator with superconducting DC excitation to avoid AC losses. A next step if HTS superconductors achieve a sufficiently low level of AC losses, will be fully superconducting alternators with both sides using superconducting coils. The case of magnetic energy storage is more evident; there is no option for resistive solutions, and the magnets have to be superconducting anyway. Their stored energy density, which is intrinsically low for these devices, is limited, curiously, by their mechanical properties (yield strength) and this means that stresses in the superconductor should be controlled. Alternatively,

the stored energy density is also proportional to the $B \cdot J$ product being the Nb3Sn the material with the best $B \cdot J$ parameter. Also, REBCO has a high value, but AC losses are a more limiting factor since the attainable wire subdivision in filaments is much higher for the first material than for the second one. Kinetic energy storage (Flywheels) is rather the opposite case. Conventional non-superconducting solutions have been running for a long time and superconductivity contributes with an improvement in the levitation/guidance systems, which allows for better performance, basically in terms of round-trip efficiency.

For energy transmission, SC cable systems have an important role to play in addressing the challenges associated with traditional power transmission lines. These are, to a great extent, related to power losses which vary from 1 to 10% in both AC and DC lines. Due to its zero-resistance characteristic, SC cable lines have the potential to minimize power losses during DC energy transmission. While AC power lines remain subjected to AC losses, advanced cable designs have been developed to effectively reduce AC-related energy dissipation. Geometric strategies allow for establishing the correct cable twisting pattern by optimizing key parameters such as twist pitch to reduce the effects of flux jumping and eddy currents. SC transmission line designs are mainly based on the use of HTS tapes refrigerated at LN2 temperature. The latter enables simpler cooling systems than those required for LTS, consequently reducing passive power losses from cooling, vacuum pumping, and coolant circulation. SC power line losses are dominated by such passive power losses which are present even when power isn't transmitted. For this reason, efficiency depends on the average load relative to the peak load, namely the load factor. It was shown that the power savings achieved by using HTS cables, outweigh their passive energy. High load factors minimize idle losses, and for 50–100% load factors with capacities of 4–10 GW, SC power losses are one to two orders of magnitude lower than those of conventional conductors. Apart from the cables themselves HTS tapes are used to limit fault currents in transmission lines. SCFCL operation is based on the SC fast resistivity increasing due to the superconductor quenching caused by the overcurrent during a fault and is especially attractive due to its self-triggered and self-recovering character.

An extremely advantageous consequence of the use of HTS power lines is related to space-reduced cross-section area due to the higher current densities that SC power cables can conduct. The use of SC lines allow to drastically reduce in two orders of magnitude the corridor widths in comparison with traditional ones.

One of the most representative examples of HTS power line application is the AMPACITY project. Such an installation has a 10 kV, 40 MVA and 1 km REBCO cable together with a SCFCL installed in the city of Essen, Germany.

For transport applications, there is an outstanding case corresponding to ship propulsion where the potential benefits of superconductivity in a scenario of increasing electrification is undoubtful. The need for more forceful and efficient ships, highly electrified, becomes the perfect scenario for introducing superconducting propulsion which is intrinsically more compact and allows the implementation of powerful pods outside the hull which contribute to improving the overall hydrodynamic efficiency of the ship and also to increase its payload. Some attempts to use homopolar motors to avoid AC coils were substituted by superconducting excitation side synchronous alternators, able to reduce significantly the motor sizes providing the same power as

the conventional ones. Additionally, a more exotic solution (magneto-hydrodynamic propulsion) is still waiting for the development of very high field magnets able to achieve much better efficiencies.

In airborne applications, the success of superconducting motors is strongly associated with the feasibility and competitiveness of the full concept of electric planes. At this moment, the energy density of the complete electrical propulsion system is lower than that of fossil fuels, even if superconducting motors are used to profit from their high-power density. Fully electrical aircrafts will dramatically change the baseline of future designs and propulsion concepts in the field, where SC technology seems to be the best candidate for future large planes. Therefore, this technology is being developed at an early stage, while the expectation is put on the future performance of the materials and cryogenic synergies are considered critical, being Hydrogen the most promising one. Finally, some of applications in the industrial sector have been addressed. While future technologies could be based on the advantages that SC can provide, at this moment, the SC technology for industry is basically focused on reducing emissions and improving efficiencies without giving big qualitative improvements on their capabilities.

Acknowledgements ICMAB authors acknowledge the Spanish Ministry of Science and Innovation and the European Regional Development Fund, MCIU/AEI/FEDER for SUPERENERTECH (PID2021-127297OB-C21), SUPERPOWER (TED2021-130004B-100), HTS-JOINTS (PDC2022-133208-I00) and FUNFUTURE "Severo Ochoa" Program for Centers of Excellence in R&D (CEX2019-000917-S), EU-COST SUPERQUMAP (CA-21144) and Hi-Scale (CA-19108), the Catalan Government for 2021 SGR 0040 and MATRANS42 (CEX2023-001263-S). CIEMAT authors acknowledge the Spanish Ministry of Science and Innovation for funding MagNext project under 2020 R&D Program, reference PID2020-120582GB-I00, and the PRISMAC program in collaboration with the Spanish Center for Technological and Industrial Development (CDTI) and CERN under contracts KE-3797 and KE-3920. CIEMAT also acknowledges the European Commission for funding the MARES Project (Proposal number 101172746 from the Call HORIZON-CL5-2024-D3-01) and the POSEIDON Project (Proposal number 101096457 from the call HORIZON-CL5-2022-D5-01).

Funding Open Access funding provided thanks to the CRUE-CSIC agreement with Springer Nature.

References

1. H.D. Stryczewska, O. Boiko, M.A. Stępień, P. Lasek, M. Yamazato, A. Higa, Selected Materials and Technologies for Electrical Energy Sector. Energies **16**(12), 4543 (2023). (**Number: 12 Publisher: Multidisciplinary Digital Publishing Institute**)
2. D. Larbalestier, A. Gurevich, D.M. Feldmann, A. Polyanskii, High-Tc superconducting materials for electric power applications. Nature **414**(6861), 368–377 (2001)
3. A. Gurevich, Challenges and Opportunities for Applications of Unconventional Superconductors. Annual Review of Condensed Matter Physics **5**(2014), 35–56 (2014)

4. W.-K. Kwok, U. Welp, A. Glatz, A.E. Koshelev, K.J. Kihlstrom, G.W. Crabtree, Vortices in high-performance high-temperature superconductors. Reports on Progress in Physics **79**(11), 116501 (2016)
5. C. Yao, Y. Ma. Superconducting materials: Challenges and opportunities for large-scale applications. iScience, **24**(6), (2021)
6. Z. S. Hartwig, R. F. Vieira, B. N. Sorbom, R. A. Badcock, M. Bajko, W. K. Beck, B. Castaldo, C. L. Craighill, M. Davies, J. Estrada, V. Fry, T. Golfinopoulos, A. E. Hubbard, J. H. Irby, S. Kuznetsov, C. J. Lammi, P. C. Michael, T. Mouratidis, R. A. Murray, A. T. Pfeiffer, S. Z. Pierson, A. Radovinsky, M. D. Rowell, E. E. Salazar, M. Segal, P. W. Stahle, M. Takayasu, T. L. Toland, L. Zhou. VIPER: an industrially scalable high-current high-temperature superconductor cable. 2020
7. C. Yao, Y. Ma, Recent breakthrough development in iron-based superconducting wires for practical applications. Superconductor Science and Technology **32**(2), 023002 (2019)
8. J.-I. Shimoyama, Potentials of iron-based superconductors for practical future materials. Superconductor Science and Technology **27**(4), 044002 (2014)
9. H. Hosono, A. Yamamoto, H. Hiramatsu, Y. Ma, Recent advances in iron-based superconductors toward applications. Materials Today **21**(3), 278–302 (2018)
10. X. Xu, X. Peng, F. Wan, J. Rochester, G. Bradford, J. Jaroszynski, M. Sumption, APC Nb_3Sn superconductors based on internal oxidation of Nb-Ta-Hf alloys. Superconductor Science and Technology **36**(3), 035012 (2023)
11. G. Bovone, F. Buta, F. Lonardo, T. Bagni, M. Bonura, D. LeBoeuf, S.C. Hopkins, T. Boutboul, A. Ballarino, C. Senatore, Effects of the oxygen source configuration on the superconducting properties of internally-oxidized internal-Sn Nb_3Sn wires. Superconductor Science and Technology **36**(9), 095018 (2023)
12. Y.E. Shujun, H. Kumakura, The development of MgB_2 superconducting wires fabricated with an internal Mg diffusion (IMD) process. Superconductor Science and Technology **29**(11), 113004 (2016)
13. M. Parizh, Y. Lvovsky, M. Sumption, Conductors for commercial MRI magnets beyond NbTi: requirements and challenges. Superconductor Science and Technology **30**(1), 014007 (2016)
14. D. Patel, A. Matsumoto, H. Kumakura, M. Maeda, S.-H. Kim, H. Liang, Y. Yamauchi, S. Choi, J.H. Kim, Md.S.A. Hossain, MgB_2 Superconducting Joint Architecture with the Functionality to Screen External Magnetic Fields for MRI Magnet Applications. ACS Applied Materials & Interfaces **14**(2), 3418–3426 (2022)
15. X. Obradors, T. Puig, Coated conductors for power applications: Materials challenges. Superconductor Science and Technology **27**, 044003 (2014)
16. J. MacManus-Driscoll, S. Wimbush, Processing and application of high-temperature superconducting coated conductors. Nature Reviews Materials **6**, 587–604 (2021)
17. T. Puig, J. Gutierrez, X. Obradors, Impact of high growth rates on the microstructure and vortex pinning of high-temperature superconducting coated conductors. Nature Reviews Physics **6**(2), 132–148 (2024)
18. T. Izumi, K. Nakaoka, Control of artificial pinning centers in REBCO coated conductors derived from the trifluoroacetate metal-organic deposition process. Superconductor Science and Technology **31**(3), 034008 (2018)
19. N. Mitchell, J. Zheng, C. Vorpahl, V. Corato, C. Sanabria, M. Segal, B. Sorbom, R. Slade, G. Brittles, R. Bateman, Y. Miyoshi, N. Banno, K. Saito, A. Kario, H.T. Kate, P. Bruzzone, R. Wesche, T. Schild, N. Bykovskiy, A. Dudarev, M. Mentink, F.J. Mangiarotti, K. Sedlak, D. Evans, D.C. Van Der Laan, J.D. Weiss, M. Liao, G. Liu, Superconductors for fusion: a roadmap. Superconductor Science and Technology **34**(10), 103001 (2021)
20. X. Obradors, T. Puig, Pin the vortex on the superconductor. Nature Materials **23**(10), 1311–1312 (2024)
21. L. Soler, J. Jareño, J. Banchewski, S. Rasi, N. Chamorro, R. Guzman, R. Yáñez, C. Mocuta, S. Ricart, J. Farjas, P. Roura-Grabulosa, X. Obradors, T. Puig, Ultrafast transient liquid assisted growth of high current density superconducting films. Nature Communications **11**(1), 344 (2020)
22. S. Rasi, A. Queraltó, J. Banchewski, L. Saltarelli, D. Garcia, A. Pacheco, K. Gupta, A. Kethamkuzhi, L. Soler, J. Jareño, S. Ricart, J. Farjas, P. Roura-Grabulosa, C. Mocuta, X. Obradors, T. Puig, Kinetic Control of Ultrafast Transient Liquid Assisted Growth of Solution-Derived $YBa_2Cu_3O_{7-x}$ Superconducting Films. Advanced Science **9**(32), 2203834 (2022)

23. J.-H. Lee, H. Lee, J.-W. Lee, S.-M. Choi, S.-I. Yoo, S.-H. Moon, RCE-DR, a novel process for coated conductor fabrication with high performance. Superconductor Science and Technology **27**(4), 044018 (2014)
24. M. Miura, G. Tsuchiya, T. Harada, K. Sakuma, H. Kurokawa, N. Sekiya, Y. Kato, R. Yoshida, T. Kato, K. Nakaoka, T. Izumi, F. Nabeshima, A. Maeda, T. Okada, S. Awaji, L. Civale, B. Maiorov, Thermodynamic approach for enhancing superconducting critical current performance. NPG Asia Materials **14**(1), 1–12 (2022)
25. X. Obradors, T. Puig, S. Ricart, A. Palau, M. Coll, J. Gutiérrez, J. Farjas, E. Bartolomé, Progress in superconducting $REBa_2Cu_3O_7$ (RE = rare earth) coated conductors derived from fluorinated solutions. Superconductor Science and Technology **37**(5), 053001 (2024)
26. A. Molodyk, D.C. Larbalestier, The prospects of high-temperature superconductors. Science **380**(6651), 1220–1222 (2023)
27. A. Godeke, High temperature superconductors for commercial magnets. Superconductor Science and Technology **36**(11), 113001 (2023)
28. D. Uglietti, A review of commercial high temperature superconducting materials for large magnets: from wires and tapes to cables and conductors. Superconductor Science and Technology **32**(5), 053001 (2019)
29. D.C. Larbalestier, J. Jiang, U.P. Trociewitz, F. Kametani, C. Scheuerlein, M. Dalban-Canassy, M. Matras, P. Chen, N.C. Craig, P.J. Lee, E.E. Hellstrom, Isotropic round-wire multifilament cuprate superconductor for generation of magnetic fields above 30 T. Nature Materials **13**(4), 375–381 (2014)
30. M. Miura, S. Eley, K. Iida, K. Hanzawa, J. Matsumoto, H. Hiramatsu, Y. Ogimoto, T. Suzuki, T. Kobayashi, T. Ozaki, H. Kurokawa, N. Sekiya, R. Yoshida, T. Kato, T. Okada, H. Okazaki, T. Yamaki, J. Hänisch, S. Awaji, A. Maeda, B. Maiorov, H. Hosono, Quadrupling the depairing current density in the iron-based superconductor SmFeAsO1-xHx. Nature Materials **23**(10), 1370–1378 (2024)
31. A. Stangl, A. Palau, G. Deutscher, X. Obradors, T. Puig, Ultra-high critical current densities of superconducting YBa2Cu3O7-d thin films in the overdoped state. Scientific Reports **11**(1), 8176 (2021)
32. Y.-H. Zhou, D. Park, Y. Iwasa, Review of progress and challenges of key mechanical issues in high-field superconducting magnets. National Science Review **10**(3), nwad001 (2023)
33. P. Barusco, H. Ben-Saad, D. Horn-Bourque, C. Lacroix, F. Sirois, T. Puig, J. Gutiérrez, X. Granados, X. Obradors, Enhanced Normal Zone Propagation Velocity in REBCO Coated Conductors Using an Intermetallic Stabilizer Coating. IEEE Transactions on Applied Superconductivity **34**(3), 1–6 (2024)
34. C. Lacroix, J. Giguère, S.-M.B. Hartman, H.B. Saad, A. Martin, T. Leduc, M. Gendron-Paul, Z. Bellil, J.-H. Fournier-Lupien, L. Moret, P. Barusco, X. Granados, X. Obradors, M. Pekarčiková, F. Gömöry, V. Grosse, M. Bauer, F. Sirois, Normal zone propagation in various REBCO tape architectures. Superconductor Science and Technology **35**(5), 055009 (2022)
35. J. Ekin, Relationships between critical current and stress in NbTi. IEEE Transactions on Magnetics **23**(2), 1634–1637 (1987)
36. A. Godeke, B. ten Haken, H.H.J. ten Kate, D.C. Larbalestier, A general scaling relation for the critical current density in Nb_3Sn. Superconductor Science and Technology **19**(10), R100 (2006)
37. N. Cheggour, T.C. Stauffer, W. Starch, L.F. Goodrich, J.D. Splett, Implications of the strain irreversibility cliff on the fabrication of particle-accelerator magnets made of restacked-rod-process Nb_3Sn wires. Scientific Reports **9**(1), 5466 (2019)
38. P. Kováč, M. Búran, J. Kováč, T. Melišek, I. Hušek, D. Berek, P. Mauceri, T. Spina, Ch.-E. Bruzek, Electrical and mechanical limits of ex situ MgB_2 wires for cabling. Superconductor Science and Technology **37**(6), 065004 (2024)
39. X. liu, Y. Shi, S. Wei, F. Liu, Y. Song, Q. Li, Y. Li, L. Liu, Z. Shi, L. Ren, Y. Xu, P. Duan, Z. Yang, J.-Y Ge, Y. Qi, H. Liu, J. Qin, Z. Zhang. Reversible critical current performance of FeSe0.5Te0.5 coated conductor tapes under uniaxial tensile strain. Superconductor Science and Technology, 35, (2022)
40. Y. Miyoshi, G. Nishijima, H. Kitaguchi, X. Chaud, Hoop stress test on new high strength alloy laminated Bi-2223 conductor. Superconductor Science and Technology **28**(7), 075013 (2015)
41. T. Kiyoshi, S. Choi, S. Matsumoto, K. Zaitsu, T. Hase, T. Miyazaki, M. Hamada, M. Hosono, H. Maeda, Bi-2223 Innermost Coil for 1.03 GHz NMR Magnet. IEEE Transactions on Applied Superconductivity **21**(3), 2110–2113 (2011)
42. A. Godeke, M.H.C. Hartman, M.G.T. Mentink, J. Jiang, M. Matras, E.E. Hellstrom, D.C. Larbalestier, Critical current of dense Bi-2212 round wires as a function of axial strain. Superconductor Science and Technology **28**(3), 032001 (2015)

43. C. Barth, G. Mondonico, C. Senatore, Electro-mechanical properties of REBCO coated conductors from various industrial manufacturers at 77 K, self-field and 4.2 K, 19 T. Superconductor Science and Technology **28**(4), 045011 (2015)
44. D.C. van der Laan, J.D. Weiss, D.M. McRae, Status of CORC® cables and wires for use in high-field magnets and power systems a decade after their introduction. Superconductor Science and Technology **32**(3), 033001 (2019)
45. A. Molodyk, S. Samoilenkov, A. Markelov, P. Degtyarenko, S. Lee, V. Petrykin, M. Gaifullin, A. Mankevich, A. Vavilov, B. Sorbom, J. Cheng, S. Garberg, L. Kesler, Z. Hartwig, S. Gavrilkin, A. Tsvetkov, T. Okada, S. Awaji, D. Abraimov, A. Francis, G. Bradford, D. Larbalestier, C. Senatore, M. Bonura, A.E. Pantoja, S.C. Wimbush, N.M. Strickland, A. Vasiliev, Development and large volume production of extremely high current density $YBa_2Cu_3O_7$ superconducting wires for fusion. Scientific Reports **11**(1), 2084 (2021)
46. J. T. Tanabe. Iron Dominated Electromagnets. Stanford Linear Accelerator Center, (2005)
47. R. Hoard, S. Mance, R. Leber, E. Dalder, M. Chaplin, K. Blair, D. Nelson, D. Van Dyke, Field enhancement of a 12.5-T magnet using holmium poles. IEEE Transactions on Magnetics **21**(2), 448–450 (1985)
48. S. Sanz, J. Calero, F.M. Aragon, J.L. Gutiérrez, I. Moya, I. Podadera, F. Toral, J.G.S. Gama, N. Bazin, P. Bosland, P. Bredy, N. Grouas, P. Hardy, V.M. Hennion, J. Migne, F. Orsini, B. Renard, G. Disset, J. Relland, and E.N. Zaplatin. Fabrication and Testing of the First Magnet Package Prototype for the SRF Linac of LIPAc. (2011)
49. F. Savary, R. Gallix, J. Knaster, N. Mitchell, K. Seo, The Toroidal Field Coils for the ITER Project. IEEE Transactions on Applied Superconductivity **22**(3), 4200904 (2012)
50. J.A. García-Matos, C. Alcázar, M. Domínguez, O.D. Lucas, L. García-Tabarés, L.A.G. Gómez, P. Gómez, J. Jiménez, T. Martínez, C.M. Jardim, J.A. Pardo, J.M. Pérez, P. Sobrino, F. Toral, J.C. Perez, E. Todesco, Fine Tuning of the Inner Dipole Design of MCBXF Magnets. IEEE Transactions on Applied Superconductivity **32**(6), 1–5 (2022)
51. P. Abramian, F. de Aragón, J. Calero, J. de la Gama, L. García-Tabarés, J.L. Gutiérrez, M. Karppinen, T. Martínez, E. Rodríguez, I. Rodríguez, L. Sánchez, F. Toral, C. Vázquez, Development of Radiation Resistant Superconducting Corrector Magnets for LHC Upgrade. IEEE Transactions on Applied Superconductivity **23**(3), 4101204 (2013)
52. M.N. Wilson, M.N. Wilson, *Superconducting Magnets. Monographs on Cryogenics.* (Oxford University Press, Oxford, New York, 1987)
53. Case Studies in Superconducting Magnets, *Design and Operational Issues* (Springer, US, Boston, MA, 2009)
54. Karl-Hubert. Mess, *Superconducting Accelerator Magnets* (Singapore, River Edge, NJ, 1996)
55. T. Benkel, Y. Miyoshi, X. Chaud, A. Badel, P. Tixador, REBCO tape performance under high magnetic field. The European Physical Journal Applied Physics **79**, 30601 (2017)
56. F.C. de Castro Sene, Review on the state-of-the-art and challenges in the MgB2 component manufacturing for superconducting applications. Superconductivity **9**, 100083 (2024)
57. L. Bortot, B. Auchmann, I. Cortes Garcia, A.M. Fernandez Navarro, M. Maciejewski, M. Mentink, M. Prioli, E. Ravaioli, S. Schps, A.P. Verweij, STEAM: A Hierarchical Cosimulation Framework for Superconducting Accelerator Magnet Circuits. IEEE Transactions on Applied Superconductivity **28**(3), 1–6 (2018)
58. P. Gao, Y. Zhang, X. Wang, Y. Zhou, Interface properties and failures of REBCO coated conductor tapes: Research progress and challenges. Superconductivity **8**, 100068 (2023)
59. M. Marchevsky, Quench Detection and Protection for High-Temperature Superconductor Accelerator Magnets. Instruments **5**, 27 (2021)
60. G. Seo, J. Mun, D. Kim, M. Park, S. Kim. Neon-helium hybrid cooling system for a 10 MW class superconducting wind power generator. IEEE Transactions on Applied Superconductivity, pages 1
61. S. Sanz, P. Abramian, J. Calero, A. Fernandez, L. Garcia-Tabares, J.L. Gutierrez, J. Lucas, E. Rodriguez, I. Rodriguez, F. Toral, C. Vazquez, Design of a HTS Solenoid for a Gyrotron Magnet Upgrade. IEEE Transactions on Applied Superconductivity **17**(2), 1406–1409 (2007)
62. J. Munilla, P. Abramian, J. Calero, L. Garcia-Tabares, P.R. Gómez, A. Estevez, L.M. Martinez, C. Oliver, J.A. Pardo, P. Sobrino, F. Toral, C. Langeber, I. Perez, C. Hernando, Commissioning of an autonomous cooling system for a compact superconducting cyclotron devoted to radioisotope production. IEEE Transactions on Applied Superconductivity **31**(5), 1–4 (2021)

63. F. Gömöry, M. Solovyov, J. Šouc, L. Frolek, T. Kujovič, E. Seiler, R. Ries, M. Mošat', T. Winkler, K. Sugita, M. Dhallé, H.J.G. Krooshoop, C. Hintze, A. Troshyn, W. Prusseit, L. Nedergaard, L. Traberg, J. Christensen, N. Jørgensen, A. Wulff, AC Loss Reduction in Round HTS Cables Achieved by Low-Cost Filamentization of Tape Conductors. IEEE Transactions on Applied Superconductivity **34**, 1–5 (2024)
64. F. Toral, P. Abramian, H. Brueck, J. Calero, L. Garcia-Tabares, J.L. Gutierrez, W. Maschmann, E. Rodriguez, S. Sanz, M. Stolper, C. Vazquez, Fabrication and testing of a combined superconducting magnet for the tesla test facility. IEEE Transactions on Applied Superconductivity **16**(2), 231–235 (2006)
65. CERN Yellow Reports: Monographs. European Strategy for Particle Physics - Accelerator R&D Roadmap. CERN Yellow Reports: Monographs, 2022
66. Superconductivity Summit Initiative for a Greener, Healthier, Prosperous and Sustainable Future - ESAS - European Society for Applied Superconductivity, June 2022
67. The 17 goals. https://sdgs.un.org/goals
68. K. Ikeda, Progress in the ITER Physics Basis. Nuclear Fusion **47**(6), E01 (2007)
69. Wendelstein 7-x fusion device produces its first hydrogen plasma. https://www.ipp.mpg.de/4010154/0216
70. L. Spitzer Jr., The Stellarator Concept. The Physics of Fluids **1**(4), 253–264 (1958)
71. C. Mercier, Equilibrium and stability of a toroidal magnetohydrodynamic system in the neighbourhood of a magnetic axis. Nuclear Fusion **4**(3), 213 (1964)
72. Y. Xu, A general comparison between tokamak and stellarator plasmas. Matter and Radiation at Extremes **1**(4), 192–200 (2016)
73. G. Xu, Z. Lu, D. Chen, B. Wan, A promising approach to steady-state fusion: High-temperature superconducting strong-field stellarator with precise omnigenity. The Innovation **5**(1), 100537 (2024)
74. ...Z.S. Hartwig, R.F. Vieira, D. Dunn, T. Golfinopoulos, B. LaBombard, C.J. Lammi, P.C. Michael, S. Agabian, D. Arsenault, R. Barnett, M. Barry, L. Bartoszek, W.K. Beck, D. Bellofatto, D. Brunner, W. Burke, J. Burrows, W. Byford, C. Cauley, S. Chamberlain, D. Chavarria, J.L. Cheng, J. Chicarello, V. Diep, E. Dombrowski, J. Doody, R. Doos, B. Eberlin, J. Estrada, V. Fry, M. Fulton, S. Garberg, R. Granetz, A. Greenberg, M. Greenwald, S. Heller, A.E. Hubbard, E. Ihloff, J.H. Irby, M. Iverson, P. Jardin, D. Korsun, S. Kuznetsov, S. Lane-Walsh, R. Landry, R. Lations, R. Leccacorvi, M. Levine, G. Mackay, K. Metcalfe, K. Moazeni, J. Mota, T. Mouratidis, R. Mumgaard, J.P. Muncks, R.A. Murray, D. Nash, B. Nottingham, C. O'Shea, A.T. Pfeiffer, S.Z. Pierson, C. Purdy, A. Radovinsky, D.K. Ravikumar, V. Reyes, N. Riva, R. Rosati, M. Rowell, E.E. Salazar, F. Santoro, A. Sattarov, W. Saunders, P. Schweiger, S. Schweiger, M. Shepard, S. Shiraiwa, M. Silveira, F.T. Snowman, B.N. Sorbom, P. Stahle, K. Stevens, J. Stillerman, D. Tammana, T.L. Toland, D. Tracey, R. Turcotte, K. Uppalapati, M. Vernacchia, C. Vidal, E. Voirin, A. Warner, A. Watterson, D.G. Whyte, S. Wilcox, M. Wolf, B. Wood, L. Zhou, A. Zhukovsky, The SPARC Toroidal Field Model Coil Program. IEEE Transactions on Applied Superconductivity **34**(2), 1–16 (2024)
75. Y.Y. Ueda, H. Iguchi, K. Matsuoka, *Helical system research* (Japan Society of Plasma Science and Nuclear Fusion Research, Japan, 1998)
76. S. Wu, An overview of the EAST project. Fusion Engineering and Design **82**(5), 463–471 (2007)
77. G. S. Lee, M. Kwon, C. J. Doh, B. G. Hong, K. Kim, M. H. Cho, W. Namkung, C. S. Chang, Y. C. Kim, J. Y. Kim, H. G. Jhang, D. K. Lee, K. I. You, J. H. Han, M. C. Kyum, J. W. Choi, J. Hong, W. C. Kim, B. C. Kim, J. H. Choi, S. H. Seo, H. K. Na, H. G. Lee, S. G. Lee, S. J. Yoo, B. J. Lee, Y. S. Jung, J. G. Bak, H. L. Yang, S. Y. Cho, K. H. Im, N. I. Hur, I. K. Yoo, J. W. Sa, K. H. Hong, G. H. Kim, B. J. Yoo, H. C. Ri, Y. K. Oh, Y. S. Kim, C. H. Choi, D. L. Kim, Y. M. Park, K. W. Cho, T. H. Ha, S. M. Hwang, Y. J. Kim, S. Baang, S. I. Lee, H. Y. Chang, W. Choe, S. G. Jeong, S. S. Oh, H. J. Lee, B. H. Oh, B. H. Choi, C. K. Hwang, S. R. In, S. H. Jeong, I. S. Ko, Y. S. Bae, H. S. Kang, J. B. Kim, H. J. Ahn, D. S. Kim, C. H. Choi, J. H. Lee, Y. W. Lee, Y. S. Hwang, S. H. Hong, K.-H. Chung, D.-I. Choi, and KSTAR Team. Design and construction of the KSTAR tokamak. Nuclear Fusion, **41**(10):1515, (2001)
78. Y. C. Saxena and SST-1 Team. Present status of the SST-1 project. Nuclear Fusion, 40(6):1069, (2000)
79. N. Chernoplekov, N. Monoszon, T-15 facility and tests. IEEE Transactions on Magnetics **23**(2), 826–830 (1987)
80. R. Aymar, B. Bareyt, G. Bon Mardion. Tore Supra Basic design Tokamak system. Technical Report INIS Reference Number: 12614695, France, (1980)

81. H. Zushi, S. Itoh, K. Hanada, K. Nakamura, M. Sakamoto, E. Jotaki, M. Hasegawa, Y.D. Pan, S.V. Kulkarni, A. Iyomasa, S. Kawasaki, H. Nakashima, N. Yoshida, K. Tokunaga, T. Fujiwara, M. Miyamoto, H. Nakano, M. Yuno, A. Murakami, S. Nakamura, N. Sakamoto, K. Shinoda, S. Yamazoe, H. Akanishi, K. Kuramoto, Y. Matsuo, A. Iwamae, T. Fuijimoto, A. Komori, T. Morisaki, H. Suzuki, S. Masuzaki, Y. Hirooka, Y. Nakashima, O. Mitarai, Overview of steady state tokamak plasma experiments in TRIAM-1M. Nuclear Fusion **43**(12), 1600 (2003)
82. Y. Kamada, E. Di Pietro, M. Hanada, P. Barabaschi, S. Ide, S. Davis, M. Yoshida, G. Giruzzi, C. Sozzi, and the JT-60SA Integrated Project Team. Completion of JT-60SA construction and contribution to ITER. Nuclear Fusion, 62(4):042002, (2022)
83. M. Huguet, The ITER magnet system. Fusion Engineering and Design **36**(1), 23–32 (1997)
84. The Magnet System of Wendelstein 7-X Stellarator in Operation
85. O. Motojima, N. Yanagi, S. Imagawa, K. Takahata, S. Yamada, R. Maekawa, H. Chikaraishi, A. Iwamoto, S. Masuzaki, T. Mito, T. Morisaki, A. Nishimura, S. Satoh, T. Satow, H. Tamura, S. Tanahashi, S. Yamaguchi, J. Yamamoto, Superconducting Magnet System of Large Helical Device. Fusion Technology **30**(3P2B), 1226–1233 (1996)
86. P. Bauer, A. Ballarino, A. Devred, K. Ding, Y. Dong, E. Niu, Q. Du, C.Y. Gung, Q. Han, R. Heller, X. Huang, T. Ichihara, S. Lee, J. Li, C. Liu, C. Liu, K. Lu, N. Mitchell, Y. Song, T. Spina, Q. Ran, T. Taylor, S. Yamada, Y. Yang, T. Zhou, Development of HTS Current Leads for the ITER Project. IOP Conference Series: Materials Science and Engineering **756**(1), 012032 (2020)
87. Commonwealth fusion systems. https://cfs.energy/
88. R.F. Vieira, D. Arsenault, R. Barnett, L. Bartoszek, W. Beck, S. Chamberlain, J.L. Cheng, E. Dombrowski, J. Doody, D. Dunn, J. Estrada, V. Fry, S. Garberg, T. Golfinopoulos, A. Greenberg, S. Heller, A. Hubbard, D. Korsun, S. Kuznetsov, B. LaBombard, C. Lammi, R. Leccacorvi, M. Levine, D.C. Mendoza, K. Metcalfe, P. Michael, T. Mouratidis, R. Mumgaard, J.P. Muncks, R. Murray, D. Nash, A. Pfeiffer, S. Pierson, A. Radovinsky, R. Rosati, M. Rowell, E. Salazar, S. Schweiger, S. Shiraiwa, B. Sorbom, P. Stahle, K. Stevens, D. Tammana, T. Toland, M. Vernacchia, E. Voirin, A. Warner, A. Watterson, D.G. Whyte, S. Wilcox, L. Zhou, A. Zhukovsky, Z.S. Hartwig, Design, Fabrication, and Assembly of the SPARC Toroidal Field Model Coil. IEEE Transactions on Applied Superconductivity **34**(2), 1–15 (2024)
89. T. Golfinopoulos, P.C. Michael, E. Ihloff, A. Zhukovsky, D. Nash, V. Fry, J.P. Muncks, R. Barnett, L. Bartoszek, W. Beck, W. Burke, W. Byford, S. Chamberlain, D. Chavarria, K. Cote, E. Dombrowski, J. Doody, R. Doos, J. Estrada, M. Fulton, R. Johnson, B. LaBombard, S. Lane-Walsh, M. Levine, K. Metcalfe, C. O'Shea, A. Pfeiffer, S. Pierson, D.K. Ravikumar, M. Rowell, F. Santoro, S. Schweiger, J. Stillerman, C. Vidal, R. Vieira, E. Voirin, A. Watterson, S. Wilcox, M.J. Wolf, Z. Hartwig, Building the runway: A new superconducting magnet test facility made for the sparc toroidal field model coil. IEEE Transactions on Applied Superconductivity **34**(2), 1–16 (2024)
90. P.C. Michael, T. Golfinopoulos, E. Ihloff, A. Zhukovsky, S. Schweiger, V. Fry, C. O'Shea, A. Watterson, D. Nash, R.F. Vieira, J. Doody, R. Barnett, E.A. Voirin, L. Bartoszek, R.F. Lations, Z.S. Hartwig, A 20-K, 600-W, Cryocooler-Based, Supercritical Helium Circulation System for the SPARC Toroidal Field Model Coil Program. IEEE Transactions on Applied Superconductivity **34**(2), 1–13 (2024)
91. The Global Fusion Industry in 2023. Fusion Companies Survey by the Fusion Industry Association. https://www.fusionindustryassociation.org/wp-content/uploads/2023/07/FIA--2023-FINAL.pdf
92. https://tokamakenergy.com/
93. https://thea.energy
94. T. Kruger, D. Gates, and Thea Energy Team. All Planar Stellarator Coil Optimization. volume 2023, page GP11.082, (2023)
95. https://renfusion.eu/
96. https://www.proximafusion.com/
97. https://typeoneenergy.com/home/, August 2024
98. L. Joyce, Z. Feng. Annual Wind Report. Technical report, (2019)
99. International Renewable Energy Agency (IRENA). Renewable capacity statistics 2024. https://www.irena.org/-/media/Files/IRENA/Agency/Publication/2024/Mar/IRENARECapacityStatistics2024.pdf
100. Wood Mackenzie. Global wind power market outlook update: Q1 2019. https://www.woodmac.com/reports/power-markets-global-wind-power-market-outlook-update-q1-2019-213626/, March 2019

101. G.E. Barter, L. Sethuraman, P. Bortolotti, J. Keller, D.A. Torrey, Beyond 15 MW: A cost of energy perspective on the next generation of drivetrain technologies for offshore wind turbines. Applied Energy **344**, 121272 (2023)
102. R. Uria-Martinez, M. M. Johnson. Hydropower_market_report. Technical report, (2023)
103. S.K. Moore, Rough seas for the superconducting wind turbine: To keep offshore turbines light, engineers look beyond superconductors to a new permanent-magnet tech. IEEE Spectrum **55**(8), 32–39 (2018)
104. T.-K. Hoang, L. Quéval, L. Vido, D.-Q. Nguyen, Levelized Cost of Energy Comparison Between Permanent Magnet and Superconducting Wind Generators for Various Nominal Power. IEEE Transactions on Applied Superconductivity **32**(7), 1–6 (2022)
105. B.B Jensen, P. J. Masson. History and latest development of superconducting machines
106. S. Nagano, T. Kitajima, K. Yoshida, Y. Kazao, Y. Kabata, D. Murata, K. Nagakura, Development of world's largest hydrogen-cooled turbine generator. In IEEE Power Engineering Society Summer Meeting **2**, 657–663 (2002)
107. M. Polikarpova, P. Ponomarev, P. Röyttä, S. Semken, Y. Alexandrova, J. Pyrhönen, Direct liquid cooling for an outer-rotor direct-drive permanent-magnet synchronous generator for wind farm applications. IET Electric Power Applications **9**(8), 523–532 (2015)
108. A. Turnbull, C. McKinnon, J. Carrol, A. McDonald, On the Development of Offshore Wind Turbine Technology: An Assessment of Reliability Rates and Fault Detection Methods in a Changing Market. Energies **15**(9), 3180 (2022)
109. https://www.vestas.com/en/energy-solutions/offshore-wind-turbines/V236-15MW, September 2024
110. https://www.gevernova.com/wind-power/offshore-wind/haliade-x-offshore-turbine
111. https://www.compositesworld.com/news/mingyang-reveals-18-mw-offshore-wind-turbine-model-with-140-meter-long-blades, September 2024
112. http://cssc-hz.com/?en/Products/WindTurbines/Product57/77.html
113. C.C.T. Chow, M.D. Ainslie, K.T. Chau, High temperature superconducting rotating electrical machines: An overview. Energy Reports **9**, 1124–1156 (2023)
114. J.X. Jian, L.H. Zheng, Y.G. Guo, G.Z. Zhu, Developement of High Termperature Superconducting Machines. Energy Reports **9**, 1124–1156 (2023)
115. J. L. Kirtley, A. Banerjee, and Steven Englebretson. Motors for Ship Propulsion. Proceedings of the IEEE, 103(12):2320–2332, (2015)
116. K. Kovalev, N. Ivanov, S. Zhuravlev, D. Rusanov, G. Kuznetsov, V. Podguzov, Calculation, design and test results of 3 kW fully HTS electric machine. Physica C: Superconductivity and its Applications **587**, 1353892 (2021)
117. T. Andrew. Superconductor Technology Makes Hydropower Debut, (2010)
118. S.S. Kalsi, K. Weeber, H. Takesue, C. Lewis, H.-W. Neumueller, R.D. Blaugher, Development status of rotating machines employing superconducting field windings. Proceedings of the IEEE **92**(10), 1688–1704 (2004)
119. P.N. Barnes, M.D. Sumption, G.L. Rhoads, Review of high power density superconducting generators: Present state and prospects for incorporating YBCO windings. Cryogenics **45**(10), 670–686 (2005)
120. R. Fair, C. Lewis, J. Eugene, M. Ingles, Development of an HTS hydroelectric power generator for the hirschaid power station. Journal of Physics: Conference Series **234**(3), 032008 (2010)
121. O. Keysan. Superconducting generators for large off shore wind turbines. PhD thesis, (2014)
122. K.F. Goddard, B. Lukasik, J.K. Sykulski, Alternative Designs of High-Temperature Superconducting Synchronous Generators. IEEE Transactions on Applied Superconductivity **19**(6), 3805–3811 (2009)
123. S. S. George, S. Regani. 'Ecomagination' at Work: GE's Sustainability Initiative. In Gilbert G. Lenssen and N. Craig Smith, editors, Managing Sustainable Business: An Executive Education Case and Textbook, pages 417–434. Springer Netherlands, Dordrecht, (2019)
124. J. Lloberas, A. Sumper, M. Sanmarti, X. Granados, A review of high temperature superconductors for offshore wind power synchronous generators. Renewable and Sustainable Energy Reviews **38**, 404–414 (2014)
125. X. Song, N. Mijatovic, B.B. Jensen, J. Holbøll, Design Study of Fully Superconducting Wind Turbine Generators. IEEE Transactions on Applied Superconductivity **25**(3), 1–5 (2015)
126. Y. Terao, M. Sekino, H. Ohsaki, Electromagnetic Design of 10 MW Class Fully Superconducting Wind Turbine Generators. IEEE Transactions on Applied Superconductivity **22**(3), 5201904 (2012)

127. G. dos Santos, F. Sass, G.G. Sotelo, F. Fajoni, C.A. Baldan, E. Ruppert, Multi-objective optimization for the superconducting bias coil of a saturated iron core fault current limiter using the T-A formulation. Superconductor Science and Technology **34**(2), 025012 (2021)
128. T. Lan, H. Liao, M. Iftikhar, W. Yuan, A. Cole, R. Abdouh, M. Zhang. Multifilament HTS Cables to Reduce AC Loss: Proof-of-Concept Experiments and Simulation. IEEE Transactions on Applied Superconductivity, PP:1–25, (2023)
129. A.B. Yahia, X.-F. Li, M. Majoros, M.D. Sumption, V. Selvamanickam, AC Loss Reduction in Multifilamentary Coated Conductors With Transposed Filaments. IEEE Transactions on Applied Superconductivity **27**(4), 1–5 (2017)
130. R. Radebaugh, Cryocoolers for aircraft superconducting generators and motors. AIP Conference Proceedings **1434**(1), 171–182 (2012)
131. A.B. Abrahamsen, D. Liu, N. Magnusson, A. Thomas, Z. Azar, E. Stehouwer, B. Hendriks, G.-J. Van Zinderen, F. Deng, Z. Chen, D. Karwatzki, A. Mertens, M. Parker, S. Finney, H. Polinder, Comparison of Levelized Cost of Energy of superconducting direct drive generators for a 10 MW offshore wind turbine. IEEE Transactions on Applied Superconductivity **28**(4), 1–5 (2018)
132. X. Song, C. Bührer, A. Mølgaard, R.S. Andersen, P. Brutsaert, M. Bauer, J. Hansen, A.V. Rebsdorf, J. Kellers, T. Winkler, A. Bergen, M. Dhalle, S. Wessel, M. ter Brake, J. Wiezoreck, H. Kyling, H. Boy, E. Seitz, Commissioning of the World's First Full-Scale MW-Class Superconducting Generator on a Direct Drive Wind Turbine. IEEE Transactions on Energy Conversion **35**(3), 1697–1704 (2020)
133. T. Winkler, on behalf of the EcoSwing Consortium. The EcoSwing Project. IOP Conference Series: Materials Science and Engineering, 502(1):012004, (2019)
134. D. Gonzalez-Delgado, P. Jaen-Sola, E. Oterkus, Design and optimization of multi-MW offshore direct-drive wind turbine electrical generator structures using generative design techniques. Ocean Engineering **280**, 114417 (2023)
135. M. Musa, L. Ghobrial, C. Sasthav, J. Heineman, M. Rencheck, K. M. Stewart, S. DeNeale, C.-Y. Tseng, D. White, L. Davis, M. Nachman, R. Kelsey. Advanced Manufacturing and Materials for Hydropower: Challenges and Opportunities. Technical Report ORNL/TM-2023/2835, Oak Ridge National Laboratory (ORNL), Oak Ridge, TN (United States), (2023)
136. A. Iwata, Ocean Current Power Generation by Superconducting MHD Method. Journal of the Cryogenic Society of Japan **15**(6), 317–328 (1980)
137. M. Takeda, Seawater Magnetohydrodynamics Power Generator / Hydrogen Generator. Advances in Science and Technology **75**, 208–214 (2010)
138. M. Blanco, J. Torres, M. Santos-Herrán, L. García-Tabarés, G. Navarro, J. Nájera, D. Ramírez, M. Lafoz. Correction to: Recent Advances in Direct-Drive Power Take-Off (DDPTO) Systems for Wave Energy Converters Based on Switched Reluctance Machines (SRM). In Abdus Samad, S.A Sannasiraj, V. Sundar, and Paresh Halder, editors, Ocean Wave Energy Systems: Hydrodynamics, Power Takeoff and Control Systems, pages C1–C1. Springer International Publishing, Cham, (2022)
139. P. Kambo, Y. Yamanouchi, A.A. Caunes, K. Yamaguchi, M. Izumi, T. Ida, Concept design of an HTS linear power generator for wave energy conversion. Superconductivity **6**, 100043 (2023)
140. L. García-Tabarés, C. Hernando, J. Munilla, J. Torres, M. Santos-Herran, M. Blanco, S. Sanz, G. Sarmiento, F.G. Lorenzo, M. Neri, D. Magrassi, Concept Design of a Novel Superconducting PTO Actuator for Wave Energy Extraction. IEEE Transactions on Applied Superconductivity **32**(6), 1–5 (2022)
141. O. Keysan, M. A. Mueller. A linear superconducting generator for wave energy converters. In 6th IET International Conference on Power Electronics, Machines and Drives (PEMD 2012), pages 1–6, (2012)
142. UHVDC Transmission Project. https://www.nsenergybusiness.com/projects/changji-guquan-uhvdc-transmission-project/
143. M. Cullinane, F. Judge, M. O'Shea, K. Thandayutham, J. Murphy, Subsea superconductors: The future of offshore renewable energy transmission? Renewable and Sustainable Energy Reviews **156**, 111943 (2022)
144. Superconducting cables: maximum transmission capacity and near-zero losses. https://www.nexans.es/en/company/Innovation/superconducting-cables.html
145. X.H. Zong, Y.W. Han, C.Q. Huang, Introduction of 35-kV kilometer-scale high-temperature superconducting cable demonstration project in Shanghai. Superconductivity **2**, 100008 (2022)
146. Executive summary – Electricity 2024 – Analysis

147. Superconducting Cables (AmpaCity). https://www.mission-innovation.net/our-work/mission-innovation-breakthroughs/superconducting-cables-ampacity/
148. SUPERCONDUCTING CABLES FOR POWER TRANSMISSION APPLICATIONS – A REVIEW. In Workshop on accelerator magnet superconductors
149. J. Oestergaard, J. Okholm, K. Lomholt, O. Toennesen, Energy losses of superconducting power transmission cables in the grid. IEEE Transactions on Applied Superconductivity **11**(1), 2375–2378 (2001)
150. H. Thomas, A. Marian, A. Chervyakov, S. Stückrad, C. Rubbia, Efficiency of superconducting transmission lines: An analysis with respect to the load factor and capacity rating. Electric Power Systems Research **141**, 381–391 (2016)
151. H. Thomas, A. Marian, A. Chervyakov, S. Stückrad, D. Salmieri, C. Rubbia, Superconducting transmission lines - Sustainable electric energy transfer with higher public acceptance? Renewable and Sustainable Energy Reviews **55**, 59–72 (2016)
152. Z. Wang, J. Qiu, S. Wang, W. Gong, H. Hong, B. Tian. Design of cold dielectric hts power cable. In 2009 International Conference on Applied Superconductivity and Electromagnetic Devices, pages 64–67, (2009)
153. M. Stemmle, F. Merschel, M. Noe, A. Hobl. AmpaCity – Installation of advanced superconducting 10 kV system in city center replaces conventional 110 kV cables. In 2013 IEEE International Conference on Applied Superconductivity and Electromagnetic Devices, pages 323–326, (2013)
154. A.T.A.M. de Waele, Basic Operation of Cryocoolers and Related Thermal Machines. Journal of Low Temperature Physics **164**(5), 179–236 (2011)
155. N. Mathias. Superconducting Cables. In EUCAS Short Course Power Applications, September 17th 2017, Geneva, (2017)
156. S. Fukui, T. Noguchi, J. Ogawa, M. Yamaguchi, T. Sato, O. Tsukamoto, Analysis of AC Loss and Current Distribution Characteristics of Multi-Layer Triaxial HTS Cable for 3-Phase AC Power Transmission. IEEE Transactions on Applied Superconductivity **16**(2), 135–138 (2006)
157. S.-J. Lee, S.Y. Kang, M. Park, D. Won, J. Yoo, H.S. Yang, Performance Analysis of Real-Scale 23 kV/60 MVA Class Tri-Axial HTS Power Cable for Real-Grid Application in Korea. Energies **13**(8), 2053 (2020)
158. S. Mukoyama, K. Miyoshi, H. Tsubouti, T. Yoshida, M. Mimura, N. Uno, M. Ikeda, H. Ishii, S. Honjo, Y. Iwata, Uniform current distribution conductor of HTS power cable with variable tape-winding pitches. IEEE Transactions on Applied Superconductivity **9**(2), 1269–1272 (1999)
159. S. Mukoyama, K. Miyoshi, H. Tsubouti, M. Mimitra, N. Uno, N. Ichtyanagi, Y. Tanaka, M. Ikeda, H. Ishii, S. Honjo, Y. Sato, T. Hara, Y. Iwata, 50-m long HTS conductor for power cable. IEEE Transactions on Applied Superconductivity **7**(2), 1069–1072 (1997)
160. R. Soika, X. Granados, S.C. Nogales, ENDESA Supercable, a 3.2 kA, 138 MVA, Medium Voltage Superconducting Power Cable. IEEE Transactions on Applied Superconductivity **21**(3), 972–975 (2011)
161. T. Hamajima, M. Tsuda, T. Yagai, S. Monma, H. Satoh, K. Shimoyama, Analysis of AC Losses in a Tri-axial Superconducting Cable. IEEE Transactions on Applied Superconductivity **17**(2), 1692–1695 (2007)
162. D. Miyagi, N. Takahashi, S. Torii, K. Ueda, K. Yasuda, 3-D FEM Analysis of Effect of Twist Pitch and Shielding Layer on Multi-Layered HTS Power Cable. IEEE Transactions on Applied Superconductivity **16**(2), 1614–1617 (2006)
163. X. Pei, A.C. Smith, M. Barnes, Superconducting Fault Current Limiters for HVDC Systems. Energy Procedia **80**, 47–55 (2015)
164. G.G. Sotelo, G. dos Santos, F. Sass, B.W. França, D.H.N. Dias, M.Z. Fortes, A. Polasek, R. de Andrade Jr, A review of superconducting fault current limiters compared with other proven technologies. Superconductivity **3**, 100018 (2022)
165. M. Song, S. Dai, C. Sheng, L. Zhong, X. Duan, G. Yan, Y. Huang, C. Chen, L. Li, L. Cai, T. Ma, Design and performance tests of a 160 kV/1.0 kA DC superconducting fault current limiter. Physica C: Superconductivity and its Applications **585**, 1353871 (2021)
166. Y. Xin, W.Z. Gong, H. Hong, X.Y. Niu, J.Y. Zhang, A.R. Ren, B. Tian, Saturated iron-core superconductive fault current limiter developed at Innopower. AIP Conference Proceedings **1573**(1), 1042–1048 (2014)

167. A. Hobl, W. Goldacker, B. Dutoit, L. Martini, A. Petermann, P. Tixador, Design and Production of the ECCOFLOW Resistive Fault Current Limiter. IEEE Transactions on Applied Superconductivity **23**(3), 5601804 (2013)
168. M. Stemmle, F. Merschel, M. Noe, A. Hobl. Ampacity project – Worldwide first superconducting cable and fault current limiter installation in a German city center. In 22nd International Conference and Exhibition on Electricity Distribution (CIRED 2013), pages 1–4, (2013)
169. J.F. Maguire, F. Schmidt, S. Bratt, T.E. Welsh, J. Yuan, A. Allais, F. Hamber, Development and Demonstration of a HTS Power Cable to Operate in the Long Island Power Authority Transmission Grid. IEEE Transactions on Applied Superconductivity **17**(2), 2034–2037 (2007)
170. V.H. Tahiliani, J.W. Porter, Fault Current Limiters an Overview of EPRI Research. IEEE Transactions on Power Apparatus and Systems, PAS- **99**(5), 1964–1969 (1980)
171. M. Noe, M. Steurer, High-temperature superconductor fault current limiters: concepts, applications, and development status. Superconductor Science and Technology **20**(3), R15 (2007)
172. P. Tixador, A. Akbar, M. Bauer, M. Bocchi, A. Calleja, C. Creusot, G. Deutscher, F. Gomory, M. Noe, X. Obradors, M. Pekarčíková, F. Sirois, Some results of the eu project fastgrid. IEEE Transactions on Applied Superconductivity **32**(4), 1–6 (2022)
173. A. Abramovitz, K.M. Smedley, F. De La Rosa, F. Moriconi, Prototyping and Testing of a 15 kV/1.2 kA Saturable Core HTS Fault Current Limiter. IEEE Transactions on Power Delivery **28**(3), 1271–1279 (2013)
174. T. Ma, S. Dai, M. Song, C. Li, Electromagnetic Design of High-Temperature Superconducting DC Bias Winding for Single-Phase 500 kV Saturated Iron-Core Fault Current Limiter. IEEE Transactions on Applied Superconductivity **28**(3), 1–5 (2018)
175. P. Tixador, Fault current limiter based on high temperature superconductors. Physica C: Superconductivity and its Applications **615**, 1354398 (2023)
176. D.A. Barton, G.O. Zimmerman, Superconducting AC/DC power coversion using high-temperature superconducting components. IEEE Transactions on Applied Superconductivity **9**(2), 685–688 (1999)
177. N. Mathias. Superconducting Transformers. In EUCAS Short Course Power Applications, September 17th 2017, Geneva, (2017)
178. D. Willén, F. Hansen, M. Däumling, C.N. Rasmussen, J. Østergaard, C. Træholt, E. Veje, O. Tønnesen, K.-H. Jensen, S.K. Olsen, C. Rasmussen, E. Hansen, O. Schuppach, T. Visler, S. Kvorning, J. Schuzster, J. Mortensen, J. Christiansen, S.D. Mikkelsen, First operation experiences from a 30 kV, 104 MVA HTS power cable installed in a utility substation. Physica C: Superconductivity **372–376**, 1571–1579 (2002)
179. NKT powers up test system for the world's longest superconducting power cable
180. S. Elschner, J. Brand, W. Goldacker, M. Hollik, A. Kudymow, S. Strauss, V. Zermeno, C. Hanebeck, S. Huwer, W. Reiser, M. Noe, 3S-Superconducting DC-Busbar for High Current Applications. IEEE Transactions on Applied Superconductivity **28**(4), 1–5 (2018)
181. Vision Electric Super Conductors – PIONEERS IN ELECTRIC POWER. https://www.vesc-superbar.de/
182. M. Tomita, Y. Fukumoto, K. Suzuki, M. Miryala, Development of prototype DC superconducting cable for railway system. Physica C: Superconductivity and its Applications **470**, S1007–S1008 (2010)
183. H. Ohsaki, Z. Lv, M. Sekino, M. Tomita, Application of Superconducting Power Cables to DC Electric Railway Systems. Physics Procedia **36**, 908–913 (2012)
184. M. Tomita, K. Suzuki, Y. Fukumoto, A. Ishihara, M. Muralidhar, Next generation of prototype direct current superconducting cable for railway system. Journal of Applied Physics **109**(6), 063909 (2011)
185. R. Takagi, Energy Saving Techniques for the Power Feeding Network of Electric Railways. IEEJ Transactions on Electrical and Electronic Engineering **5**(3), 312–316 (2010)
186. A. Allais, J.-M. Saugrain, B. West, N. Lallouet, H. Caron, D. Ferandelle, L. Terrien, G. Bouvier, G. Hajiri, K. Berger, L. Quéval, Superrail-world-first hts cable to be installed on a railway network in france. IEEE Transactions on Applied Superconductivity **34**(3), 1–7 (2024)
187. P.J. Ferrara, M.A. Uva, J. Nowlin, Naval ship-to-shore high temperature superconducting power transmission cable feasibility. IEEE Transactions on Applied Superconductivity **21**(3), 984–987 (2011)
188. X. Chen, S. Jiang, Y. Chen, Y. Lei, D. Zhang, M. Zhang, H. Gou, B. Shen, A 10 MW class data center with ultra-dense high-efficiency energy distribution: Design and economic evaluation of superconducting DC busbar networks. Energy **250**, 123820 (2022)

189. N. Lei, E. Masanet, Statistical analysis for predicting location-specific data center PUE and its improvement potential. Energy **201**, 117556 (2020)
190. C. Jin, X. Bai, C. Yang, W. Mao, X. Xu, A review of power consumption models of servers in data centers. Applied Energy **265**, 114806 (2020)
191. N. Chikumoto, H. Watanabe, Y.V. Ivanov, H. Takano, S. Yamaguchi, H. Koshizuka, K. Hayashi, T. Sawamura, Construction and the circulation test of the 500-m and 1000-m dc superconducting power cables in ishikari. IEEE Transactions on Applied Superconductivity **26**(3), 1–4 (2016)
192. Superconductor LVDC data center power cables. https://www.amsc.com/wp-content/uploads/LVDC_BRO_0412_web.pdf
193. A. Ballarino, Development of superconducting links for the Large Hadron Collider machine. Superconductor Science and Technology **27**(4), 044024 (2014)
194. https://hebergement.universite-paris-saclay.fr/supraconductivite/supra/en/applications-electricite-smes.php
195. R.W. Boom, The UW-SMES design. IEEE Transactions on Applied Superconductivity **3**(1), 320–327 (1993)
196. H.J. Boenig, J.F. Hauer, Commissioning Tests Of The Bonneville Power Administration 30 MJ Superconducting Magnetic Energy Storage Unit. IEEE Transactions on Power Apparatus and Systems **PAS–104**(2), 302–312 (1985)
197. J. Cerulli. Operational experience with a superconducting magnetic energy storage device at Brookhaven National Laboratory, New York. In IEEE Power Engineering Society. 1999 Winter Meeting (Cat. No.99CH36233), **2**, 1247–1252 (1999)
198. H. Khodzhibagiyan, V. Drobin, G. Dorofeev, V. Karpinskiy, A. Shurygin, M. Novikov, D. Kashaev, M. Zaslavskiy, G. Kachlishvili, An approach to development of the HTS magnet for SMES at JINR. Journal of Physics: Conference Series **1590**(1), 012057 (2020)
199. R. Schottler, R.G. Coney, Commercial application experiences with SMES. Power Engineering Journal **13**(3), 149–152 (1999)
200. S. Nagaya, N. Hirano, M. Kondo, T. Tanaka, H. Nakabayashi, K. Shikimachi, S. Hanai, J. Inagaki, S. Ioka, S. Kawashima, Development and performance results of 5 MVA SMES for bridging instantaneous voltage dips. IEEE Transactions on Applied Superconductivity **14**(2), 699–704 (2004)
201. P. Mukherjee, V.V. Rao, Design and development of high temperature superconducting magnetic energy storage for power applications - A review. Physica C: Superconductivity and its Applications **563**, 67–73 (2019)
202. T. Christen, M.W. Carlen, Theory of Ragone plots. Journal of Power Sources **91**(2), 210–216 (2000)
203. A. Rufer, On the efficiency of energy storage systems - the influence of the exchanged power and the penalty of the auxiliaries. FACTA UNIVERSITATIS Series Electronics and Energetics **34**, 173–185 (2021)
204. N.S. Ghiasi, S.M.S. Ghiasi, A review on superconducting magnetic energy storage system applications, in *Energy Storage Applications in Power Systems, chapter 2*. ed. by Z. Wang, A. Younesi (IntechOpen, Rijeka, 2023)
205. Superconducting Magnetic Energy Storage. Technical Report Fact Sheet 01, (2019)
206. P. Tixador, M. Deléglise, A. Badel, K. Berger, B. Bellin, J.-C. Vallier, A. Allais, C.-E. Bruzek, First tests of a 800 kJ HTS SMES. IEEE Transactions on Applied Superconductivity **18**(2), 774–778 (2008)
207. Y. Makida, T. Shintomi, T. Hamajima, N. Ota, M. Katsura, K. Ando, T. Takao, M. Tsuda, D. Miyagi, H. Tsujigami, S. Fujikawa, J. Hirose, K. Iwaki, T. Komagome, Performance of a 10-kJ SMES model cooled by liquid hydrogen thermo-siphon flow for ASPCS study. IOP Conference Series: Materials Science and Engineering **101**(1), 012028 (2015)
208. B. Kondratowicz-Kucewicz. Study on impact of HTS winding configuration on energy value and magnetic field distribution in SMES. Prace Instytutu Elektrotechniki, Z. 278, (2018)
209. M.H. Ali, B. Wu, R.A. Dougal, An Overview of SMES Applications in Power and Energy Systems. IEEE Transactions on Sustainable Energy **1**(1), 38–47 (2010)
210. P.N. Murgatroyd, The Brooks inductor: a study of optimal solenoid cross-sections. IEE Proceedings B (Electric Power Applications) **133**(5), 309–314 (1986)
211. A. Morandi, M. Fabbri, B. Gholizad, F. Grilli, F. Sirois, V.M.R. Zermeño, Design and Comparison of a 1-MW/5-s HTS SMES With Toroidal and Solenoidal Geometry. IEEE Transactions on Applied Superconductivity **26**(4), 1–6 (2016)
212. S.M. Schoenung, W.R. Meier, W.V. Hassenzahl, A comparison of large-scale toroidal and solenoidal SMES systems. IEEE Transactions on Magnetics **27**(2), 2324–2328 (1991)

213. S. Nomura, H. Tsutsui, Structural Limitations of Energy Storage Systems Based on the Virial Theorem. IEEE Transactions on Applied Superconductivity **27**(4), 1–6 (2017)
214. H. Kamada, A. Ninomiya, S. Nomura, T. Yagai, T. Nakamura, H. Chikaraishi, Development of 1-T Class Force-Balanced Helical Coils Using REBCO Tapes. IEEE Transactions on Applied Superconductivity **30**(4), 1–5 (2020)
215. A. Anand, A.S. Gour, T.S. Datta, V.V. Rao, Novel-Shape-Based HTS Magnet Coil for SMES Application. Journal of Superconductivity and Novel Magnetism **36**(4), 1121–1131 (2023)
216. S.S. Peng, J. Zheng, W.Y. Li, Y.J. Dai, AC Loss Analysis of a Single-Solenoid HTS SMES Based on H-formulation. IOP Conference Series: Earth and Environmental Science **233**(2), 022018 (2019)
217. J. Zheng, Y. Cheng, M. Li, F. Liu, X. Liu, H. Liu, High temperature superconducting CORC cable with variable winding angles for low AC loss and high current carrying SMES system. Superconductor Science and Technology **36**(11), 115032 (2023)
218. P. Song, J. Zhu, T. Qu, P. Chen, F. Feng, M. Qiu, Design and Test of a Double Pancake Coil for SMES Application Wound by HTS Roebel Cable. IEEE Transactions on Applied Superconductivity **28**(4), 1–5 (2018)
219. G. Genta. Kinetic Energy Storage: Theory and Practice of Advanced Flywheel Systems. (2013)
220. K. Xu, Y. Guo, G. Lei, J. Zhu, A Review of Flywheel Energy Storage System Technologies. Energies **16**(18), 6462 (2023)
221. M.A. Conteh, E.C. Nsofor, Composite flywheel material design for high-speed energy storage. Journal of Applied Research and Technology **14**(3), 184–190 (2016)
222. H. Dongxu, D. Xingjian, L. Wen, Z. Yangli, Z. Xuehui, C. Haisheng, Z. Zhilai, A review of flywheel energy storage rotor materials and structures. Journal of Energy Storage **74**, 109076 (2023)
223. K.S. Haran, S. Kalsi, T. Arndt, H. Karmaker, R. Badcock, B. Buckley, T. Haugan, M. Izumi, D. Loder, J.W. Bray, P. Masson, E.W. Stautner, High power density superconducting rotating machines-development status and technology roadmap. Superconductor Science and Technology **30**(12), 123002 (2017)
224. S. Kalsi, K. Hamilton, R. Buckley, R. Badcock, Superconducting AC Homopolar Machines for High-Speed Applications. Energies **12**, 86 (2018)
225. High efficiency UPS system for a power-hungry world. Active Power White Paper. https://www.activepower.com/wp-content/uploads/2023/11/high-efficiency-ups-systems-for-a-power-hungry-world_compressed.pdf
226. M.L. Pastor, L.G.-T. Rodriguez, C.V. Velez, Flywheels Store to Save: Improving railway efficiency with energy storage. IEEE Electrification Magazine **1**(2), 13–20 (2013)
227. B. V. Jayawant. Electromagnetic levitation and suspension techniques. (1981)
228. F.C. Moon, P.-Z. Chang, *Superconducting Levitation: Applications to Bearing and Magnetic Transportation*, 1st edn. (Wiley-VCH, Weinheim, 1994)
229. H. Bleuler. A Survey of Magnetic Levitation and Magnetic Bearing Types. JSME international journal. Ser. 3, Vibration, control engineering, engineering for industry, 35:335–342, (1992)
230. L. Lu, W. Wu, X. Yu, Z. Jin, High-Temperature Superconducting Non-Insulation Closed-Loop Coils for Electro-Dynamic Suspension System. Electronics **10**, 1980 (2021)
231. R. Post, Maglev: A New Approach. Scientific American - SCI AMER **282**, 82–87 (2000)
232. J.H. Jeans, *The Mathematical Theory of Electricity and Magnetism*, 2nd edn. (The University Press, 1911)
233. A.B. Abrahamsen. Superconducting bearings for flywheel applications. Number 1265(EN) in Denmark. Forskningscenter Risoe. Risoe-R. Risø National Laboratory, (2001)
234. E. Chaidez, S.P. Bhattacharyya, A.N. Karpetis, Levitation Methods for Use in the Hyperloop High-Speed Transportation System. Energies **12**(21), 4190 (2019)
235. J.G. Bai, X.Z. Zhang, L.M. Wang, A Flywheel Energy Storage System with Active Magnetic Bearings. Energy Procedia **16**, 1124–1128 (2012)
236. P. Bernstein, J. Noudem, Superconducting magnetic levitation: principle, materials, physics and models. Superconductor Science and Technology **33**(3), 033001 (2020)
237. M. Strasik, J.R. Hull, J.A. Mittleider, J.F. Gonder, P.E. Johnson, K.E. McCrary, C.R. McIver, An overview of Boeing flywheel energy storage systems with high-temperature superconducting bearings. Superconductor Science and Technology **23**(3), 034021 (2010)
238. F.N. Werfel, U. Floegel-Delor, T. Riedel, R. Rothfeld, D. Wippich, B. Goebel, HTS Magnetic Bearings in Prototype Application. IEEE Transactions on Applied Superconductivity **20**(3), 874–879 (2010)

239. M. Komori, H. Kato, K.-I. Asami, Suspension-Type of Flywheel Energy Storage System Using High Tc Superconducting Magnetic Bearing (SMB). Actuators **11**, 215 (2022)
240. World's Largest Superconducting Flywheel Power Storage System Test Machine Completed and Test Operation Started. Furukawa Electric News Release, (2015)
241. M. Strasik, P.E. Johnson, A.C. Day, J. Mittleider, M.D. Higgins, J. Edwards, J.R. Schindler, K.E. McCrary, C.R. McIver, D. Carlson, J.F. Gonder, J.R. Hull, Design, Fabrication, and Test of a 5-kWh/100-kW Flywheel Energy Storage Utilizing a High-Temperature Superconducting Bearing. Applied Superconductivity, IEEE Transactions on **17**, 2133–2137 (2007)
242. Y. Arai, H. Seino, K. Yoshizawa, K. Nagashima, Development of superconducting magnetic bearing with superconducting coil and bulk superconductor for flywheel energy storage system. Physica C: Superconductivity **494**, 250–254 (2013)
243. K. Kwon. Flywheels turn superconducting to Reinvigorate Grid Storage Potential. IEEE Spectrum, (2021)
244. International shipping. https://www.iea.org/energy-system/transport/international-shipping
245. How Much Does the Shipping Industry Contribute to Global CO2 Emissions?
246. M. Breschi, A Godeke, L Queval, Z Melhem, Mark Ainslie, L. Cavallucci, Peter Cheetham, L Cooley, Kiruba Haran, Mark Husband, E Nilsson, Sastry Pamidi, Michael Parizh, and Xiaoze Pei. A strategic roadmap for implementing superconductivity towards zero-emission transport. To be Published
247. W. Soong. Sizing of electrical machines, (2008)
248. P. Tixador, Superconducting electrical motors. International Journal of Refrigeration **22**(2), 150–157 (1999)
249. M. Bauer, B. Massuti-Ballester, R. O'Regan, M.L.R. Betancourt, *Technology trends and challenges for superconductor-based ship propulsion* (Stockholm, Sweden, 2019)
250. H.W. Neumüller, W. Nick, B. Wacker, M. Frank, G. Nerowski, J. Frauenhofer, W. Rzadki, R. Hartig, Advances in and prospects for development of high-temperature superconductor rotating machines at Siemens. Superconductor Science and Technology **19**(3), S114 (2006)
251. B. Gamble, G. Snitchler, T. MacDonald, Full Power Test of a 36.5 MW HTS Propulsion Motor. IEEE Transactions on Applied Superconductivity **21**(3), 1083–1088 (2011)
252. S. Kalsi. Design of MW-Class Ship Propulsion Motors for US Navy by AMSC, (2019)
253. K. Umemoto, K. Aizawa, M. Yokoyama, K. Yoshikawa, Y. Kimura, M. Izumi, K. Ohashi, M. Numano, K. Okumura, M. Yamaguchi, Y. Gocho, E. Kosuge, Development of 1 MW-class HTS motor for podded ship propulsion system. Journal of Physics: Conference Series **234**(3), 032060 (2010)
254. T. Yanamoto, M. Izumi, K. Umemoto, T. Oryu, Y. Murase, M. Kawamura, Load Test of 3-MW HTS Motor for Ship Propulsion. IEEE Transactions on Applied Superconductivity **27**(8), 1–5 (2017)
255. M. Parizh, D. Torrey, J. Bray, W. Stautner, N. Tapadia, M. Xu, A. Wu, J. Zierer. Superconducting Synchronous Motors for Electric Ship Propulsion. IEEE Transactions on Applied Superconductivity, PP:1, (2020)
256. M. B. Nezhad. Study of homopolar dc generator. (2013)
257. T. Nitta, Superconducting rotating machines: A review of the past 30 years and future perspectives. Journal of Physics: Conference Series **1054**(1), 012081 (2018)
258. W. Li, T.W. Ching, K.T. Chau, C.H.T. Lee, A Superconducting Vernier Motor for Electric Ship Propulsion. IEEE Transactions on Applied Superconductivity **28**(3), 1–6 (2018)
259. J. Li, K.T. Chau, A Novel HTS PM Vernier Motor for Direct-Drive Propulsion. IEEE Transactions on Applied Superconductivity **21**(3), 1175–1179 (2011)
260. C. L. Goodzeit, R. B. Meinke, H. M. Gutierrez, P. J. Masson, H. J. Schneider-Muntau. High power density marine propulsion motors with double-helix coils
261. K. L. J. Kan, K.W.E. Cheng. Review of Marine Magnetohydrodynamic Motor Development. In 2022 IEEE 9th International Conference on Power Electronics Systems and Applications (PESA), pages 1–3, (2022)
262. A. Salerno-Garthwaite. DARPA's silent MHD magnetic drives for replacing naval propellers, (2023)
263. P. Cheetham, C.H. Kim, S. Pamidi, R. Smart, N. Robertson, D. Mavris, M. Balchanos, J. McNabb, A. Card, R. Leonard, A. Sudol, J. Chalfant, J. Ordonez, SuPErShip - A Multidisciplinary Collaborative Study on System-Level Benefits of Superconducting Power Devices on Electric Ships. IEEE Transactions on Applied Superconductivity **33**(5), 1–4 (2023)
264. N.G. Suttell, J.V.C. Vargas, J.C. Ordonez, S.V. Pamidi, C.H. Kim, Modeling and optimization of gaseous helium (GHe) cooled high temperature superconducting (HTS) DC cables for high power density transmission. Applied Thermal Engineering **143**, 922–934 (2018)

265. L. García-Tabarés. The Poseidon Project. Funded by the European Commision within the call Clean and competitive solutions for all transport modes as a Research and Innovation Action. 2023-2026
266. A. Zhang, S.V. Gudmundsson, T.H. Oum, Air transport, global warming and the environment. Transportation Research Part D: Transport and Environment **15**(1), 1–4 (2010)
267. X. S. Zheng, D. Rutherford. Fuel Burn of New Commercial Jet Aircraft: 1960 to 2019. (2020)
268. Y. Cohen, D. Hauglustaine, N. Bellouin, S. Eastham, M. T. Lund, S. Matthes, M. Righi, A. Skowron, R. Thor. Impact of aircraft NOx and aerosol emissions on atmospheric composition: a model intercomparison, and a multimodel assessment using the airborne IAGOS data. Technical Report EGU24-20326, Copernicus Meetings, (2024)
269. Fuel burn of new commercial jet aircraft: 1960 to 2019. https://theicct.org/publication/fuel-burn-of-new-commercial-jet-aircraft-1960-to-2019/
270. H. Southall, C. Oberly, System considerations for airborne, high power superconducting generators. IEEE Transactions on Magnetics **15**(1), 711–714 (1979)
271. Pat Wheeler, Sergei Bozhko, The More Electric. Aircraft, Technology and challenges. IEEE Electrification Magazine **2**(4), 6–12 (2014)
272. J. Swanke, D. Bobba, T. M. Jahns, B. Sarlioglu. Comparison of Modular PM Propulsion Machines for High Power Density. In 2019 IEEE Transportation Electrification Conference and Expo (ITEC), pages 1–7, (2019)
273. Directorate-General for Climate Action (European Commission), Directorate-General for Energy (European Commission), Directorate-General for Mobility and Transport (European Commission), M. Zampara, M. Obersteiner, S. Evangelopoulou, A. De Vita, W. Winiwarter, Heinz-Peter Witzke, S. Tsani, Monika Kesting, L. Paroussos, L. Höglund-Isaksson, D. Papadopoulos, P. Capros, M. Kannavou, P. Siskos, N. Tasios, N. Kouvaritakis, P. Karkatsoulis, P. Fragkos, A. Gomez-Sanabria, A. Petropoulos, P. Havlík, S. Frank, P. Purohit, K. Fragiadakis, N. Forsell, M. Gusti, and Ch Nakos. EU reference scenario 2016: energy, transport and GHG emissions : trends to 2050. Publications Office of the European Union, (2016)
274. C.E. Oberly. Lightweight superconducting generators for mobile military platforms. In 2006 IEEE Power Engineering Society General Meeting, pages 8 pp.–, (2006)
275. N. K. Madavan, R. Del Rosario, A. L. Jankovsky. Hybrid-Electric and Distributed Propulsion Technologies for Large Commercial Transports: A NASA Perspective, (2015)
276. K. Sivasubramaniam, T. Zhang, M. Lokhandwalla, E.T. Laskaris, J.W. Bray, B. Gerstler, M.R. Shah, J.P. Alexander, Development of a High Speed HTS Generator for Airborne Applications. IEEE Transactions on Applied Superconductivity **19**(3), 1656–1661 (2009)
277. C.E. Jones, P.J. Norman, S.J. Galloway, M.J. Armstrong, A.M. Bollman, Comparison of Candidate Architectures for Future Distributed Propulsion Aircraft. IEEE Transactions on Applied Superconductivity **26**(6), 1–9 (2016)
278. A. Patel, V. Climente-Alarcon, A. Baskys, B. A, Glowacki, T. Reis. Design considerations for fully superconducting synchronous motors aimed at future electric aircraft. In 2018 IEEE International Conference on Electrical Systems for Aircraft, Railway, Ship Propulsion and Road Vehicles & International Transportation Electrification Conference (ESARS-ITEC), pages 1–6, (2018)
279. A. Colle, T. Lubin, S. Ayat, O. Gosselin, J. Leveque, Test of a Flux Modulation Superconducting Machine for Aircraft. Journal of Physics: Conference Series **1590**(1), 012052 (2020)
280. Z. Zhu, Y. Wang, S. Venuturumilli, J. Sheng, M. Zhang, W. Yuan, Influence of Harmonic Current on Magnetization Loss of a Triaxial CORC REBCO Cable for Hybrid Electric Aircraft. IEEE Transactions on Applied Superconductivity **28**(4), 1–5 (2018)
281. C.D. Manolopoulos, M.F. Iacchetti, A.C. Smith, K. Berger, M. Husband, P. Miller, Stator Design and Performance of Superconducting Motors for Aerospace Electric Propulsion Systems. IEEE Transactions on Applied Superconductivity **28**(4), 1–5 (2018)
282. P.J. Masson, C.A. Luongo, High power density superconducting motor for all-electric aircraft propulsion. IEEE Transactions on Applied Superconductivity **15**(2), 2226–2229 (2005)
283. P.J. Masson, G.V. Brown, D.S. Soban, C.A. Luongo, HTS machines as enabling technology for all-electric airborne vehicles. Superconductor Science and Technology **20**(8), 748 (2007)
284. S.S. Kalsi, R.A. Badcock, J.G. Storey, K.A. Hamilton, Z. Jiang, Motors Employing REBCO CORC and MgB_2 Superconductors for AC Stator Windings. IEEE Transactions on Applied Superconductivity **31**(9), 1–7 (2021)

285. G. Messina, M. Yazdani-Asrami, F. Marignetti, A.D. Corte, Characterization of HTS Coils for Superconducting Rotating Electric Machine Applications: Challenges, Material Selection, Winding Process, and Testing. IEEE Transactions on Applied Superconductivity **31**(2), 1–10 (2021)
286. M. Yazdani-Asrami, S.M. Seyyedbarzegar, M. Zhang, W. Yuan, Insulation Materials and Systems for Superconducting Powertrain Devices in Future Cryo-Electrified Aircraft: Part I-Material Challenges and Specifications, and Device-Level Application. IEEE Electrical Insulation Magazine **38**(2), 23–36 (2022)
287. Md M. Hossain, A. Ur Rashid, Y. Wei, R. Sweeting, H. A. Mantooth. Cryogenic Characterization and Modeling of Silicon IGBT for Hybrid Aircraft Application. In 2021 IEEE Aerospace Conference (50100), pages 1–8, (2021)
288. N. Clayton, M. Crouchen, A. Devred, D. Evans, C.Y. Gung, I. Lathwell, Manufacture and mechanical characterisation of high voltage insulation for superconducting busbars - (Part 1) Materials selection and development. Cryogenics **83**, 64–70 (2017)
289. J.S. Bennett, B.E. Vyhnalek, H. Greenall, E.M. Bridge, F. Gotardo, S. Forstner, G.I. Harris, F.A. Miranda, W.P. Bowen, Precision Magnetometers for Aerospace Applications: A Review. Sensors **21**(16), 5568 (2021)
290. M. Vietze, S. Weiland, System analysis and requirements derivation of a hydrogen-electric aircraft powertrain. International Journal of Hydrogen Energy **47**(91), 38793–38810 (2022)
291. G. Squadrito, G. Maggio, A. Nicita, The green hydrogen revolution. Renewable Energy **216**, 119041 (2023)
292. N. Ma, W. Zhao, W. Wang, X. Li, H. Zhou, Large scale of green hydrogen storage: Opportunities and challenges. International Journal of Hydrogen Energy **50**, 379–396 (2024)
293. T. Yusaf, A.S.F. Mahamude, K. Kadirgama, D. Ramasamy, K. Farhana, H.A. Dhahad, A.B.D.R.A. Talib, Sustainable hydrogen energy in aviation – A narrative review. International Journal of Hydrogen Energy **52**, 1026–1045 (2024)
294. F. Grilli, T. Benkel, J. Hänisch, M. Lao, T. Reis, E. Berberich, S. Wolfstädter, C. Schneider, P. Miller, C. Palmer, B. Glowacki, V. Climente-Alarcon, A. Smara, L. Tomkow, J. Teigelkötter, A. Stock, J. Büdel, L. Jeunesse, M. Staempflin, G. Delautre, B. Zimmermann, R. van der Woude, A. Perez, S. Samoilenkov, A. Molodyk, E. Pardo, M. Kapolka, S. Li, A. Dadhich, Superconducting motors for aircraft propulsion: the Advanced Superconducting Motor Experimental Demonstrator project. Journal of Physics: Conference Series **1590**(1), 012051 (2020)
295. Airbus takes superconductivity research for hydrogen-powered aircraft a step further | Airbus, May 2024. Section: Innovation
296. L. Chapman, Transport and climate change: a review. Journal of Transport Geography **15**(5), 354–367 (2007)
297. L.S. Mattos, E. Rodriguez, F. Costa, G.G. Sotelo, R. de Andrade, R.M. Stephan, MagLev-Cobra Operational Tests. IEEE Transactions on Applied Superconductivity **26**(3), 1–4 (2016)
298. R.M. Stephan, A.O. Pereira, The Vital Contribution of MagLev Vehicles for the Mobility in Smart Cities. Electronics **9**(6), 978 (2020)
299. J. Wang, S. Wang, Y. Zeng, H. Huang, F. Luo, Z. Xu, Q. Tang, G. Lin, C. Zhang, Z. Ren, G. Zhao, D. Zhu, S. Wang, H. Jiang, M. Zhu, C. Deng, P. Hu, C. Li, F. Liu, J. Lian, X. Wang, L. Wang, X. Shen, X. Dong, The first man-loading high temperature superconducting Maglev test vehicle in the world. Physica C: Superconductivity **378–381**, 809–814 (2002)
300. H.-W. Lee, K.-C. Kim, J. Lee, Review of maglev train technologies. IEEE Transactions on Magnetics **42**(7), 1917–1925 (2006)
301. V.S. Murty, S. Jain, A. Ojha, Development of single linear induction motor for high-speed transit system. Soft Computing **28**(2), 887–902 (2024)
302. Y. Gao, T. Nakamura, Experimental study of a high-temperature superconducting induction/synchronous motor with REBCO bulk bars for transportation applications. Physica C: Superconductivity and its Applications **611**, 1354284 (2023)
303. F. Dong, D. Park, Z. Huang, M. Wang, Y. Iwasa, On the future sustainable ultra-high-speed maglev: A superconductor magnet technology enabling high energy efficiency and robustness. Energy Conversion and Management **314**, 118725 (2024)
304. K. Kuwano, M. Igarashi, S. Kusada, K. Nemoto, T. Okutomi, S. Hirano, T. Tominaga, M. Terai, T. Kuriyama, K. Tasaki, T. Tosaka, K. Marukawa, S. Hanai, T. Yamashita, Y. Yanase, H. Nakao, M. Yamaji, The Running Tests of the Superconducting Maglev Using the HTS Magnet. IEEE Transactions on Applied Superconductivity **17**(2), 2125–2128 (2007)

305. Z. Deng, W. Zhang, J. Zheng, Y. Ren, D. Jiang, X. Zheng, J. Zhang, P. Gao, Q. Lin, B. Song, C. Deng, A High-Temperature Superconducting Maglev Ring Test Line Developed in Chengdu. China. IEEE Transactions on Applied Superconductivity **26**(6), 1–8 (2016)
306. X. Zhao, J. Fang, Z. Jiang, W. Song, N. Liu, Y. Gao, X. Li, F. Zeng, Y. Xia, R.A. Badcock, N.J. Long, M.P. Staines, R.G. Buckley, X. Fang, Y. Li, B. Liu, J. Zhang, W. Han, L. Li, J. Wang, P. Gao, Design, development, and testing of a 6.6 MVA HTS traction transformer for high-speed train applications. Superconductor Science and Technology **36**(8), 085009 (2023)
307. A. Ingo, Hansen, Hyperloop transport technology assessment and system analysis. Transportation Planning and Technology **43**(8), 803–820 (2020)
308. Z. Deng, W. Zhang, J. Zheng, B. Wang, Y. Ren, X. Zheng, J. Zhang, A High-Temperature Superconducting Maglev-Evacuated Tube Transport (HTS Maglev-ETT) Test System. IEEE Transactions on Applied Superconductivity **27**(6), 1–8 (2017)
309. M. Tomita, Y. Fukumoto, Y. Kobayashi, A. Ishihara, T. Akasaka, K. Suzuki, T. Onji, Laying of superconducting cable and cooling test on the field of subway. Cryogenics **123**, 103433 (2022)
310. M. Tomita, T. Akasaka, Y. Fukumoto, A. Ishihara, Y. Kobayashi, T. Onji, Practical Verification of Superconducting Feeder Cable on Commercial Rail Lines. IEEE Transactions on Applied Superconductivity **34**(3), 1–5 (2024)
311. O. Vakaliuk, S. Song, U. Floegel-Delor, F. Werfel, K. Nielsch, Z. Ren, A multifunctional highway system incorporating superconductor levitated vehicles and liquefied hydrogen. APL Energy **1**(1), 016107 (2023)
312. T. Shinzato, S. Arakawa, H. Oyama, H. Saka, T. Hayasaki. Development of high-temperature superconducting motor for automobiles. pages 62–65, (2012)
313. T. Nakamura, Y. Yamada, H. Nishio, K. Kajikawa, M. Sugano, N. Amemiya, T. Wakuda, M. Takahashi, M. Okada, Development and fundamental study on a superconducting induction/synchronous motor incorporated with MgB_2 cage windings. Superconductor Science and Technology **25**(1), 014004 (2011)
314. T. Nakamura, M. Yoshikawa, T. Terazawa, K. Matsuki, Y. Gao, T. Kiss, Development of 50-kw-class high-temperature superconducting induction/synchronous motor with continuous drive characteristics from room temperature. IEEE Transactions on Applied Superconductivity **33**(5), 1–5 (2023)
315. H. Oyama, T. Shinzato, K. Hayashi, K. Kitajima, T. Ariyoshi, T. Sawai. Application of Superconductors for Automobiles. (2008)
316. E.-L. Molina-Ibáñez, E. Rosales-Asensio, C. Pérez-Molina, F.M. Pérez, A. Colmenar-Santos, Analysis on the electric vehicle with a hybrid storage system and the use of Superconducting magnetic energy storage (SMES). Energy Reports **7**, 854–873 (2021)
317. J. Oberteuffer, Magnetic separation: A review of principles, devices, and applications. IEEE Transactions on Magnetics **10**(2), 223–238 (1974)
318. J. Svoboda, T. Fujita, Recent developments in magnetic methods of material separation. Minerals Engineering **16**(9), 785–792 (2003)
319. Drum Separators | Magnetic Drum Separators. https://www.imt-inc.com/products/magnetic-drum-separators/
320. S.P. Veetil, G. Mercier, J.-F. Blais, E. Cecchi, S. Kentish, Magnetic separation of serpentinite mining residue as a precursor to mineral carbonation. International Journal of Mineral Processing **140**, 19–25 (2015)
321. T. Ohara, H. Kumakura, H. Wada, Magnetic separation using superconducting magnets. Physica C: Superconductivity **357–360**, 1272–1280 (2001)
322. K. Yokoyama, T. Oka, H. Okada, Y. Fujine, A. Chiba, K. Noto, Solid-liquid magnetic separation using bulk superconducting magnets. IEEE Transactions on Applied Superconductivity **13**(2), 1592–1595 (2003)
323. D.W. Ha, J.M. Kwon, S.K. Baik, Y.J. Lee, K.S. Han, R.K. Ko, M.H. Sohn, K.C. Seong, Purification of condenser water in thermal power station by superconducting magnetic separation. Physica C: Superconductivity and its Applications **471**(21), 1530–1532 (2011)
324. T. Oka, H. Kanayama, K. Tanaka, S. Fukui, J. Ogawa, T. Sato, M. Ooizumi, T. Terasawa, Y. Itoh, R. Yabuno, Waste water purification by magnetic separation technique using HTS bulk magnet system. Physica C: Superconductivity **469**(15), 1849–1852 (2009)
325. R.D. Ambashta, M. Sillanpää, Water purification using magnetic assistance: A review. Journal of Hazardous Materials **180**(1), 38–49 (2010)

326. T. Oka, H. Kanayama, S. Fukui, J. Ogawa, T. Sato, M. Ooizumi, T. Terasawa, Y. Itoh, R. Yabuno, Application of HTS bulk magnet system to the magnetic separation techniques for water purification. Physica C: Superconductivity **468**(15), 2128–2132 (2008)
327. A. Moradnouri, A. Ardeshiri, M. Vakilian, A. Hekmati, M. Fardmanesh, Survey on High-Temperature Superconducting Transformer Windings Design. Journal of Superconductivity and Novel Magnetism **33**(9), 2581–2599 (2020)
328. M.P. Staines, Z. Jiang, N. Glasson, R.G. Buckley, and M. Pannu. 12 - high-temperature superconducting (hts) transformers for power grid applications. In Christopher Rey, editor, Superconductors in the Power Grid, Woodhead Publishing Series in Energy, pages 367–397. Woodhead Publishing, (2015)
329. H. Zueger, 630kva high temperature superconducting transformer. Cryogenics **38**(11), 1169–1172 (1998)
330. B. Grzesik, M. Stepien, Toroidal superconducting transformer with cold magnetic core - results of analysis and measurements. Journal of Physics: Conference Series **507**(3), 032043 (2014)
331. S. Hellmann, M. Abplanalp, L. Hofstetter, M. Noe, Manufacturing of a 1-mva-class superconducting fault current limiting transformer with recovery-under-load capabilities. IEEE Transactions on Applied Superconductivity **27**(4), 1–5 (2017)
332. F. Irannezhad, H. Heydari, Conducting a Survey of Research on High Temperature Superconducting Transformers. IEEE Transactions on Applied Superconductivity **30**(6), 1–13 (2020)
333. M. Miryala, *High-Tc Superconducting Technology: Towards Sustainable Development Goals* (CRC Press, 2021)
334. O. Lucía, P. Maussion, E.J. Dede, J.M. Burdío, Induction Heating Technology and Its Applications: Past Developments, Current Technology, and Future Challenges. IEEE Transactions on Industrial Electronics **61**(5), 2509–2520 (2014)
335. X. Wang, S. Dai, T. Ma, G. Jiang, Design and Operating Characteristics Analysis of HTS Magnets for Dipole-Type DC Induction Heating. Journal of Superconductivity and Novel Magnetism **37**(2), 311–324 (2024)